Effect of Notch Size on the Reliability of Composite Laminates Based on Stochastic Finite Element Analysis and Experimental Investigation

Md Ibrahim

A Thesis

in

The Department

of

Mechanical and Industrial Engineering

Presented in Partial Fulfillment of the Requirements

for the Degree of Master of Applied Science at

Concordia University

Montreal, Quebec, Canada

March 2005

Your file Votre référence
ISBN: 0-494-04418-7
Our file Notre référence
ISBN: 0-494-04418-7

ABSTRACT

Effect of Notch Size on the Reliability of Composite Laminates based on Stochastic Finite Element Analysis and Experimental Investigation

Ibrahim Md

This work considers the reliability of notched composite laminates based on stochastic mechanics. The reliability of composite laminates with different notch sizes is evaluated using point stress criterion and average stress criterion. Reliability values are calculated based on the stresses developed over certain characteristic distances from the notch edge and the strength of the corresponding un-notched laminates. In practical applications, it is very difficult to achieve a perfect circular profile during the drilling operation on a composite laminate and also there is a possibility that the driven hole is offset from the desired location. These imperfections affect the reliability of the laminate. In the present work the perturbation in the circular profile of the hole is modeled using a hypotrochoid variation and further, the location of the hole center is modeled using a Gaussian random variable. Tests are conducted on specimens made of graphite/epoxy material to determine the material properties that are required for stochastic analysis. The material properties are modeled using Markov model based on the test data by two dimensional stochastic processes. Tests are also conducted on $[0/90]_{4s}$ cross-ply specimens to determine the notched and un-notched strengths of the laminate. The characteristic length to be used in design is shown to follow a stochastic distribution. Therefore, in order to design a notched laminate with required reliability and safety, i) the stress analysis of the laminate has to be conducted based on a stochastic approach, ii) the strength distribution and its

probabilistic parameters have to be determined based on a number of tests, iii) the notch size effect on the reliability of the laminates has to be studied. Notched and un-notched strength values of $[0/90]_{4s}$ cross-ply specimens obtained from experiments are used to determine the sets of characteristic length values for both the point stress criterion and average stress criterion for different notch sizes. The distributions of the strength and characteristic length of laminates are determined.

Two dimensional stochastic finite element analysis of symmetric cross-ply $[0/90]_{4s}$ laminate with three different notch sizes is conducted. Stochastic simulations are performed on the laminates by subjecting them to tensile load. Probabilistic moments of the point stress and average stress parameters are found out for the so-called controlled hole and un-controlled hole laminates. The reliability values are calculated for three notch sizes using point stress criterion and average stress criterion by combining the stochastic finite element analysis and the test results.

Acknowledgements

At first I would like to express my gratitude to the creator of this universe who gave me the ability to complete this thesis. Secondly, I wish to express my sincere gratitude to my supervisor Dr. Rajamohan Ganesan for his invaluable guidance, financial support and stimulating suggestions through out the entire thesis work. It is with his encouragement that this study is completed.

I would also like to acknowledge the financial support provided by National Science and Engineering Research Council (NSERC) of Canada through the research grant to my supervisor, and the support provided through that work study program of Concordia University.

I would also like to thank many people in the department who have assisted me in doing experimental work. Among them, Ming Xie, Robert Oliver, John Elliott and J. Bowles, who have been particularly generous with their time and expertise. I am also grateful to Shashank M. Venugopal who helped me by showing the details of making the composite laminates.

I also wish to thank my parents and family members, who have always inspired me by wishing every accomplishment in my research work. I am especially grateful to my father from whom I learnt to be patient, hardworking, honest and sincere in life.

I wish to thank my wife Kazi Basneen Haseen for her every support in the entire course of work. Lastly, and importantly, I wish to thank my son Saadat Mohammad Najib, who always keeps me vibrant and cheered me up in every step of my life. To him I dedicate this thesis.

Table of Contents

List of Tables

List of Figures

Nomenclature

N_i	Shape functions
ξ,η	Local co-ordinates
$[\sigma]$	Stress vector
τ	Shear stress
ε	Normal strain
γ	Shear strain
E	Young's modulus
ν	Poisson's ratio
$\{u\ v\}^T$, $\{d\}$	Displacement vector
[B]	Strain-nodal displacement matrix
$[K]^e$	Element stiffness matrix
h	Thickness of the element; Thickness of the plate
[J]	Jacobian matrix
[E]	Elasticity matrix
W_p, W_q	Weight factors used for Gaussian integration
r,s	Position of Gauss point in the element
q	Uniformly distributed load
l	Element length
x,y,z	Global co-ordinates
r	Radius of the hole

d	Diameter of the hole
[A]	Axial stiffness matrix
[B]	Axial-bending coupling stiffness matrix
[D]	Bending stiffness matrix
[κ]	Curvature matrix
[N]	Stress resultant matrix
[a]	Compliance matrix
$E_x, E_y, G_{xy}, \nu_{xy}, m_{xy}$	Effective laminate moduli, Shear modulus, Poisson's ratio and tension-shear coupling coefficient in the x and y co-ordinate system
R_{aa}	Auto-correlation function
$[\zeta_x \ \zeta_y]^T$	Separation vector
a(X)	Fluctuating component of E_1
[L]	Lower triangular matrix
$[C_{aa}]$	Covariance matrix
θ, t	Ply orientation angle; ply thickness
δ	Small perturbation parameter
σ_o	Applied stress at infinity; Un-notched strength of the laminate
σ_y^{∞}	Y component of normal stress for an infinite width plate
σ_y	Y component of normal stress for a finite width plate
μ_1, μ_2	Roots of the characteristic equation
K_T, K_T^{α}	Stress concentration factors for finite and infinite plates

	respectively
W	Width of the plate
M	Magnification factor
$E_1, E_2, \nu_{12}, G_{12}$	Young's modulus values of the graphite/epoxy material in the fiber and transverse directions, major Poisson's ratio and shear modulus
{f}	Equivalent nodal force vector
s	Standard deviation
Z_R	Standardized variable
R	Reliability
R_{Point}	Reliability obtained using point stress criterion
R_{Avg}	Reliability obtained using average stress criterion
c	Correlation length

CHAPTER 1

INTRODUCTION

1.1 Composites in Structural Applications

The use of advance composite materials in both military and commercial aircraft structures has progressed steadily over the last 30 years. Current generation aircrafts now use composites in primary structures and the weight of composites are approaching 30-40% of the total aircraft structure. Examples of composite primary structures include the horizontal and vertical tails, cabin floor structure and the wing center section keel beam. Secondary structure application includes engine nacelle components, landing gear doors, wing trailing edges, flight controls, stabilizers, etc [1]. Cutouts of different sizes and shapes are introduced in these structures for fastening and weight reduction purposes. Introduction of cutouts leads to stress concentrations in addition to lowering the load carrying capability of the structure.

The fundamental benefits that composite materials offer are weight savings. The specific strength and stiffness of graphite epoxy composite materials allow for novel design applications that can reduce the weight of a component by as much as 50% or greater when compared to an equivalent metallic design. Secondary benefits of composite structure include improved acoustic performance, higher damage tolerance, better manufacturability and structural fatigue properties with better durability.

The primary benefit to the aircraft operator that utilizes a high percentage of composite materials is reduced direct operating cost. Since the airframe is lighter, the fuel burn is

reduced in proportion to the savings in weight. Alternatively, the weight saved in structure can be put to effective use as either increased cargo load/or increased passenger load thus increasing the revenue generation.

Improvement in flight performance is one of the most important criteria in the design of aerospace structures. Weight reduction measures, coupled with strength, stiffness and stability requirements are important. Investigators have long been in search of materials that have less weight as well as sufficient strength and stiffness to withstand aerodynamic loads experienced by a structure in various flight conditions. Fiber reinforced composite materials have been found to have promising properties in this regard.

Composites have also found many applications as advanced engineering materials, and they are effectively employed in various structural systems such as automobiles, power plants, ships, etc. In recent years, composite materials have become widely recognized as a vital construction material too. The increasing use of composite materials in the design of structural parts with high mechanical performance requires a better understanding and modeling the behavior of these structures. The safety and reliability of these structures depend on the design of the constituent components.

The design of composite laminates typically involves optimization of the following four parameters [2]:

1. Ply property
2. Ply thickness
3. Ply orientation, and
4. Stacking or lay-up sequence

The true optimization of a composite laminate, simultaneously considering the coupling effects of the four design parameters mentioned above, is a mathematical challenge in structural optimization. Characterization of stress distribution in a composite laminate is not trivial and simulations need to be accompanied by experimental verification before various laminate theories can be used with confidence.

Carbon fiber composite materials are sensitive to open holes, defects, and low-velocity impact damage that can significantly reduce their stiffness and strength properties. Holes in composites will create stress concentrations. There are no criteria capable of predicting failure under a broad range of general stress state. A good design methodology in the presence of stress concentration in composite structures is also deficient. To utilize these advance materials to their full potential, the establishment of the strength criterion is important. Considerable efforts have been devoted to recent developments of strength/failure criteria for composite materials [3].

1.2 Cutouts in Composite Structure

It is well known that holes and cutouts cause serious problems of stress concentrations due to the geometry discontinuity. These problems are even more serious in structures made of composite materials since the materials exhibit anisotropic behavior, and the structures are more sensitive to stress concentrations due to its brittle behavior. Because of its importance, engineers must know how to analyze it, to predict failure and strength, and to develop methods to reduce the effects of stress concentration. Stress concentration in a structure can be caused by many reasons and they are listed below [3]:

1. Cutouts

2. Material and geometric discontinuities

3. Joints which include bolted joints, bonded joints and other mechanical joints

4. Voids and damage due to material fabrication

Solutions to many issues related to stress concentration in laminated composites are still in the early stages of development. In this regard, finite element method is found as one of the most effective numerical tools for the analysis of composite laminates.

Composite materials are used in the structures to withstand important mechanical loads. The design of these structures requires the thorough knowledge of the mechanical behavior of the material used. This is generally obtained by the testing of laminate coupons. However, the preparation of these coupons often involves cutting operations (cutting coupons from panel, machining notches, drilling holes, etc.). These tend to create damage on the cut surfaces, the cutting conditions are a possible source of strength reduction at the coupon level. Also, standards tend to contain limited information in terms of specimen cutting.

1.3 Randomness in the Behavior of Composite Structure

The parameters of any mechanical or structural system possess a random variation as a function of space and/or time. The randomness in stress and strength parameters of notched composite laminates encompasses the uncertainties involved at the design and manufacturing stages as well as uncertainty that exist in the geometric profile of the notches. At the design stage, randomness is present in the test data regarding material strength values of notched laminates, engineering constants, damage parameters, and the material properties pertinent to the service life. The randomness in material properties

significantly affects the functioning of the mechanical component and is unavoidable even with the best quality control measures.

Tests on a single material specimen or structure yield a definite value for each material parameter such as the elastic constant, damage parameter, strength value, etc. But when a number of specimens are tested, i) the parameter values randomly fluctuate from specimen to specimen, ii) within the same structure itself, the values of any parameter display an uncertain spatial variation, iii) due to environmental degradation the parameters have uncertain fluctuations. The sample to sample variation, spatial fluctuations within the structure, structure to structure variations and variation due to environmental effects of strength, deformation and damage parameters together imply that most present day engineering materials are random in nature [4]. This is particularly the case with fiber reinforced composite materials. Variations in fiber size, fiber volume fraction, fiber orientation, void content, matrix properties and thickness of lamina are always present and unavoidable. As a result, the engineering constant and strength values of fiber reinforced composite materials possess random variation [5].

1.4 Literature Review

The effects of a load free circular hole on the tensile strength of a metallic plate are characterized by the stress concentration factor (SCF). Consequently, the use of SCF as a design parameter in metallic construction is widespread, and the effects of plate, hole, and loading configuration on the value of this parameter have been extensively characterized [6]. However, the exact analytical solutions for the finite-width anisotropic plate are not available. The stress distribution of an infinite anisotropic laminate containing holes of different shapes using the series method is given by Lekhnitskii [7].

Green [8] has given solutions for stress concentration problems in isotropic and allotropic plates. The first analytical solution for multi-layered composite laminates with a circular hole has been given by Greszczuk [9]. Greszczuk found out the failure strength and location of failure based on Hencky-Von Mises theory using the equations given by Fischer [10]. Approximate solution for normal stress distribution adjacent to a circular hole in an infinite orthotropic plate is given by Konish and Whitney [11]. They consider the solution for normal stress in the form of a polynomial by adding sixth and eighth order terms to the isotropic solution.

The effect of fiber orientation on stress concentration in a finite width composite laminate has been studied by Rao and Shastry [12]. They have found that stress concentration factor is maximum when the fiber directions are parallel to the loading and minimum when they make an angle of 45^0. In three-dimensional analysis, Lucking et al. [13] have studied the effect of the radius-to-thickness ratio R/t on the interlaminar stresses around the hole in a $[0/90]_{4s}$ laminate. The tangential interlaminar shear stress near the hole edge increases as the ratio of R/t increases. They have also concluded that interlaminar stress could play a significant role in influencing the strength of notched laminates. The hole size and shape affecting the overall strength of the composite laminate have been investigated by Dana [14] using three dimensional finite element method. For large holes, interlaminar shear failures probably begin at the edge of the hole, rather than at the free straight edges of the laminate. If the hole is of some critical size, the failures may start at both curved and straight edges and grow toward one another. Notched strengths of angle ply laminates of configurations $[0_2/\pm\theta]_s$ are studied for larger hole sizes by Fung-En Harn [15]. The hole size and fiber orientation are considered as two parameters for this study.

The extensive study of boundary layer theory and interlaminar stresses can be found in the literature [16-20]. It is believed that interlaminar stresses play an important role in the delamination at the ply interface. Chan and Ochoa [21] have developed a finite element scheme to study the delamination characteristics of laminates subjected to various loading conditions. They found that the interlaminar stresses can be significantly reduced by minimizing the Poisson's ratio mismatch. Shah and Chan [22] applied the Chan and Ochoa's finite element scheme to investigate the interlaminar stress distribution around a hole. Notches of different shapes and sizes other than a circular hole are studied in many literatures. Hufenbach et al. [23] gave a solution for the case of an elliptical hole in an anisotropic plate under uni-axial tension at different angles. Daoust and Hoa [24] gave the solution for a triangular hole in an anisotropic plate. Their solution considers any ratio of base length and height of the triangle. Ugadgaonkar and Rao [25] have extended Daoust and Hoa's [24] solution for multi-layered plates and considered several cases of in-plane loading. Theocaris and Petrou [26-27] considered triangular and rectangular holes in isotropic plates. The stress distribution around these holes is determined considering singular points at the rounded corners.

Cutouts are used in structures for various reasons such as: to make passages for hydraulic lines, avionic harnesses, and on a larger scale, an access door in an aircraft fuselage. Optimizing the size and shape of the cutouts in composite structures is still a challenge for the designer due to the anisotropic nature of the material. Many other researchers have conducted work on single and elliptical cutouts and to name a few: Tan, S.C. [28-30], Lin and Ueng [31], X. W. Xu et al. [32], Rowlands et al. [33].

Many of the solutions cited for a circular hole involve analytical work with complex method, series expansion, conformal mapping and boundary collocation techniques. Most of them are not verified by experimental work. It is felt that a solution based on a simple mathematical approach is needed to consider any shape of hole in multi-layered plates. Such a solution will be useful to study the effect of hole size and shape, type of loading and laminate geometry on stress distribution around the hole.

Traditionally, the stress concentration factor (SCF) around holes of ideal shapes has been considered. However, in practice the manufacturing process of structural parts inevitably produces imperfections which may affect the stress distribution around hole. Givoli and Elishakoff [34] studied the stress concentration on the boundary of an uncertain nearly circular hole in an infinite elastic circular plate under uniform radial tension at infinity. This work considers a certain set of bounded profiles and finds the profile which yields the maximum stress concentration factors. Irregularities of ideally shaped holes have been modeled using a probabilistic description by Pal'mov [35]. Lomakin [36] has developed a double perturbation scheme for a hole with a rapidly oscillating boundary. The boundary was characterized as a random stationary Gaussian function with zero mean and with a specified autocorrelation function. The stress concentration factor was calculated as suggested by Pal'mov. The profile of the hole as a random function was treated by Sayles [37].

The analysis of structures, whether subjected to random or deterministic external loads, has been developed mainly under the assumption that the structure's parameters are deterministic quantities. For a significant number of cases, this assumption is not valid, and the probabilistic aspects of the structure need to be taken into account. The necessity

to account for random effects in determining the response of a mechanical system is due , in general, to three different sources: random external loadings, random boundary conditions, and random material parameters. With many recent developments, the finite element method is now capable of incorporating these random effects and is now known as the Stochastic Finite Element Method (SFEM). Amongst all numerical procedures in non-deterministic computational mechanics the SFEM has been developed and applied to the reliability and response variability assessment of static and dynamic, linear and non-linear problems. The well known probabilistic theories for the tensile strength of unidirectional composites have been proposed by Rosen [38] and Zweben [39] and further developments have been reported in detail by different authors [40-44]. These models give us satisfactory strength estimation when the composite failure is predominantly affected by the stochastic distribution of reinforcement fibers but are not suitable when there are other competing failure mechanisms.

Most SFEM applications in the literature involve uncertain parameters of material or mechanical nature and rarely of geometrical nature. Many of the works done in the context of stochastic finite elements have been based on the assumption that only one material or geometric property is described by a stochastic field, e.g. [45-47]. For example, the assumption is often made that Young's modulus is randomly varying over space, while Poisson's ratio is a deterministic constant. However, many of the physical mechanisms those lead to random variations of Young's modulus also lead to random variations in other material properties such as Poisson's ratio and shear modulus. Random shape variables result in uncertain domains and boundaries, which complicate the stochastic analysis. Shashank [3] has used a stochastic finite element methodology for

the stress concentration analysis of composite laminates which incorporates the probability distributions of material and geometric properties. Two laminate configurations, $[0/90]_{4s}$ and $[0_2/\pm45]_{2s}$ with hole of diameter 5.10 mm were considered for analysis. He also conducted a reliability study based on Gaussian distribution using average stress criterion. The effect of hole size on the stress distribution and reliability of the laminates was not considered in that study. Ganesan and Hoa [48] presented the stress analysis of composite structures with stochastic parameters. Ganesan and Podugala [49] have developed an effective finite element analysis methodology for evaluating the stochastic J-integral of laminated composites. Ganesan and Haque [50] developed a stochastic finite element methodology for the probabilistic fracture behavior of composite laminates. The developments in this field are also reviewed by Contreras [51], Vanmarcke and Grigoriu [52] and Yamazaki, shinozuka and Dasgupta [53].

1.5 Failure Criteria for Composite Laminates

The main objective of stress analysis is strength prediction. Stress analysis can be performed by many methods. They all require physical boundary conditions in the form of traction, displacements or both to solve unknowns. But there is no specific boundary condition that can be used for the strength criteria. They are semi-empirical and phenomenological in nature [2]. For most failure criteria, a few basic strength parameters are defined and evaluated experimentally first, then used to predict the failure of a material in general stress or strain state.

Once the stress distribution of the structure is known, the point of interest should be examined using a failure criterion to determine whether the structure will fail or not. The notched strength of a composite laminate depends on laminate configuration, laminate

stacking sequence, hole size, and laminate width. A different lay-up or material system may exhibit a different failure mechanism. Researchers have long been in the search for a failure criterion which can be applied to laminates of different configurations, notch sizes and shapes and width.

Waddoups, Eisenmann and Kaminski model [54]: the model is an application of linear elastic fracture mechanics to the hole problem. The criterion involves two unknowns: the un-notched strength and the length of the intense energy region (or characteristic length). These unknowns have to be determined empirically using experimental data.

Mar and Lin model [55]: they modified the model proposed by Waddoups et al.[54] for laminated composites. The model is analogous to the stress analysis for the case of a crack at the interface of fiber and matrix.

Whitney and Nuismer model [56-57]: the model hypothesized that the strength of a laminate with a hole can be evaluated at a characteristic distance based on the point or average stress across the region from the edge of the hole. In point stress criterion, the failure is assumed to occur when the normal stress at a characteristic distance from hole edge is equal to the un-notched strength of the laminate. In average stress criterion, it is assumed that failure occurs when the average of the normal stress over some characteristic distance from hole edge is equal to the un-notched strength of the laminate.

Karlak model [57] : the model is a modified Whitney and Nuismer's point stress criterion for quasi–isotropic laminates where the characteristic distance is considered to be related with the hole radius.

Many other researchers proposed other models which are the modifications or extensions of the Whitney and Nuismer model. Some of them are Pipes, Wetherhold and Gillespie model [57] and El-zein and Reifsnider model [58].

The purpose of a failure model is to establish a theoretical margin of safety that has been validated by experiments. Most of the models mentioned here are valid only for unidirectional composites. These models have been widely used to predict the strength of laminated composites with very good results. They should be considered as models rather than failure criteria because they do not take into account the details of the complex failure mechanisms.

1.6 Scope and Objective of the Thesis

Most practical engineering structures contain holes and cutouts of different sizes designed as parts of basic design, such as assembling or maintenance. These cutouts can induce higher stress concentration and stress gradient in composites than in conventional isotropic materials. Achieving a perfect circular hole in the drilling operation of composite laminates is very difficult and also there is a possibility that the hole is offset from the desired location. These facts change the stress distribution in the vicinity of the hole. This variation in the stress distribution caused as a result of hole eccentricity and imperfection of the hole profile, is due to a single hole. A typical F-16XL military aircraft has thousands of tiny holes (2,500 holes over an area of 10 sq. feet) and there exists a possibility that a series of holes drilled over an area, might generate a multiple effect of the variation in the stress distribution over the region. This calls for a study of stress distributions in notched finite composite laminates with different hole sizes subjected to uniformly distributed tensile load, considering the hole profile as nearly circular and

offset from the center of the laminate. Thus a better understanding of the behavior of stress parameters of composite laminates leads to a reliable design and safer operation of the mechanical components. Composite materials are inherited with random elastic and strength properties, which require the stress analysis based on a stochastic approach.

The objectives of the present thesis are:

(1) To use a combined experimental and stochastic finite element analysis methodology for the stress concentration problem of notched finite composite laminates with various notch sizes which incorporates the probability distribution of material and geometric parameters of laminates.

(2) To develop the associated computer program using the MATLAB® code.

(3) To calculate the stochastic stress parameters for both the so-called controlled hole and un-controlled hole laminates using point stress criterion and average stress criterion and to analyze the hole size effect on those stress parameters. (A controlled hole laminate exhibits the stochastic variation in the material properties over the laminate but does not exhibit the geometric variation around the circumference of the hole and hole eccentricity. Whereas, an un-controlled hole laminate takes into account the stochastic variation in material properties over the laminate, the geometric variation around the circumference of the hole, and hole eccentricity.)

(4) To compute the reliability of composite laminates with various notch sizes based on Gaussian distribution using the stochastic stress parameters obtained from simulation and the strength of un-notched laminate.

(5) To find out the effects of hole-width ratio on the reliability of notched composite laminates using both the average stress and point stress criteria.

1.7 Organization of Thesis

The present Chapter provides a brief introduction about the composite material and its applications in various structural components. It discusses the stochastic behavior of composite structures followed by a literature survey. It also highlighted some failure models for composite laminates proposed by different researchers. The previous section provides the scope and objectives of the thesis.

In Chapter 2, the basic concepts and formulation of finite element method in the calculation of stress distribution in notched finite isotropic plate and orthotropic laminate are presented. Composite laminates are analyzed using stochastic finite element method. A two-dimensional, 8-node isoparametric element is used to model the laminates. MATLAB® programs are written to conduct the stress analysis on notched isotropic plate and composite laminate. Program validation is demonstrated by using some suitable example applications.

In Chapter 3, detailed procedures of manufacturing and tensile testing of laminated coupons to determine the stochastic material properties are described. In total 75 specimens are tested to find out the stochastic material properties like E_1, E_2, ν_{21} and G_{12}. Tests are also conducted on notched and un-notched cross-ply specimens. A total of 50 notched specimens with hole sizes of 6.35 mm and 7.54 mm with each set having 25 specimens and 25 un-notched specimens are tested to determine the tensile strength. Finally these strength values are used to calculate the characteristic length values d_o and a_o using both the point stress and average stress criteria. An explanation of the micro

structural study using optical microscope is also provided and check for defects in the laminates is made. Photographs of the specimens before and after testing are presented to explain the failure modes of different laminates.

Chapter 4 is completely devoted to simulation of the behavior of controlled and un-controlled hole laminate conditions using the stochastic finite element methodology. Simulations are performed on $[0/90]_{4s}$ cross-ply laminates with various notch sizes for both the above mentioned conditions and the corresponding stochastic stress parameters for both the criteria are collected and analyzed. Useful conclusions are drawn from the results, which reflect the behavior of a laminate with a particular notch size.

Chapter 5 deals with the reliability of composite laminates with various notch sizes. Probability distributions for the stress parameters are determined using Gaussian distribution method for both the point stress criterion and average stress criterion. Reliability values are calculated for both the controlled and un-controlled hole laminate conditions for various notch sizes by applying factor of safety on the ultimate load of the corresponding notched laminate. Finally, all the reliability values obtained from the analysis of laminates with various notch sizes are plotted against the hole-width ratios for both the criteria and hole conditions.

The thesis ends with Chapter 6, which provides the conclusions of the present thesis work and some recommendations for future work.

CHAPTER 2

STOCHASTIC FINITE ELEMENT ANALYSIS OF NOTCHED PLATE

2.1 Introduction

Metals and fiber reinforced composite laminates find wide applications in aerospace, automobiles, boats, playground structures, high-rise buildings etc. Cutouts of different shapes and sizes in the structure have many practical applications and they are normally the cause of failure. Any such discontinuities in the structure alter the stress distribution and cause an increase of stresses in places near cutouts. These discontinuities are called stress raisers and the regions in which they occur are called areas of stress concentration. In order to predict the behavior of these structures with some degree of assurance, a detailed study of the effects of cutout size and shape on the stress distribution is necessary.

The present Chapter deals with problems related to the determination of stresses in a plate with circular hole and deformed by forces applied to the middle plane. Both isotropic plate and composite laminate are considered. Study of stress concentration effect in anisotropic laminates is much more complicated than that for isotropic plates, because of the directional anisotropy. As the closed form solutions exist only for very few cases it becomes very difficult to analyze the stress concentration around hole in many practical applications. Thus in this Chapter, stress distribution around hole is found out by using finite element method.

Formulation of finite element method used to calculate the stress concentration factors is described in detail in the present Chapter. A study on the minimum number of elements to be used in the finite element mesh to achieve results, that will be close enough to the exact solution, is made. A MATLAB® program is written to solve for the stress concentration factor in a plate with hole, which inherits the concept of finite element method. In order to validate the correctness of program, few examples are considered and the results are compared with experimental results, exact solution and also with ANSYS® solution where available.

2.2 Finite Element Formulation for Isotropic Plates

An eight-node two dimensional isoparametric element is employed to analyze the stress concentration effect in the plates subjected to in plane loadings. A rectangular element of this type is known as serendipity element and is shown in Figure 2.1. The interpolation or shape functions for this element with local co-ordinates [66] are

$$N_i = \begin{cases} \frac{1}{4}(1+\xi\xi_i)(1+\eta\eta_i)(\xi\xi_i+\eta\eta_i-1) & ; \quad i = 1,2,3,4 \\ \frac{\xi_i^2}{2}(1+\xi\xi_i)(1-\eta^2)+\frac{\eta_i^2}{2}(1+\eta\eta_i)(1-\xi^2) & ; \quad i = 5,6,7,8 \end{cases} \tag{2.1}$$

The node numbering system used for the elements is also shown in Figure 2.1.

A two dimensional plane stress case is considered for the analysis because the loading is in-plane and the thickness of the plate is negligible compared to the in-plane dimensions. In the plane stress case a two dimensional stress state exists in the x-y plane when the

stresses σ_{zz}, τ_{xz} and τ_{yz} are equal to zero. The stresses along the direction of the thickness can be ignored.

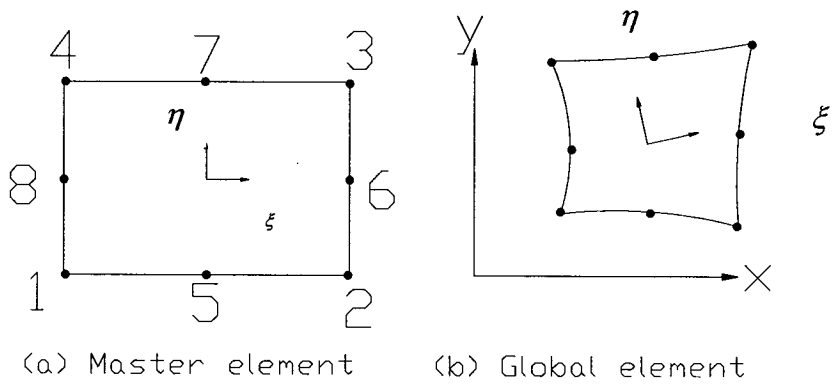

Figure 2.1 2-D eight-node quadrilateral element

Considering only x and y directions, the matrices of displacements and strains can be expressed as

$$\{u\} = \begin{Bmatrix} u \\ v \end{Bmatrix} \quad \text{and} \quad \{\varepsilon\} = \begin{Bmatrix} \varepsilon_x \\ \varepsilon_y \\ \gamma_{xy} \end{Bmatrix} \tag{2.2}$$

where

$$\varepsilon_x = \frac{\partial u}{\partial x}; \quad \varepsilon_y = \frac{\partial v}{\partial y}; \quad \gamma_{xy} = \frac{\partial u}{\partial y} + \frac{\partial v}{\partial x} \tag{2.3}$$

The stresses and strains are related by,

$$\{\sigma\} = [E]\{\varepsilon\} \tag{2.4}$$

in which the matrix representing the stresses is given by

$$\{\sigma\} = \{\sigma_x \quad \sigma_y \quad \tau_{xy}\}^T \tag{2.5}$$

For linear elastic plane stress conditions, the elasticity matrix is given by

$$[E] = \frac{E}{1-\nu^2}\begin{bmatrix} 1 & \nu & 0 \\ \nu & 1 & 0 \\ 0 & 0 & \frac{(1-\nu)}{2} \end{bmatrix} \tag{2.6}$$

where E and ν are the Young's modulus and the Poisson's ratio respectively.

The element displacement matrix can be written as [68]

$$\{u\}^{(e)} = [N]^{(e)}\{d\}^e \tag{2.7}$$

where matrix of the shape function is given by

$$[N]^{(e)} = \begin{bmatrix} N_1 & 0 & N_2 & 0 & \dots & \dots & N_8 & 0 \\ 0 & N_1 & 0 & N_2 & \dots & \dots & 0 & N_8 \end{bmatrix} \tag{2.8}$$

and the displacement vector is given by

$$\{d\}^e = \{u_1 \quad v_1 \quad u_2 \quad v_2 \quad \dots \quad \dots \quad u_8 \quad v_8\}^T \tag{2.9}$$

Details about the strain-displacement matrix and Jacobian matrix are presented in Appendix-A.

The element stiffness matrix can be written as

$$[K]^{(e)} = \int_{V_{(e)}} [B^{(e)}]^T [E][B^{(e)}] dV_{(e)} \tag{2.10}$$

where $dV_{(e)} = h|J|d\xi d\eta$ (2.11)

and h is the thickness of the element.

The stiffness matrix coefficient linking nodes i and j in any element is given by

$$K_{ij}^{(e)} = \sum_{r=1}^{NGAUS} \sum_{s=1}^{NGAUS} \left[B_{ir}^{(e)}\right]^T \left[E_{rs}^{(e)}\right] \left[B_{sj}^{(e)}\right] h \left|J^{(e)}\right| d\xi d\eta \tag{2.12}$$

where NGAUS represents the order of Gauss quadrature used for numerical integration. The elements of the stiffness matrix can be numerically evaluated as

$$K_{ij}^{(e)} = \sum_{r=1}^{NGAUS} \sum_{s=1}^{NGAUS} T\left(\xi_p, \eta_q\right)_{ij}^{(e)} W_p W_q \tag{2.13}$$

where

$$T_{ij}^{(e)} = \sum_{r=1}^{NGAUS} \sum_{s=1}^{NGAUS} \left[B_{ir}^{(e)}\right]^T \left[E_{rs}^{(e)}\right] \left[B_{sj}^{(e)}\right] h \left|J^{(e)}\right| \tag{2.14}$$

In equation (2.13), $\left(\xi_p, \eta_q\right)$ represent the sampling position and W_p, W_q are the weighting factors. If q is the uniformly distributed load acting along the edge of the length l of an element (e), the nodal loads can be expressed as

$$\begin{bmatrix} Equivalent\ load\ at\ the\ left\ node \\ Equivalent\ load\ at\ the\ central\ node \\ Equivalent\ load\ at\ the\ right\ node \end{bmatrix} = \frac{ql}{6} \begin{bmatrix} 1 \\ 4 \\ 1 \end{bmatrix} \tag{2.15}$$

The flowchart for the computation of the element stiffness matrix, nodal loads and nodal displacements is given in Figure 2.2. The main MATLAB® program is given in Appendix- B.

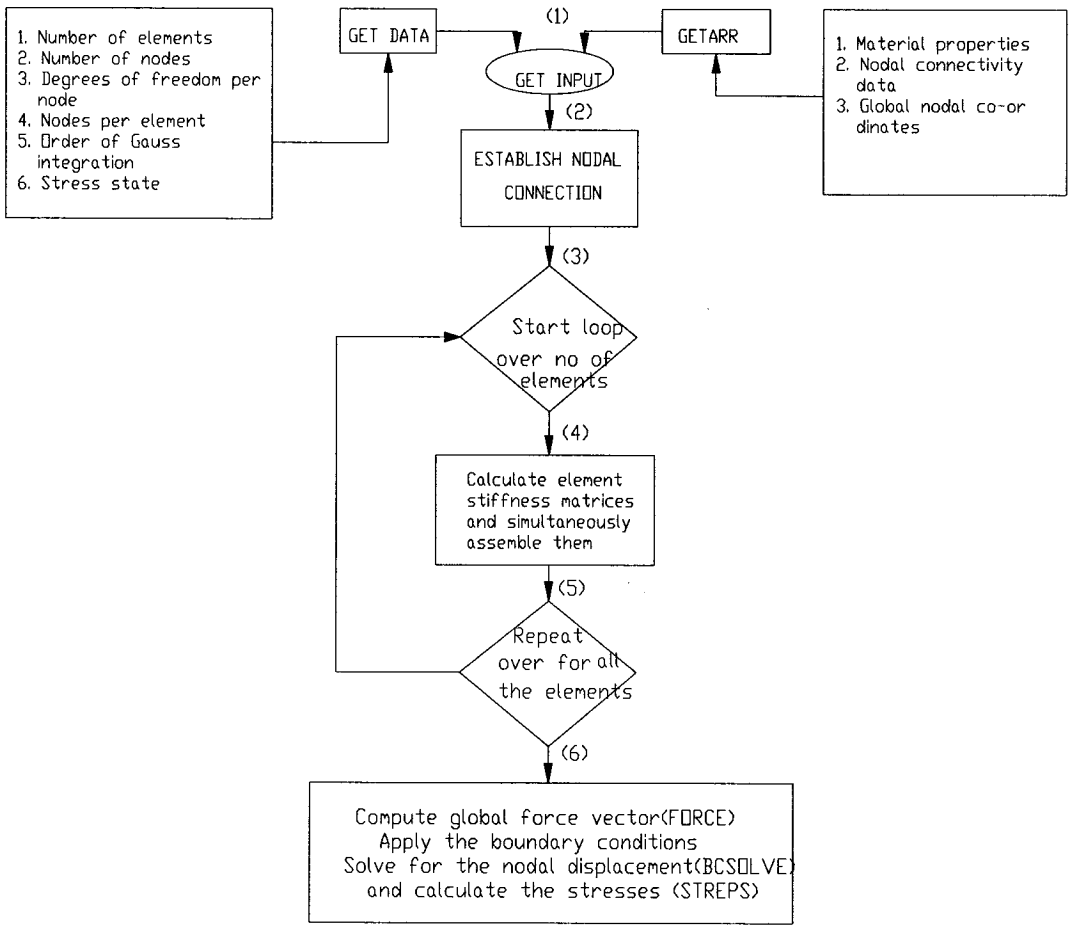

Figure 2.2 Flowchart for finite element modeling of isotropic plate

A typical finite element mesh using 200 elements with the applied loading and boundary conditions is shown in Figure 2.3

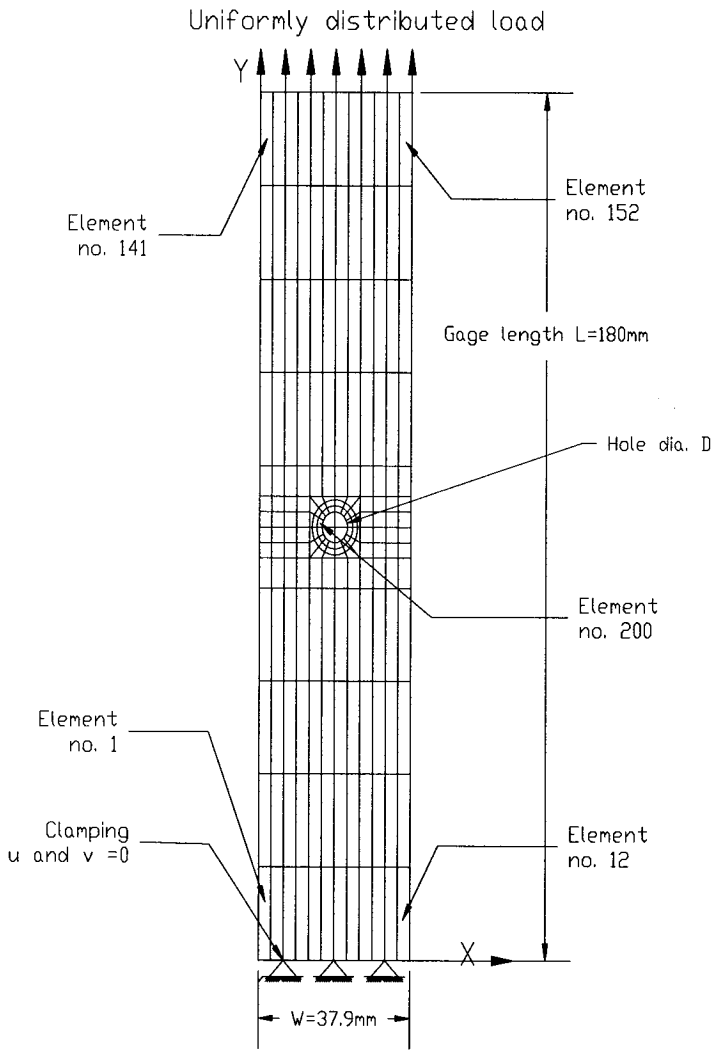

Figure 2.3 Finite element mesh using 200 elements along with the applied loading and boundary conditions

To understand the stress distribution at important nodes the finite element mesh of Figure 2.3 is enlarged and shown more clearly on Figure 2.4, where nodes from hole edge A to plate boundary B along X axis and the important boundary nodes are clearly defined.

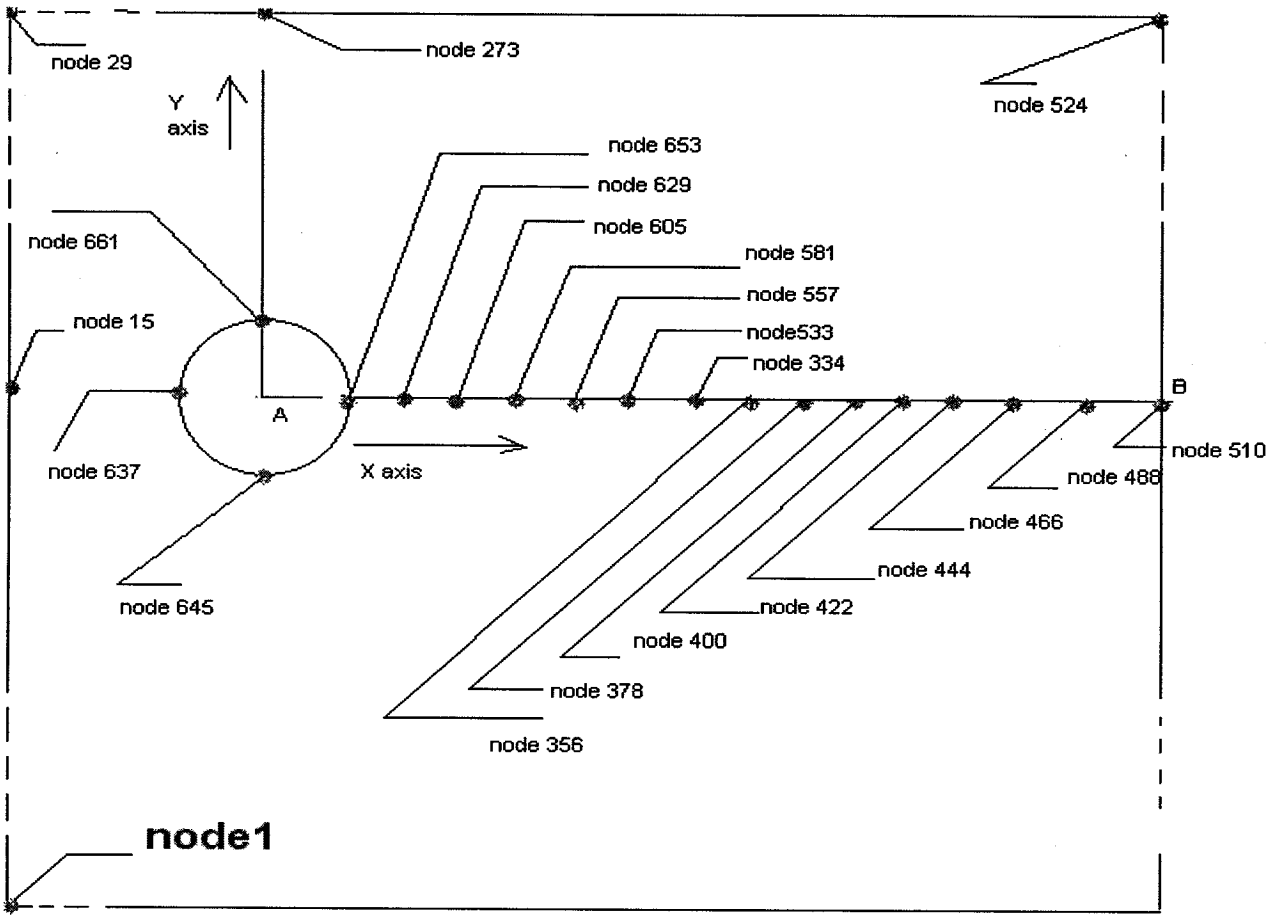

Figure 2.4 Enlarged view of the plate showing important nodes near hole and plate boundary

2.2.1 Finite Element Mesh and Example Solution for Isotropic Plate

An attempt has been made to see the convergence of solution for stresses at hole edge with the number of elements, used for finite element meshing. Solutions obtained from MATLAB® program are compared with exact solution for an isotropic plate.

As per the references [59] and [60], for an isotropic plate taking any point at a distance 'x' from the center of the hole, the normal stress at that point from the exact solution is given as follows:

$$\sigma_y = \frac{\sigma}{2}\left(2 + \frac{r^2}{x^2} + 3\frac{r^4}{x^4}\right) \tag{2.16}$$

where σ is the remote applied stress, 'x' is the distance measured along x axis and 'r' is the radius of the hole. It is found that maximum stress occurs at a distance 'x=r', which is at the edge of the hole boundary. Thus,

$$\sigma_y = 3\sigma \tag{2.17}$$

For validating the program and also to see the convergence in stresses with the increase of finite elements in the mesh, an isotropic plate with a hole of diameter 6.35 mm, gage length 180mm, width 37.9mm and thickness 2mm is considered. Dimension of the plate is chosen by keeping conformity with the dimension of the composite laminate that will be used to do the tensile test in uni-axial mode, which has been discussed in Chapter 3. The dimensions used for composite laminate testing are based on previous work [2-3]. Material properties assumed are as follows: Young's modulus 210 GPa and Poisson's ratio 0.3. A uniformly distributed load of 1.5 x 10^6 N/m is applied on the top edge of the plate and appropriate boundary conditions are imposed which are already described in Figure 2.3.

At first 48 elements are used to mesh the entire isotropic plate. After that the number of elements used for meshing is increased to 80 and finally to 200. The value of stress σ_y at the hole edge with the increase of number of elements is given in Table 2.1.

Total no. of Elements used	MATLAB® results	Exact solution	Difference
	σ_y (GPa)	σ_y (GPa)	%
48	1.991	2.250	11.51
80	2.008	2.250	10.75
200	2.132	2.250	5.24

Table 2.1 Comparison of stress σ_y at hole edge in an isotropic plate obtained by using different meshes in MATLAB® program and exact solution

From Table 2.1, one can see how the solutions for stress σ_y converge with exact solution with increase in the number of elements. Difference between MATLAB® program result and exact solution reduces to 5.24% from 11.51%, when the number of elements increases from 48 to 200. Thus, entire finite element analysis in the present work will be done by using 200 elements with total nodes of 668.

In Tables 2.2 and 2.3, displacement values obtained at the plate boundary and hole edges using MATLAB® program and ANSYS® solution are listed respectively. Displacements in the X and Y (loading) directions are denoted by u and v respectively.

Analysis in ANSYS® software is conducted using plane82 element, which is 8 node quadrilateral, same type that is used for MATLAB® program. An attempt is made to keep the number of elements near 200. For ANSYS® analysis, plane stress case with thickness is considered.

Node near the plate boundary	MATLAB® Results		ANSYS® Results	
	u (mm)	v(mm)	u(mm)	v(mm)
15	0.02536	0.3241	0.0255	0.3238
29	0.0203	0.6501	0.0203	0.6504
273	0.0000	0.6501	0.00001	0.6504
524	-0.0203	0.6501	-0.0203	0.6504
510	-0.02536	0.3241	-0.0255	0.3248

Table 2.2 Displacement values obtained for an isotropic plate near plate boundary using MATLAB® program and ANSYS® solution.

Node near the hole boundary	MATLAB® results		ANSYS® solution	
	u (mm)	v(mm)	u(mm)	v(mm)
653 (Hole right edge)	-0.01202	0.3241	-0.01235	0.3243
661 (Hole top edge)	0	0.3588	0	0.3595
637 (Hole left edge)	0.0120	0.3241	0.01235	0.3244
645 (Hole bottom edge)	0	0.2894	0	0.2892

Table 2. 3 Displacement values obtained for an isotropic plate near hole boundary using MATLAB® program and ANSYS® solution.

From Tables 2.2 and 2.3, one can see that the variations in nodal displacements in MATLAB® program and ANSYS® solution are around 1-2% only.

Nodal stresses (σ_y) from hole edge A to plate boundary B in the loading direction obtained by using MATLAB® program, and exact and ANSYS® solutions are listed in Table 2.4.

Global Node	MATLAB® results	Exact solution	ANSYS® solution
	Stress σ_y (GPa)	Stress σ_y (GPa)	Stress σ_y (GPa)
653	2.132	2.250	2.291
629	1.658	1.634	**
605	1.349	1.319	1.367
581	1.148	1.138	**
557	1.044	1.034	1.036
533	0.978	0.962	**
334	0.869	0.914	0.929
356	0.788	0.839	0.815
378	0.769	0.805	**
400	0.753	0.788	0.792
422	0.751	0.778	0.788
444	0.7502	0.771	**
466	0.7501	0.767	0.771
488	0.75004	0.764	**
510	0.7500	0.761	0.726

** *There is no node in ANSYS® at the corresponding position.*

Table 2.4 Nodal stress values obtained for a isotropic plate near hole boundary using MATLAB® program, exact solution and ANSYS® solution.

The nodal stresses (σ_y) from hole edge A to plate boundary B along X axis at different nodal positions are plotted against corresponding nodal distances and are shown in Figure 2.5.

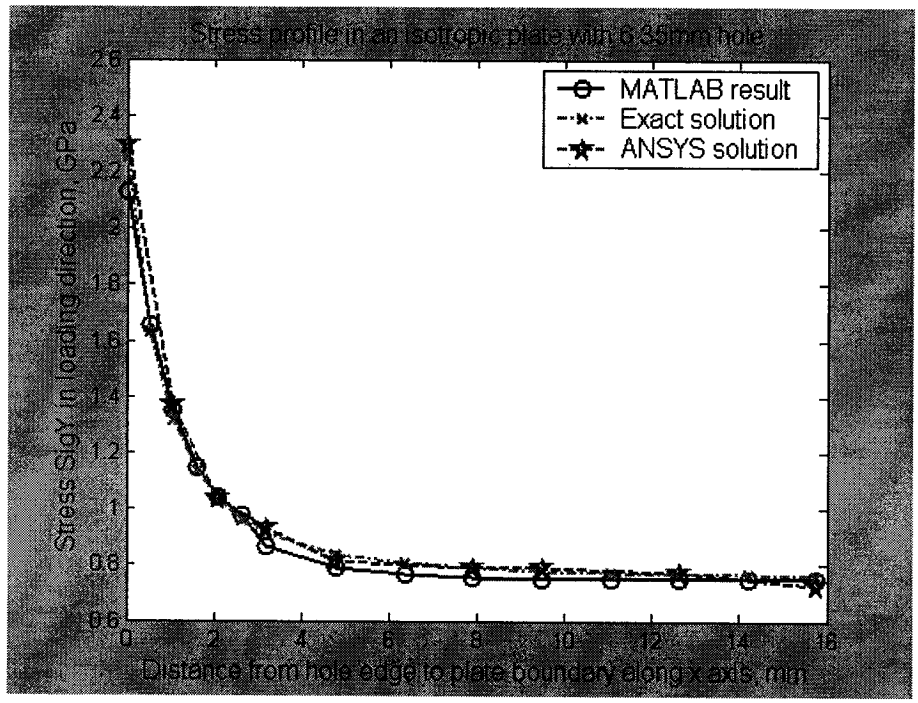

Figure 2.5 Stress profile in an isotropic plate with a hole of diameter 6.35 mm, from hole edge A to plate boundary B along x axis

In Table 2.4 nodal stress values from hole edge A to plate boundary B are given according to their positions in the plate. From those values one can see that stress obtained in MATLAB® program are very close to the exact and ANSYS® solutions. Maximum differences between MATLAB® and exact solutions for all the stresses are in the range of 1 to 6 %. Maximum differences between MATLAB® and ANSYS® solutions are in the range of 2 to 6%.

Stress concentration factor (SCF) is well defined for uniform uniaxial loading as the local stress divided by the applied stress. In Figure 2.6, stress concentration factors at various

nodal positions are plotted against the corresponding nodal distances from hole edge A along X axis.

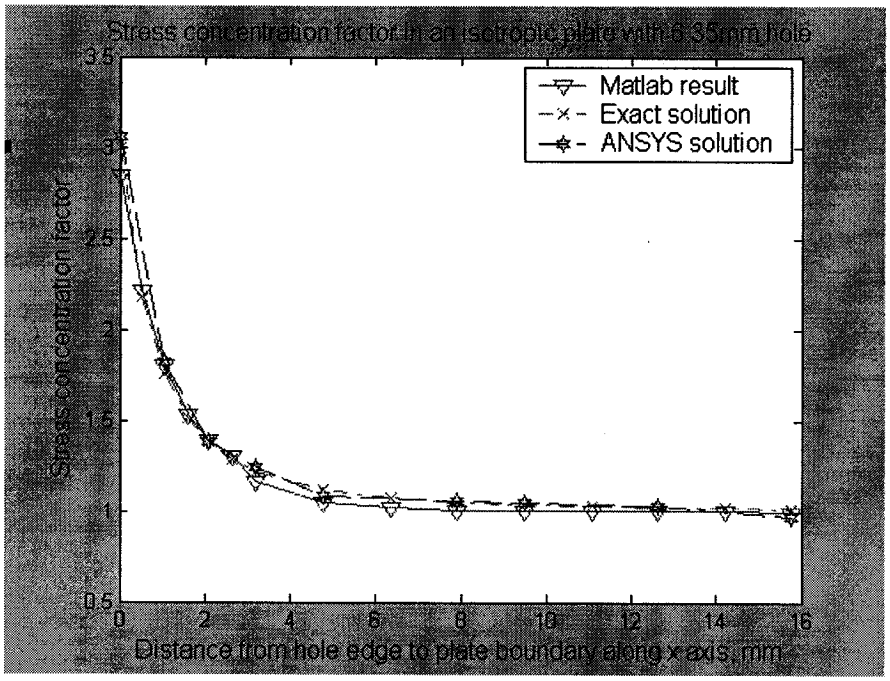

Figure 2.6 Stress concentration effect in an isotropic plate with 6.35 mm hole from hole edge A to plate boundary B along x axis

From Figures 2.5 and 2.6, one can also see that maximum stress concentration effect is at hole edge A, with SCF values of 2.84, 3.0 and 3.05 respectively in MATLAB® program, exact and ANSYS® solutions. Maximum stress value at hole edge A in MATLAB®, exact and ANSYS® solutions are respectively 2.132 GPa, 2.250 GPa and 2.291 GPa.

2.3 Finite Element Formulation for Composite Laminate

The constitutive equation of a laminated plate according to first order theory is given by [61]

$$\begin{Bmatrix} N_x \\ N_y \\ N_{xy} \\ M_x \\ M_y \\ M_{xy} \end{Bmatrix} = \begin{bmatrix} A_{11} & A_{12} & A_{16} & B_{11} & B_{12} & B_{16} \\ & A_{22} & A_{26} & & B_{22} & B_{26} \\ symm & & A_{66} & symm & & B_{66} \\ B_{11} & B_{12} & B_{16} & D_{11} & D_{12} & D_{16} \\ & B_{22} & B_{26} & & D_{22} & D_{26} \\ symm & & B_{66} & symm & & D_{66} \end{bmatrix} \begin{Bmatrix} \varepsilon_x^o \\ \varepsilon_y^o \\ \gamma_{xy}^o \\ \kappa_x \\ \kappa_y \\ \kappa_{xy} \end{Bmatrix} \tag{2.18}$$

In a concise form we can write the above equation as

$$\begin{Bmatrix} N \\ M \end{Bmatrix} = \begin{bmatrix} A & B \\ B & D \end{bmatrix} \begin{Bmatrix} \varepsilon \\ \kappa \end{Bmatrix} \tag{2.19}$$

For symmetric laminate Axial-Bending coupling stiffness matrix [B] is a null matrix; so for axial load there is no coupling between tension and bending. Thus for a plate loaded in tension, constitutive equation reduces to

$$\{N\} = [A]\{\varepsilon\} \tag{2.20}$$

where, the co-efficient of axial stiffness matrix [A] can be written as

$$A_{ij} = \sum_{k=1}^{n} Q_{ij}^k (h_k - h_{k-1}) \tag{2.21}$$

with i,j = 1,2,6 and k=1,2,6. Further Q_{ij} denotes transformed reduced stiffness matrix coefficient.

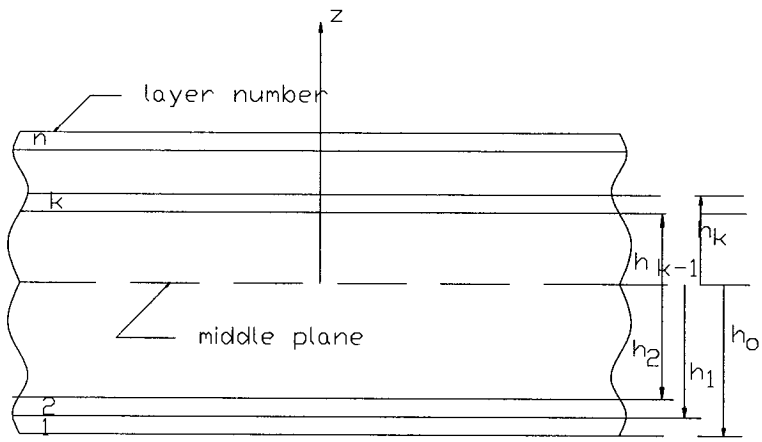

Figure 2.7 Orientation of layers in a laminate with respect to mid plane

In the case of multilayer laminate the total forces are obtained by summing the contribution from all layers. Thus for the laminate with n layers, as shown in Figure 2.7, the forces can be written as

$$\begin{Bmatrix} N_x \\ N_y \\ N_{xy} \end{Bmatrix} = \sum_{k=1}^{n} \int_{h_{k-1}}^{h_k} \begin{Bmatrix} \sigma_x \\ \sigma_y \\ \tau_{xy} \end{Bmatrix}_k dz \tag{2.22}$$

Equation (2.20) can be rewritten as follows

$$\begin{Bmatrix} N_x \\ N_y \\ N_{xy} \end{Bmatrix} = \begin{bmatrix} A_{11} & A_{12} & A_{16} \\ A_{12} & A_{22} & A_{26} \\ A_{16} & A_{26} & A_{66} \end{bmatrix} \begin{Bmatrix} \varepsilon_x^o \\ \varepsilon_y^o \\ \gamma_{xy}^o \end{Bmatrix} \tag{2.23}$$

Inversion of equation (2.23) gives

$$\begin{Bmatrix} \varepsilon_x^o \\ \varepsilon_y^o \\ \gamma_{xy}^o \end{Bmatrix} = \begin{bmatrix} a_{11} & a_{12} & a_{16} \\ a_{12} & a_{22} & a_{26} \\ a_{16} & a_{26} & a_{66} \end{bmatrix} \begin{Bmatrix} N_x \\ N_y \\ N_{xy} \end{Bmatrix} \tag{2.24}$$

in which [a] is the extensional laminate compliance matrix, which is the inverse of the corresponding stiffness matrix, [A], as given below

$$[a] = [A]^{-1} \tag{2.25}$$

The average laminate stresses can be defined as

$$\overline{\sigma_x} = \frac{N_x}{h} \; ; \qquad \overline{\sigma_y} = \frac{N_y}{h} \; ; \qquad \overline{\tau_{xy}} = \frac{N_{xy}}{h} \tag{2.26}$$

in which h is the laminate thickness.

So, equation (2.24) can be rewritten in terms of average laminate stresses as

$$\begin{Bmatrix} \varepsilon_x^o \\ \varepsilon_y^o \\ \gamma_{xy}^o \end{Bmatrix} = \begin{bmatrix} ha_{11} & ha_{12} & ha_{16} \\ ha_{12} & ha_{22} & ha_{26} \\ ha_{16} & ha_{26} & ha_{66} \end{bmatrix} \begin{Bmatrix} \frac{N_x}{h} = \overline{\sigma_x} \\ \frac{N_y}{h} = \overline{\sigma_y} \\ \frac{N_{xy}}{h} = \overline{\tau_{xy}} \end{Bmatrix} \tag{2.27}$$

By superposition of the three loadings σ_x , σ_y and τ_{xy} the following stress-strain relation can be obtained in terms of engineering constants.

$$\begin{Bmatrix} \varepsilon_x \\ \varepsilon_y \\ \gamma_{xy} \end{Bmatrix} = \begin{bmatrix} \frac{1}{E_x} & -\frac{\nu_{yx}}{E_y} & -\frac{1}{G_{xy} m_x} \\ -\frac{\nu_{xy}}{E_x} & \frac{1}{E_y} & -\frac{1}{G_{xy} m_y} \\ -\frac{m_x}{E_x} & -\frac{m_y}{E_y} & \frac{1}{G_{xy}} \end{bmatrix} \begin{Bmatrix} \sigma_x \\ \sigma_y \\ \tau_{xy} \end{Bmatrix} \tag{2.28}$$

where E_x, ν_{xy} and $m_x = -\frac{\gamma_{xy}}{\varepsilon_x}$ are the x directional modulus, Poisson's ratio and shear

coupling coefficient respectively and E_y , ν_{yx} and $m_y = -\frac{\gamma_{yx}}{\varepsilon_y}$ are the y directional modulus, Poisson's ratio and shear coupling coefficient respectively.

The equivalent elasticity matrix [E] for a composite laminate can be calculated by inverting equation (2.27) as

$$\begin{Bmatrix} \overline{\sigma_x} \\ \overline{\sigma_y} \\ \overline{\tau_{xy}} \end{Bmatrix} = \begin{bmatrix} ha_{11} & ha_{12} & ha_{16} \\ ha_{12} & ha_{22} & ha_{26} \\ ha_{16} & ha_{26} & ha_{66} \end{bmatrix}^{-1} \begin{Bmatrix} \varepsilon_x^o \\ \varepsilon_y^o \\ \gamma_{xy}^o \end{Bmatrix} \tag{2.29}$$

Now comparing equation (2.29) with equation (2.4) for calculating the elasticity matrix [E], one gets

$$[E] = \begin{bmatrix} ha_{11} & ha_{12} & ha_{16} \\ ha_{12} & ha_{22} & ha_{26} \\ ha_{16} & ha_{26} & ha_{66} \end{bmatrix}^{-1} \tag{2.30}$$

The elasticity matrix thus obtained will be incorporated in the finite element formulation through equation (2.10).

2.4 Stochastic Finite Element Analysis of Composite Plate

Composite laminates exhibit significant randomness in their material property due to the variations in fiber volume fraction, void content, fiber orientation angles in various layers, thickness of lamina, etc. As a result, tests on a single specimen provide a specific value for each material parameter and mechanical property. However when a number of specimens are tested, randomly distributed values are obtained for the same material property. Therefore the analysis of the laminate has to be performed based on a

probabilistic approach so that a stochastic description of the material property can be provided.

2.4.1 Stochastic Field Modeling of Material Properties

The material properties are modeled in terms of two dimensional homogeneous stochastic processes that have zero mean. To this end, the procedure employed in the earlier works [3,52] is used here. Further, for the purpose of clarity, the procedure is presented in detail.

Material properties such as Young's modulus, Poisson's ratio and shear modulus which have been obtained from experiments (the details will be given in Chapter 3), are considered here for stochastic process. Sample realizations are obtained at each Gauss point in the finite element mesh. Using the sample realizations of material properties at each Gauss point, the stochastic elasticity matrix, [E], is calculated for each Gauss point. Stochastic elasticity matrix thus generated is incorporated in the determination of the element stiffness matrix. The flow chart for computing the stochastic fields of the elastic constants is given in Figure 2.8.

Variations of the material properties such as the Young's modulus, Poisson's ratio and shear modulus are brought about using a fluctuating component a(X) associated with a material property, which has zero mean. For instance, the stochastic field of the Young's modulus in the fiber direction (E_1) is described below and a similar procedure is adopted for the other material properties such as E_2, G_{12}, ν_{12} and ν_{21} that are required for stochastic finite element analysis.

$$E_1 = \overline{E_1}[1 + a(X)] \quad ; \quad E\,[a(X)] = 0 \tag{2.31}$$

The auto-correlation function is given by [50]

$$R_{aa}(\zeta) = E[a(X)a(X+\zeta)] \tag{2.32}$$

where, $X = [x, y]^T$ indicates the position vector and $\zeta = [\zeta_x, \zeta_y]^T$ represents the separation vector between two points X and (X + ζ). Material property is considered to vary at each Gauss point. Thus if n represents the number of finite elements present in the structure, and m represents the order of Gauss quadrature, then there are N (equal to m x n) material property values associated with the structure. Only the fluctuating component of the homogeneous stochastic field is considered to model the material property variations around the expected value. These N values $a_i = a(X_i)$, (i = 1,2,3.... N) are correlated random variables with zero mean. Also X_i corresponds to the location of each Gauss point. Their correlation characteristics can be specified in terms of the covariance matrix C_{aa} of order N x N, whose ijth component is given by

$$C_{ij} = Cov\lfloor a_i a_j \rfloor = E\lfloor a_i a_j \rfloor = R_{aa}(\zeta_{ij}); \quad \text{i,j= 1,2,3 ..... ,N} \tag{2.33}$$

in which $\zeta_{ij} = (X_j - X_i)$ is the separation distance between the Gauss points i and j. Now a vector $\{a\} = [a_1 \quad a_2 \quad a_3 \quad .... \quad a_N]^T$ can be generated by

$$\{a\} = [L]\ \{Z\} \tag{2.34}$$

in which $\{Z\} = [Z_1 \quad Z_2 \quad Z_3 \quad .... \quad Z_N]^T$ is a vector consisting of N independent Gaussian random variables with zero mean and unit standard deviation, and L is a lower triangular matrix obtained by Cholesky decomposition of the covariance matrix $[C_{aa}]$. Thus

$$[L][L]^T = [C_{aa}] \tag{2.35}$$

Once the Cholesky decomposition is accomplished, different sample vectors of {a} are easily obtained by generating different samples for the Gaussian random vectors {Z}. The correlation properties of the stochastic fields representing the fluctuating components of the material properties are expressed using the Markov correlation model, also known as the First-order autoregressive model. The choice of this model in this work is due to its wide use in the literature [52].

2.4.2 Markov Model

The First-order autoregressive correlation model or the Markov model is given by

$$R_{aa}(\zeta) = s_o^{\,2} \exp\left[-\left(\frac{|\zeta|}{c}\right)\right] \tag{2.36}$$

in which s_o is the standard deviation of the stochastic field a(X) and further c is a positive parameter called correlation length, which is defined such that correlation disappears more slowly when c is large. The stochastic field a(X) represents the deviatoric components of the material property with auto correlation function as given in equation (2.36). The stochastic field value for each Gauss point is represented by the value of a_g of a(X) at the Gauss point X_g of the structure i.e., $a_g = a(X_g)$.

The Young's modulus along the fiber direction can now be assumed to have a distribution as given by the vector {a} and can be represented by

$$E_{1g} = E_{1m}(1+a_g) \tag{2.37}$$

where, E_{1g} is the value of Young's modulus in the fiber direction at a Gauss point. Moreover E_{1m} is the mean value of the Young's modulus in the fiber direction.

Young's modulus in the transverse direction,

$$E_{2g} = E_{2m}(1+b_g) \tag{2.38}$$

Major Poisson's ratio,

$$\nu_{12g} = \nu_{12m}(1+c_g) \tag{2.39}$$

Shear modulus,

$$G_{12g} = G_{12m}(1+d_g) \tag{2.40}$$

in which E_{2m} is the mean value of the Young's modulus in the transverse direction and further , ν_{12m} and G_{12m} are the mean values of the major Poisson's ratio and the shear modulus respectively.

It should be noted here that the standard deviations of a_g, b_g, c_g and d_g represent the coefficients of variation of the material properties E_{1g}, E_{2g}, ν_{12g} and G_{12g}. Also the variation of the ply orientation angle, θ_g and the ply thickness t_g are evaluated in a manner similar to equations (2.37 - 2.40) as

$$\theta_g=\theta_m(1+e_g) \tag{2.41}$$

$$t_g=t_m(1+f_g) \tag{2.42}$$

in which θ_m and t_m are the mean values of the ply orientation angle and ply thickness respectively. The assumption of Gaussian distribution implies the possibility of generating negative values for the material properties. In order to avoid this difficulty, the values of the random variable, a_g in the case of Monte-Carlo simulation are confined to the range

$$-1+\delta \le a_g \le 1-\delta \tag{2.43}$$

where, δ is a very small perturbation parameter.

2.4.3 Stochastic Finite Element Analysis

Sample realizations at each Gauss point in the finite element mesh are found out by applying stochastic processes using equations (2.36 - 2.40) for the material properties, like Young's modulus, shear modulus, Poisson's ratio, etc (the data for which will be obtained from experiments). A similar procedure applies to θ and t. Using the generated sample realizations of material properties at each Gauss point the stochastic elasticity matrix, [E], is calculated for each Gauss point. The stochastic elasticity matrix thus generated is incorporated into the equation (2.12) for the element stiffness matrix. The flow chart for computing the stochastic fields of the elastic constants is given below in Figure 2.8.

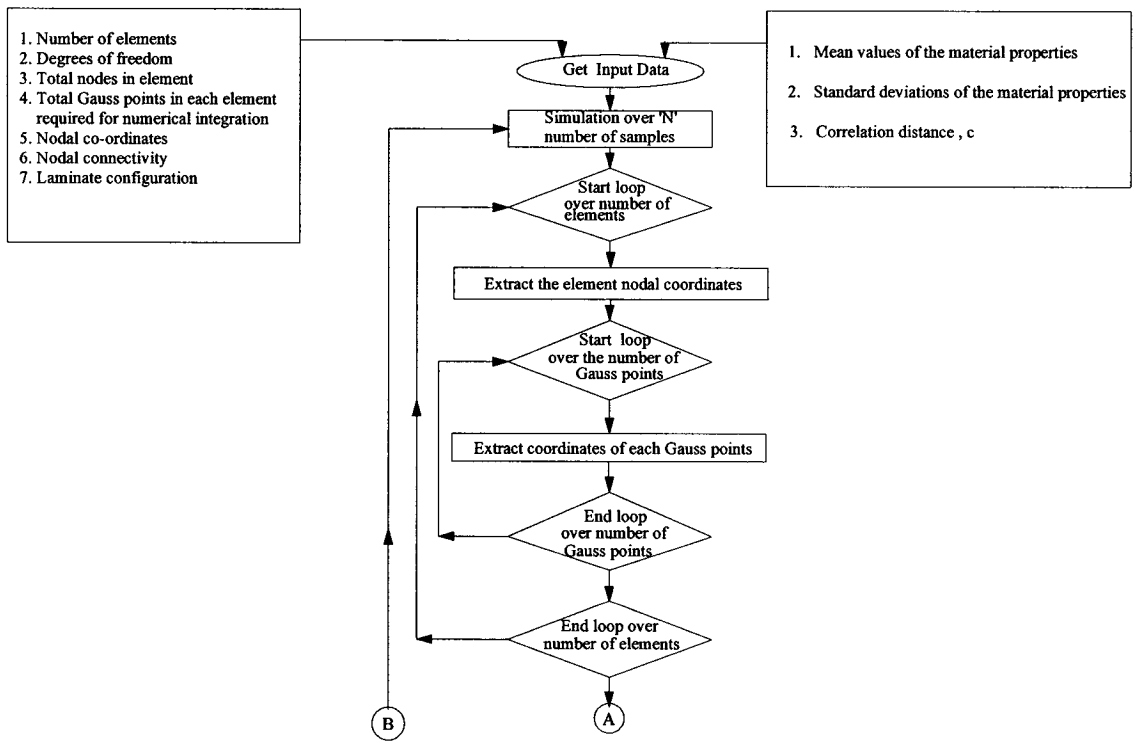

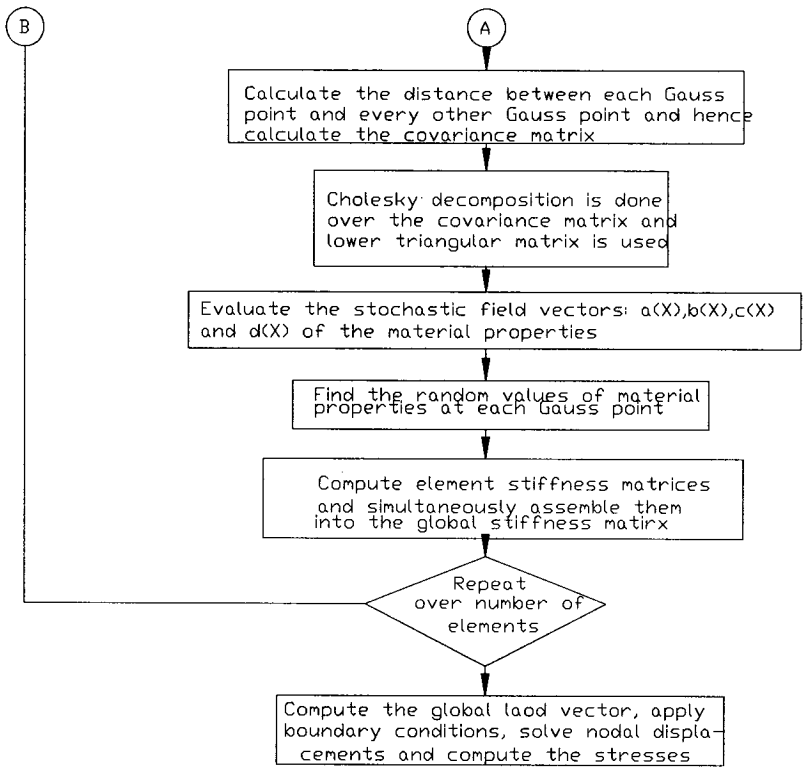

Figure 2.8 Flow chart used for the calculation of stochastic material properties, stiffness matrix, displacements and stresses for composite plate

2.5 Stress Concentration Effects in Composite Laminates

Stress concentration factor (SCF) is well defined for uniform uniaxial loading as the local stress divided by the applied stress that is

$$SCF_{\sigma y} = \frac{\sigma_y}{\sigma_o}$$

where σ_y is the local stress near hole and σ_o is the remote applied stress

The use of the SCF as a design parameter in metallic construction is widespread and the effects of hole, plate, geometry and loading configuration on the value of this parameter have been extensively characterized [6]. However, direct application of this methodology to fibrous composite laminates has produced some anomalous results, such as the "hole size effect". These anomalies apparently stem from the fact that the methodology is based on the conditions at a point on the hole boundary, while the strength of a perforated composite laminate seems related to the in-plane elastic stresses within a region adjacent to the hole boundary [55]. Thus the SCF is not itself an adequate measure of strength for a composite laminate containing a circular hole; such a measure must be based on a more complete description of the stresses near the hole.

The transverse stress components $\sigma_y(x,0)$ along the x axis in an infinite orthotropic composite laminate containing a circular hole can be written as [18]

$$\sigma_y(x,0)=\sigma_o\left\{1+\mathrm{Re}\frac{1}{\mu_1-\mu_2}\left[\frac{-\mu_2(1-i\mu_1)}{\sqrt{(\lambda^2-1-\mu_1^2)}\left(\lambda+\sqrt{\lambda^2-1-\mu_1^2}\right)}+\frac{\mu_1(1-i\mu_2)}{\sqrt{(\lambda^2-1-\mu_2^2)}\left(\lambda-1-\mu_2^2\right)}\right]\right\} \tag{2.44}$$

where, σ_o is the applied stress at infinity, $\lambda=\frac{x}{r}$; r is the radius of the hole, μ_1 and μ_2 are the roots of the characteristic equation given below

$$a_{22}\mu^4-2a_{26}\mu^3+(2a_{12}+a_{66})\mu^2-2a_{16}\mu+a_{11}=0 \tag{2.45}$$

Coefficients a_{11}, a_{12}, a_{16}, a_{22}, a_{26} and a_{66} are the components of extensional laminate compliance matrix obtained from equation (2.25).

Only the principal roots should be chosen, i.e., two of the four roots that have a positive imaginary part.

2.5.1 Finite Width Correction (FWC) Factor for Composite Laminates

The finite-width correction factor is a scale factor which is applied to multiply the notched infinite plate solution to obtain the solution for the notched finite plate. According to the definition of the FWC factor stated above, and an assumption that the normal stress profile for a finite plate is identical to that for an infinite plate except for an FWC factor the following relation is obtained:

$$\frac{K_T}{K_T^{\infty}}\sigma_y^{\infty}(x,0) = \sigma_y(x,0) \tag{2.46}$$

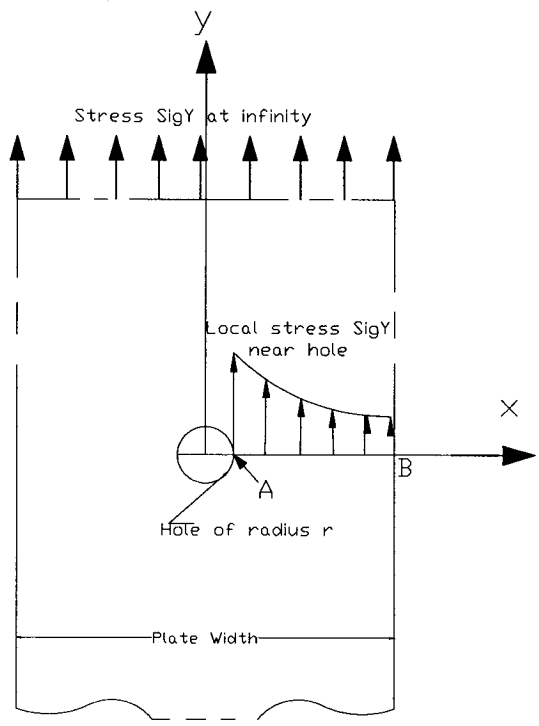

Figure 2.9 Stress distributions near a circular hole in an infinite orthotropic composite plate

where, $\frac{K_T}{K_T^\infty}$ is the finite width correction factor; K_T denotes the stress concentration factor at point A (in Figure 2.9) along X axis for a finite width plate and K_T^∞ for an infinite width plate. The parameter σ_y is the normal stress acting along y-axis for a finite width plate and σ_y^∞ is the normal stress acting along y-axis for an infinite width plate.

For orthotropic laminate containing a central circular hole, the derivation of the FWC factor is based on an approximate stress analysis. The solution for the inverse of the FWC factor is given by [1]:

$$\frac{K_T^\infty}{K_T} = \frac{3(1-\frac{2r}{w})}{2+(1-\frac{2r}{w})^3} + \frac{1}{2}\left(\frac{2r}{w}M\right)\left(K_T^\infty - 3\right)\left[1-\left(\frac{2r}{w}M\right)^2\right] \tag{2.47}$$

where, M is the magnification factor, defined as:

$$M^2 = \frac{\sqrt{1-8\left[\frac{3\left(1-\frac{2r}{w}\right)}{2+\left(1-\frac{2r}{w}\right)^3}-1\right]}-1}{2\left(\frac{2r}{w}\right)^2} \tag{2.48}$$

Also the SCF of an infinite orthotropic plate, K_T^∞, is defined by

$$K_T^\infty = 1+\sqrt{\frac{2}{A_{66}}\left(\sqrt{A_{11}A_{22}}-A_{12}+\frac{A_{11}A_{22}-A_{12}^2}{2A_{66}}\right)} \tag{2.49}$$

where, A_{ij}, i,j=1,2,6 denote the effective laminate stiffness values. Axes 1 and 2 are parallel and transverse to the loading direction respectively.

2.6 Example Applications of Finite Element Analysis for Composite Laminates

To validate the MATLAB® program, written for stochastic analysis of a composite laminate some example applications are considered below. One is a quasi-isotropic laminate $[0/90/\pm45]_{2s}$ and the other one is a matrix dominated laminate $[\pm45]_{4s}$. The nodal displacements at the plate loading end are compared with the experimental displacements for $[\pm45]_{4s}$ laminate with 6.35 mm hole and also with $[0/90]_{4s}$ laminate with 6.35 mm and 7.54 mm hole sizes. For all the example applications, a composite plate made of NCT-301 prepreg with gage length 180mm, width 37.9mm and thickness 2mm is considered. Layer thickness of the prepreg is 0.125mm. Experimental material properties of NCT-301 that are listed in Table 3.7 will be used here for all the analysis. The finite element mesh, boundary conditions and applied loading are already described in Figure 2.3. Numbering of the nodes from hole edge to plate boundary are shown in Figure 2.4.

2.6.1 Application 1

Experiments were conducted on NCT-301 material as described in Chapter 3, on different laminates with and without holes to determine their strength values. Experimental values of displacements of those laminates for different loads are listed in Tables 3.14 and 3.15. Results of those displacements are compared here with the results of MATLAB® program written for stochastic analysis of composite laminate and given in Table 2.5. Plate geometry, loading direction and node numbering at loading end are shown in Figure 2.10.

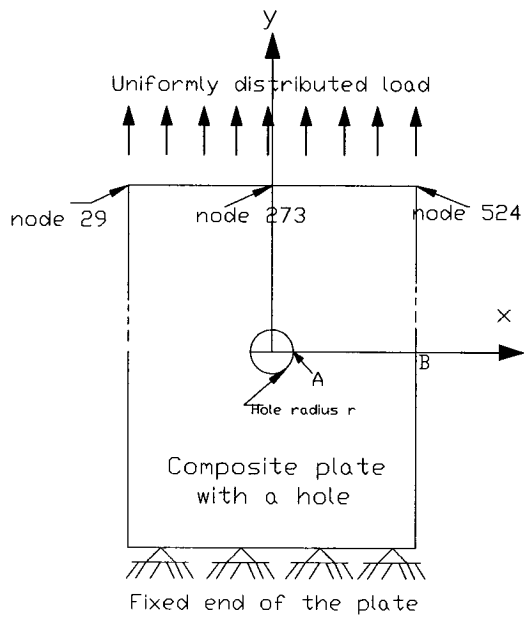

Figure 2.10 Boundary conditions, applied loading and global node numbering at the at the loading end in a composite laminate

Laminate configu-rations	Hole diameter	Applied load	Displacement at loading boundary (by experiment)	Displacements at boundary nodes 29 , 273 and 524 (by MATLAB® analysis)	Difference between MATLAB® and experim-ental results
	mm	Newtons	mm	mm	%
$[0/90]_{4s}$	6.35	38017	1.8864	1.573	16.61
$[0/90]_{4s}$	7.54	34932	1.9468	1.521	21.87
$[\pm 45]_{4s}$	6.35	3000	0.5382	0.5513	2.43

Table 2.5 Comparison of nodal displacements at the plate loading end in two different laminates obtained using both MATLAB® program and experiment.

From Table 2.5, one can see that there is a maximum difference in displacements of 21.87% for cross ply laminate and 2.3% for $[\pm 45]_{4s}$ laminate. Difference of this amount between experimental and analytical analysis is acceptable. Because in doing experiments many practical problems, such as, keeping the geometry of plate accurate in dimension during cutting, keeping the fiber angle in different layers accurate during hand lay up, drilling a notch without creating damage in the laminate, misalignment in the machine during testing, keeping fiber volume fraction constant, the effect of cross head displacement, etc., which all together lead to this error.

2.6.2 Application 2

A quasi-isotropic laminate with $[0/90/\pm 45]_{2s}$ configuration and a hole of diameter 6.35 mm at the center of the laminate is considered for the analysis. A uniformly distributed load of $1x10^6$ Newtons/meter is applied at the top edge of the plate and the plate is clamped at the bottom. Nodal stresses from hole edge A to plate boundary B are found out by using MATLAB® program. The corresponding nodal stresses are also obtained using exact solution given by equation (2.16).

Simulation is carried out over 300 laminates and the results are shown in Table 2.6 and in Figures 2.10 and 2.11. Nodal stresses at the corresponding nodes given by exact solution are also listed in Table 2.6 in a different column.

Global Node	MATLAB® results	Exact solution
	Stress σ_y (GPa)	Stress σ_y (GPa)
653	1.5417	1.5477
629	1.2425	1.2576
605	1.0473	1.0683
581	0.8303	0.8490
557	0.7214	0.7347
533	0.6553	0.6615
334	0.6224	0.6288
356	0.5724	0.5770
378	0.5495	0.5541
400	0.5368	0.5422
422	0.5270	0.5352
444	0.5192	0.5307
466	0.5096	0.5276
488	0.4976	0.5254
510	0.4826	0.5238

Table 2.6 Nodal Stress distribution from the hole edge A to the plate boundary B in a $[0/90/\pm45]_{2s}$ laminate with 6.35 mm hole obtained using MATLAB® program and exact solution

From Table 2.6, one can see that maximum stress occurs at hole edge A, at node 653 that is 1.5417 GPa and the corresponding exact stress at that point is 1.5477 GPa. There is a difference of 0.39% only.

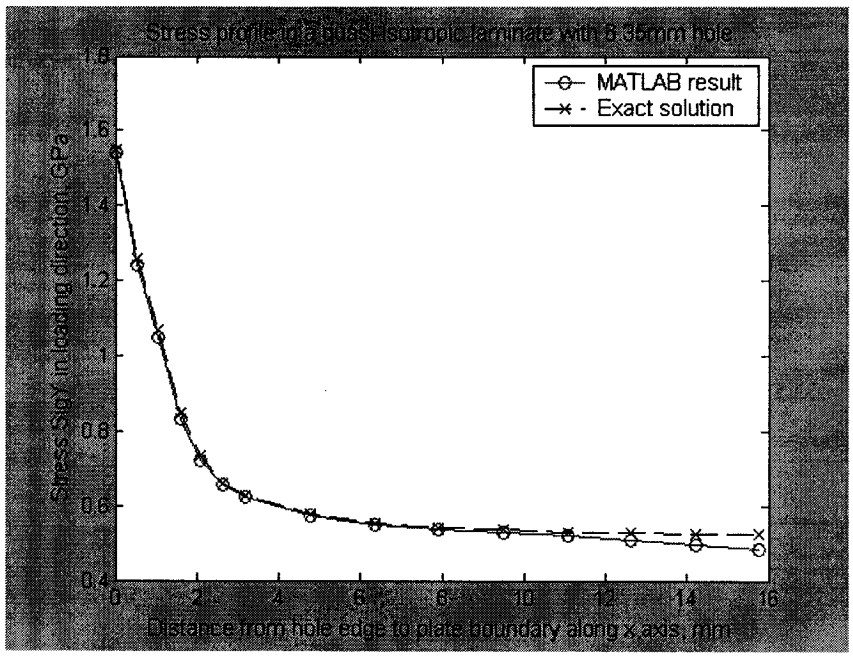

Figure 2.11 Stress profile in a $[0/90/\pm45]_{2s}$ laminate with 6.35 mm hole, from hole edge A to plate boundary B along x axis

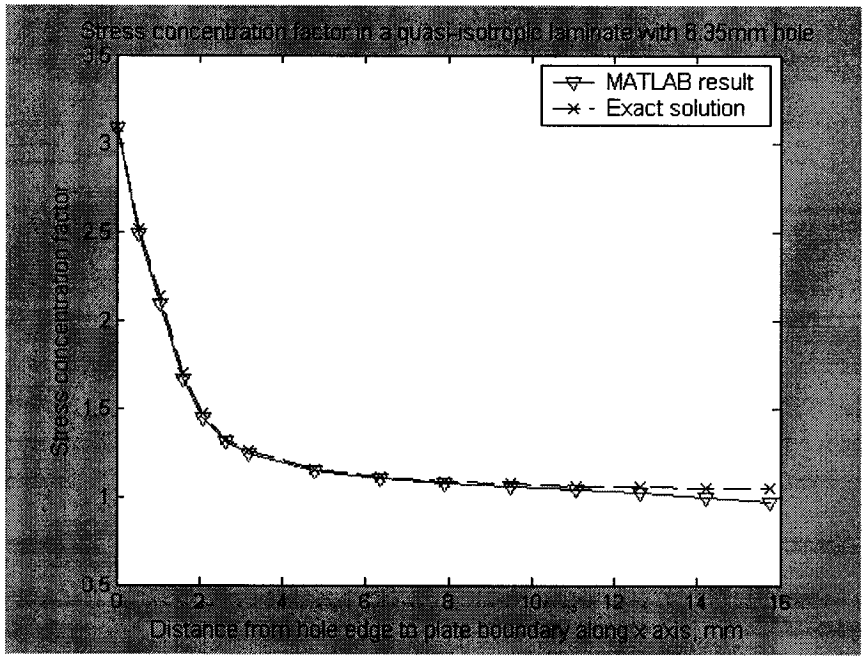

Figure 2. 12 Stress concentration effect in a $[0/90/\pm45]_{2s}$ laminate with 6.35 mm hole, from hole edge A to plate boundary B along x axis

From Figure 2.12, one can see that stress concentration factor is maximum at hole edge A that is 3.08 in MATLAB® program and 3.09 by exact solution. One can also see from Figure 2.11, how gradually the stress concentration effect goes away from hole edge to the plate boundary for quasi-isotropic laminate. From all these results one can conclude that the MATLAB® results are in a good correlation with exact solution.

2.6.3 Application 3

As another example [11], we consider a laminate of configuration $[\pm 45]_{4s}$ with a hole of 6.35 mm at the center. The boundary conditions and geometry of the plate are same, as described at the beginning of Section 2.6. A distributed load of 0.095 MN/m is applied on the top edge of the laminate and the nodal stresses are determined by MATLAB® program near the hole boundary and compared with closed form and reference solutions in Table 2.6. Choice of the load was based on experiments done on this type of laminate in Chapter 3.

Global Node	MATLAB® results	Exact Solution	Reference results from James and Whitney [5]
	Stress σ_y	Stress σ_y	Stress σ_y
	GPa	GPa	GPa
653	0.09633	0.09098	0.09098
629	0.10120	0.09620	0.10445
605	0.10263	0.09870	0.09964
581	0.08862	0.08915	0.08313
557	0.07781	0.07347	0.07119
533	0.06575	0.06290	0.06294
334	0.06072	0.05877	0.05925

356	0.05373	0.05314	0.05358
378	0.05218	0.05097	0.05121
400	0.05042	0.04989	0.05002
422	0.04871	0.04926	0.04934
444	0.04785	0.04886	0.04891
466	0.04730	0.04859	0.04862
488	0.04687	0.04839	0.04842
510	0.04648	0.04825	0.04826

Table 2.7 Nodal Stress distribution in a $[\pm 45]_{4s}$ laminate with 6.35 mm hole obtained using MATLAB® program, exact and reference solutions.

Stress profile and stress concentration factor for the laminate are plotted in Figures 2.13 and 2.14 respectively.

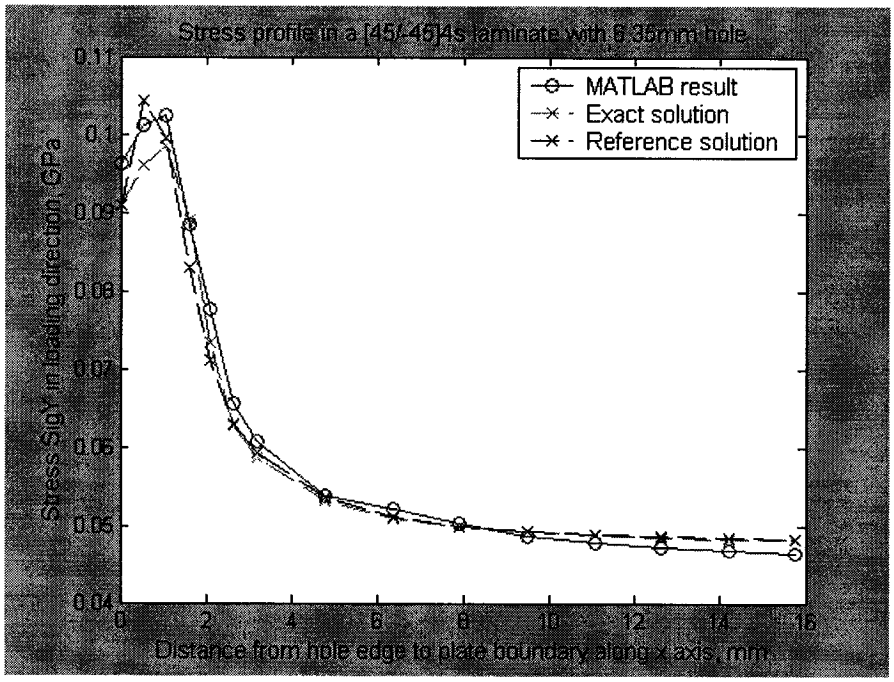

Figure 2.13 Stress profile in a $[\pm 45]_{4s}$ laminate with 6.35 mm hole

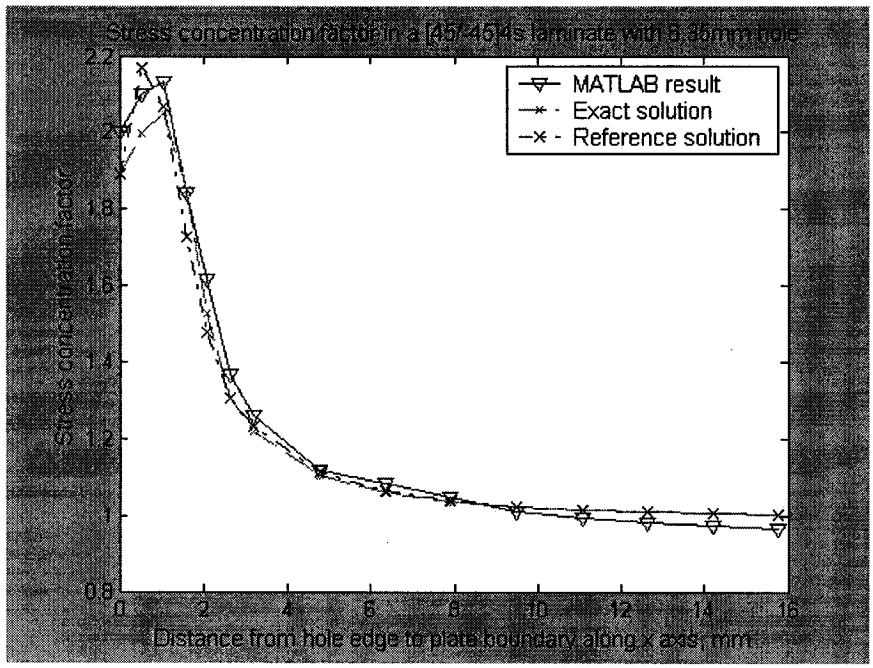

Figure 2. 14 Stress concentration effect in a $[\pm 45]_{4s}$ laminate with 6.35m hole

From Table 2.7 and Figures 2.13 and 2.14, one can see that the maximum stress for $[\pm 45]_{4s}$ laminate does not occur at the edge of the hole A. For MATLAB® program, and exact and reference solutions maximum stress occurs at 0.635 mm away from the hole edge at node 605. Value of stress at that node by MATLAB® is 0.10263 GPa and by exact and reference solutions are 0.09870 GPa and 0.09964 GPa respectively. Maximum difference in those values is 3.83%.

From Figure 2.13, one can see that the stress profile obtained by MATLAB® program is almost same in nature to that of exact and reference solutions. From Figure 2.14, one can see that stress concentration factor at hole edge A, at node 653 is 2.026, whereas at 0.635mm away from hole edge, at node 605 is 2.159. Stress concentration factor increases by a factor of 1.066 from hole edge A to the point at a distance (0.635mm) away from hole edge.

So, it is clear from all the example applications that MATLAB® program written for stochastic finite element analysis of composite laminate provides results that have very good agreement with all the experimental, exact and reference solutions.

2.7 Conclusions and Discussions

Finite element analysis of an isotropic plate under plane stress condition subjected to uniaxial tension is conducted using a MATLAB® program. Convergence of stress, with number of elements used to mesh the structure is shown in Table 2.1. Effect of stress concentration and stress profile near hole boundary are given in Table 2.4 and in Figures 2.5 and 2.6. Nodal displacements and stresses of MATLAB® results are compared with the solution that is obtained using commercial ANSYS® software and also by exact solution. It is found that the MATLAB® program results for isotropic plate have excellent agreement with the results of ANSYS® and exact solutions.

Finite element formulation for composite laminates is given in Section 2.3. Stochastic field modeling of material parameters is given in Section 2.4. Stochastic variations in material properties over the laminate are established using Markov model and sample realizations of the material properties at each and every Gauss point are obtained. Now the entire analysis is performed for number of plates.

Necessary modifications are made in the MATLAB® program written for isotropic plate, to do the stochastic analysis of composite laminates. The normal stress distribution near the hole boundary in an infinite orthotropic plate under the in-plane loading is presented. The output includes the stress distribution along the axis perpendicular to the loading direction. Finite width correction factor is used to multiply the infinite plate solution to obtain the stress distribution of a finite plate.

Example applications for composite laminates are given in Section 2.6 involving different ply configurations; stress concentration factor for each case is also calculated. Nodal displacements at the boundary of the plate obtained using MATLAB® program are also compared with experimental test data which are listed in Table 2.5.

Stress concentration factor for a quasi-isotropic laminate $[0/90/\pm45]_{2s}$ is 3.08, whereas for a $[\pm45]_{4s}$ laminate it is 2.159. It is to be noted here that in the case of composites, SCF is not the only parameter of consideration for prediction of failure of notched composite laminates. Thus, the measure of strength for a composite laminate with circular cutouts needs a more complete description of the stresses near the hole. This will be discussed in detail in Chapters 3 and 4.

CHAPTER 3

EXPERIMENTAL CHARACTERIZATION OF COMPOSITE LAMINATES

3.1 Introduction

Most modern structural systems possess a high degree of structural complexity. Therefore, when their behavior is to be predicted under various loading and environmental conditions, advanced analytical and numerical techniques are required. However, most of these applications are limited to dealing with deterministic loading and environmental conditions despite the fact that they intrinsically involved randomness and uncertainty to a considerable degree.

In the case of composite laminates, significant randomness is present. This is due to the stochastic spatial variations of properties in fiber, in matrices and at interfaces. In addition the fiber volume fraction, void content, fiber orientation angles at various plies, thickness of lamina, etc., display significant variability due to manufacturing conditions. As a result, tests on a single material specimen provide a specific value for each material parameter and mechanical property. However when a number of specimens are tested different randomly distributed values are obtained for the same material property or the material parameter.

Therefore, the analysis of composite laminates based on a probabilistic approach is more logical than the deterministic approach. When finite element analysis (FEA) is performed based on a stochastic approach, where randomness of the material property, geometry of

structure, applied loading, etc. are included , the resulting FEA is known as Stochastic finite element Analysis (SFEA). The parameters to be used in SFEA of laminates should be obtained from testing. Depending on the type, experiments are categorized into two sub groups:

1) Tensile testing of specimens to get the material properties of uni-directional prepreg or lamina

2) Tensile testing of notched and un-notched cross-ply specimens to determine the strength.

3.2 Manufacturing of Composite Laminate

In the present thesis preimpregnated NCT-301 graphite/epoxy material supplied by Newportad Company, USA is considered for experiments and analysis. Thickness of the prepreg is 0.125 mm.

The manufacturing of composite laminates can be divided into two phases:

1) Fabrication
2) Processing

In the fabrication phase the fiber reinforcement and accompanying matrix material are placed or shaped into a structural form such as a flat or curved plate, a cylinder or other body of revolution, and the like. In the present work, flat plates are made from layers or plies of preimpregnated NCT-301. During the processing phase, an autoclave is used which provides the proper level of pressure and heat to solidify and consolidate the structure.

3.2.1 Fabrication

Tooling:

All fabrication methods require tools to provide the shape of the composite structure/laminate during the processing. In this case a flat aluminum tool is used to manufacture flat composite plate.

Specialty Materials:

Many secondary or specialty materials are used in composite manufacturing such as release agent, peel plies, release films, bleeder plies, breather ply, vacuum bags and sealant tape. Each of these materials serves a specific function [60]. A cross section of typical lay-up of a composite structure prepared for autoclave processing is shown in Figure 3.1

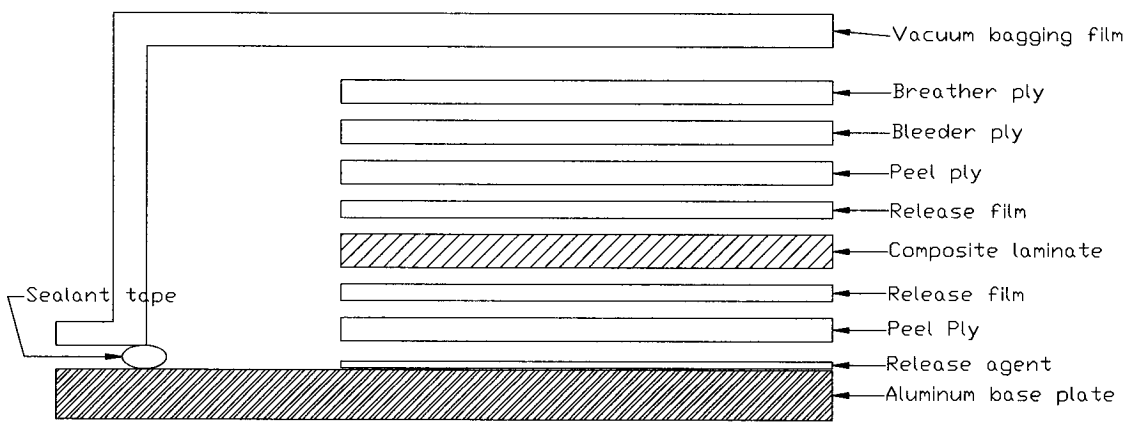

Figure 3.1 A typical cross section of an autoclave lay-up

Hand Lay-up:

The lay-up of preimpregnated material by hand is the oldest and common fabrication method for most advanced composite structures. Each step in hand lay-up of a flat composite laminate must follow in successive fashion in order to obtain a high quality composite laminate after final processing.

At first the surface of the plate is cleaned and a release agent is applied followed by one layer of release film and peel ply. The preimpregnated plies are cut according to the required dimensions of the respective specimen, usually 12"x12" or 12"x 6". The first ply is oriented and placed upon the tool. Subsequent plies are placed one upon another according to the laminate configuration. A roller is used to compact the plies and remove entrapped air that could lead to voids or delaminations in between layers. After that a peel ply, a sheet of porous release film, the bleeder ply and the breather plies are placed on top of the laminate one by one according to Figure 3.1. When the lay-up of all the plies are completed the sealant tape is placed around the periphery of the laid laminate and the vacuum bag is placed over the entire lay up. Before starting the autoclave for processing, the vacuum pump is turned on and checked for leaks, a vacuum of 28 mm of Hg is maintained for 5 minutes and again checked for leaks.

3.2.2 Processing

Once the hand lay-up is completed, the entire base plate with all set up is carefully put inside the autoclave for processing. The autoclave is a large metal pressure vessel with thermal insulation. Laminates properly cured using an autoclave, always produce high quality specimens.

Inside the autoclave laminates are passed through a definite cure cycle, where required pressure and temperature are applied following a time cycle, which is precisely controlled by computer program supplied by the manufacturer.

Figure 3.2 Autoclave used for making laminate

The cure cycle is a two step process .The laminate is heated from room temperature to 106° C at constant rate and it is held at this temperature for a period of 20 minutes (first dwell). The purpose of the first dwell is to allow the entrapped air, water vapor, or volatiles to escape from the matrix material and to allow a matrix flow, resulting in the compaction of the part. Afterwards, the temperature is again increased to 145° C and held constant for 45 minutes (2^{nd} dwell). In this dwell, cross linking of the resin takes place and the related material properties are developed. A constant pressure of 60 psi is maintained inside the autoclave throughout the process cycle. Later the laminate is cooled to room temperature at constant rate and after that kept at that stage for 10 hrs. Finally the laminate is removed from the aluminum base plate. A typical cure cycle for the curing of specimen inside an autoclave is given in Figure 3.3.

The laminate thus prepared is cut to the required size by using the water cooled rotary type diamond cutter shown in Figure 3.4.

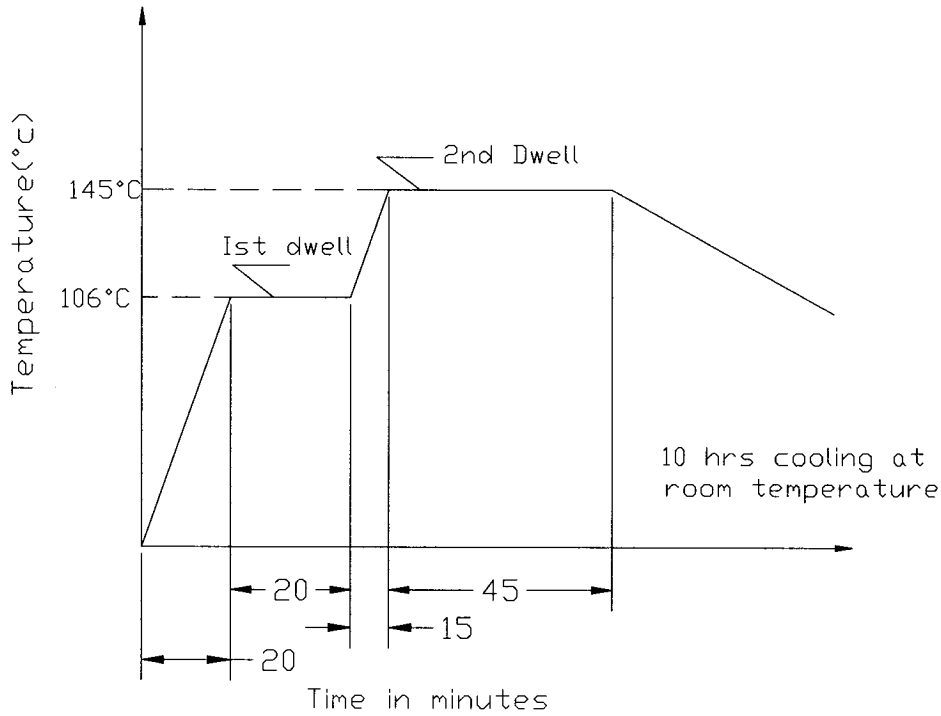

Figure 3.3 Cure cycle for NCT-301 graphite/epoxy composite material

Figure 3.4 Water cooled Rotary Diamond cutter

3.3 Experiments to Determine the Material Properties

For most composites in use today, the individual lamina (i.e., the individual layer or ply) is the basic unit or building block, whether it is in the design, analysis, or the fabrication

process stage. Therefore the properties of the individual lamina must be known for design and analysis purposes.

Experiments are conducted on different laminate configurations to get lamina properties like Young's modulus values in the fiber and transverse directions, E_1 and E_2, major and minor Poisson ratios ν_{12} and ν_{21} and shear modulus G_{12}. 25 specimens of each laminate configuration are tested to get the mean, standard deviation and co-efficient of variation of the material properties that are required for stochastic analysis.

Three different types of coupons with different geometry and laminate configurations are tested to get all the required data. All the specimens are straight sided coupons of constant cross section and are tested using end tabs. At the beginning trial tests are conducted by using adhesively bonded continuous woven E-glass and graphite/epoxy (same material) tabs with different types of adhesive. Four different adhesives like Fastweld-10 from Ciba Geigy, Lansing, Michigan, USA and Araldite-1258, Araldite-2043, Araldite-2015 from Vantico A and T, Michigan, USA are used to bond the E-glass and graphite/epoxy tab with the specimens and many trial tests are conducted. Unfortunately no adhesives can withstand the load until failure for unidirectional laminate. All the tabs (added to the specimen by using adhesives) came out from specimen under tensile load (before failure of the specimen) when they are tested in the MTS machine.

After that a different approach is followed to make the tab. Tabs of the same material (used for specimen), graphite/epoxy prepreg, are used. Prepreg layers for the tab and the specimen are precisely laid on the base plate at the same time and cured in one shot inside the autoclave. To protect the laminate from bending due to autoclave pressure, some false layers of the prepreg (that make up the thickness of the tab) are used on the bottom of the

laminate and isolated by release film. These tabs work very well during the testing of the machine and produce very much consistent results. There are no immature failures on any specimen in the tab. A schematic diagram of this lay-up is shown below:

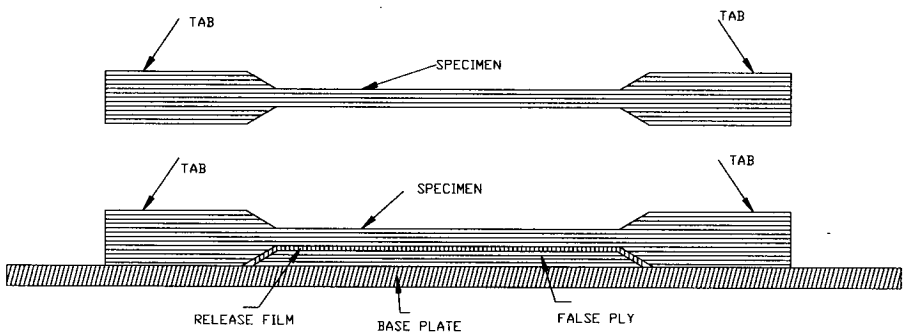

Figure 3.5 Cross section of the lay up showing the technique used to make tab and specimen at the same time

All the specimens are tested on displacement control mode in a Universal MTS machine (100 Kilo Newton Capacity, hydraulic grips control) by using special smooth grips used for composite material.

Two different types of strain gages are used to get the axial and transverse strains during the test. Axial strains are obtained by using strain gage of model CEA-06-125UW-350. Axial and transverse strains are obtained at the same time by using strain gage of model CEA-06-125UT-350. Strain gages are supplied by Micro Measurements; Measurements group Inc., Raleigh, North Carolina, USA.

3.3.1 Bonding of strain gage with the specimen

Strain gages are usually utilized in testing of composite materials for the acquisition of strain data. A careful and rational gage selection will result in obtaining accurate and reliable strain measurements, ease of installation and minimizing cost. In most cases larger gages are preferred because they are easier to handle and they improve heat dissipation which could affect gage performance and accuracy. Strain gages with higher resistance are also preferable because they reduce heat generation by a big factor than the smaller resistance gage for the same applied voltage across the gage [15].

Considering all the above mentioned factors gage of 6mm in length and 350 ohms is chosen for the present work.

In bonding the strain gage and soldering the wire with the specimen, manufacturer instructions are followed. At first, surface of the specimen is rubbed by using very fine grid emery cloth for smoothing and then a drop of acid (phosphoric) and neutralizer (Ammonia water) are used to clean the surface. After that very small amount of catalyst (Isopropyl alcohol) followed by a drop of M bond 200 adhesive is applied on the surface. Then strain gage is put over the adhesive and pressed and held on for two minutes. Misalignment of strain gages in testing of isotropic materials can cause negligible measurement error, but induces significant measurement error in testing of composite materials. The bubbles or gap between the gage grids and the specimen are fatal to the strain gage readings.

Finally gages are fitted with the wires by soldering .Very small amounts of soldering flux (Isopropyl alcohol) are put on the solder and on strain gage and then a fine needle like heated solder unit is used to fit the strain gage with the wire.

Testing of three different laminate configurations are described as follows:

3.3.2 Tensile Testing of Unidirectional Laminate (fiber direction)

This test is conducted to get the Young's modulus of the material in the fiber direction. Procedure followed to do the test is available in ASTM D 3039/3039M-00 [62]. Four laminates of size 12" x 6" are made. Specimens are taken from them according to the required dimensions. A graphical presentation of the specimen is shown in Figure 3.6.

Specimen geometry: 250 x 15 x 1 (All dimensions in mm) .

Laminate Configuration: $[O]_8$, thickness of each layer is 0.125mm.

Tab dimensions: Length = 56mm, Thickness = 1mm.

Strain gage model: CEA-06-125UW-350.

During the tensile test in the MTS machine, fiber direction load P_i (Newtons) and corresponding strain data ϵ_i (micro strain) are recorded on the computer, attached with the testing machine at some predefined time interval.

Then the fiber direction stress at each point i is calculated by using the formula

$$\sigma_i = P_i / A \qquad (3.1)$$

where

A =bt ;

b and t are the width and thickness of the specimen respectively in the units of mm.

Fiber direction stresses are plotted against the fiber direction strains in Figure 3.9. The slope of this curve $\Delta\sigma/\Delta\epsilon$ in the linear region is the fiber direction Young's modulus E_1.

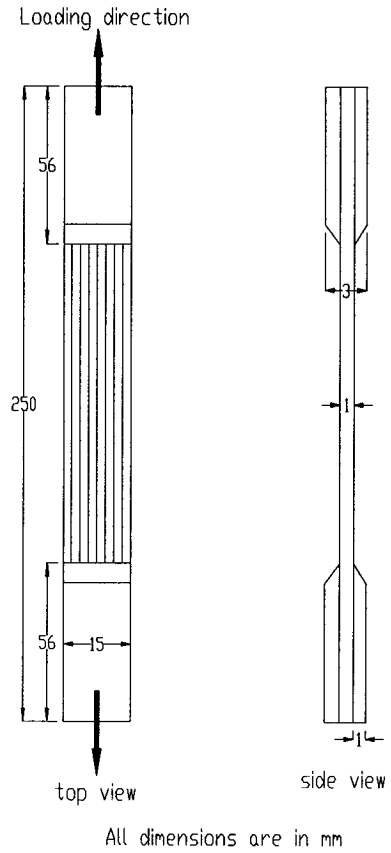

Figure 3.6 Unidirectional tensile testing specimens

3.3.3 Tensile Testing of Unidirectional Laminate (transverse dir.)

This test is conducted to get the Young's modulus of the material in the transverse direction and minor Poisson's ratio ν_{21}. Procedure followed to do the test is available in ASTM D 3039/3039M-00 [62]. Six different laminates of size 12" x 6" were made. Specimens are taken from them according to the required dimensions. A graphical presentation of the specimen is shown in Figure 3.7.

Specimen geometry: 175 x 25 x 2 (All dimensions in mm) .

Laminate Configuration: $[90]_{16}$

Tab dimensions: Length = 25mm , Thickness = 1mm.

Strain gage model: CEA-06-125UT-350.

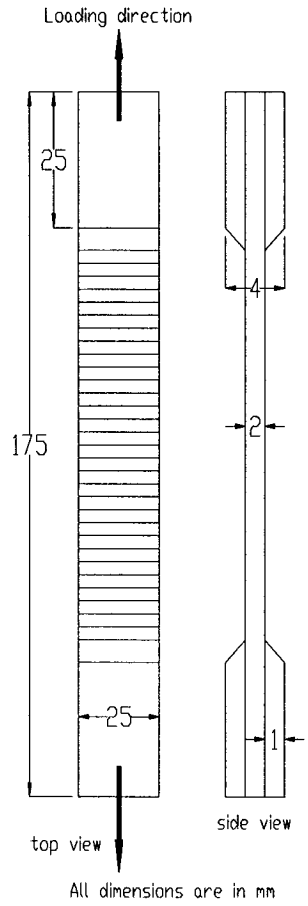

Figure 3.7 Transverse tensile testing specimen

During the tensile test in the MTS machine, transverse direction load P_i (Newtons) and corresponding axial and transverse strains data ϵ_{xi} (micro strain) and ϵ_{yi} (micro strain) are recorded on the computer attached with the testing machine at some predefined time interval.

Then the transverse direction stress at each point i is calculated by using the formula

$$\sigma_{xi}=P_{xi}/A \qquad (3.2)$$

where A =bt ;

b and t are the width and thickness of the specimen respectively in the units of mm.

Transverse direction stress σ_{xi} is plotted against the transverse direction strain ϵ_{xi} in Figure 3.10. The slope of this curve $\Delta\sigma_{xi}$ /$\Delta\epsilon_{xi}$ in the linear region is the transverse direction Young's modulus E_2. x is the direction of loading . Minor Poisson ratio ν_{21} is obtained by plotting ϵ_1 versus ϵ_2 which is shown in Figure 3.11.

3.3.4 Testing of angle ply laminate to get the shear modulus

This test is conducted to get the shear modulus G_{12} of the material. Procedure followed to do the test is available in ASTM D 3518/3518M-94 [63].

Six different laminates of size 12" x 6" were made. Specimens are taken from them according to the required dimensions. A graphical presentation of the specimen is shown in Figure 3.8.

Specimen geometry: 250 x 25 x 2 (All dimensions in mm) .

Laminate Configuration: $[\pm 45]_{4s}$

Tab dimensions: Length = 56mm, Thickness = 1mm.

Strain gage model: CEA-06-125UT-350.

During the tensile test in the MTS machine, Axial load P_{xi} (Newtons) and corresponding axial and transverse strain data ϵ_{xi} (micro strain) and ϵ_{yi} (micro strain) are recorded on the computer attached with the testing machine at some predefined time interval.

Then the shear stress and shear strain at each point i are calculated by using the formula

$$\tau_{12}=P_{xi}/2*A \qquad (3.3)$$

where A =bt ;

$$\gamma_{12}=\epsilon_{xi} - \epsilon_{yi} \qquad (3.4)$$

where

b and t are the width and thickness of the specimen respectively in the units of mm.

τ_{12} is in-plane shear stress in 1-2 plane

γ_{12} is in-plane shear strain in 1-2 plane

P_{xi} is applied tensile load in Newtons

ϵ_{xi} is longitudinal strain

ϵ_{yi} is transverse strain

Shear stress τ_{12} is plotted against the shear strain γ_{12} in Figure 3.12. The slope of this curve $\Delta\tau_{12}/\Delta\gamma_{12}$ in the linear region is the shear modulus G_{12}.

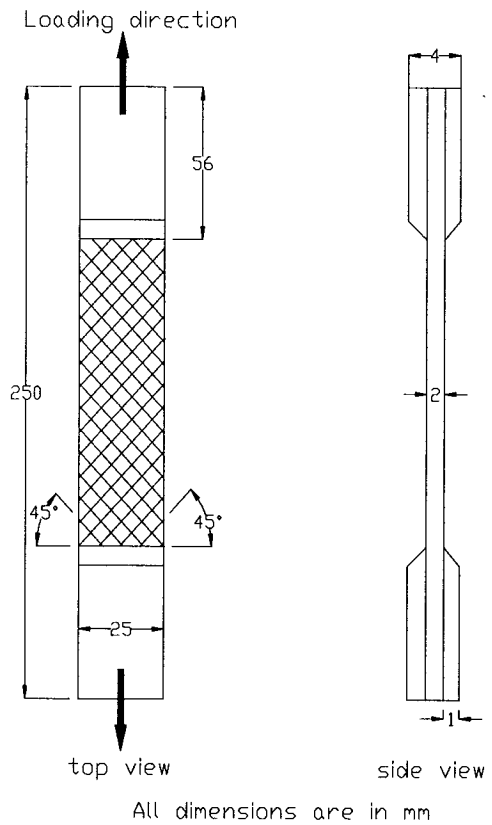

Figure 3.8 Tensile testing specimen to determine shear modulus

3.3.5 Statistical Parameters

To get the mean, standard deviation and coefficient of variation for each material property, 25 specimens of each type are tested .These values are calculated as follows:

$$\overline{X} = \frac{1}{n}\sum_{i=1}^{n} X_i \tag{3.5}$$

$$s = \sqrt{\frac{\sum_{i=1}^{n} X_i^2 - n\left(\overline{X}\right)^2}{n-1}} \tag{3.6}$$

$$\text{C.O.V.} = 100 \times \frac{s}{\overline{X}} \tag{3.7}$$

where

$\overline{X}$ = Mean value

s = Standard deviation

C.O.V. = Coefficient of variation

X_i = Test value obtained for the i^{th} specimen.

n= number of specimens tested

3.3.6 Tensile Testing Data of Unidirectional Laminate (fiber direction)

Table 3.1 lists the experimental results for specimens loaded in the fiber direction. An effort has been made to control the specimen geometry in the required dimensions.

Sl. No.	Width W	Area A	Failure load	Ultimate Strain	Ultimate Strength	E_1
	mm	mm^2	Newtons	Micro strain	MPa	GPa
1	15.15	15.3523	28,072	13,885	1829	131.9
2	14.55	14.1587	29,238	14,554	2065	141.5
3	15.18	14.6811	31,385	14,398	2138	141.7
4	14.82	14.3754	29,478	11,862	2051	136.5
5	15.06	14.6244	32,307	15,826	2209	143.5
6	15.01	14.5629	31,316	14,874	2150	143.6
7	15.06	14.6082	22,582	11,556	1546	137.0
8	15.16	14.6616	25,853	13,440	1763	132.7
9	15.00	14.5468	31,137	15,679	2140	129.0
10	15.08	14.6799	29,209	12,407	1990	136.0
11	15.10	14.8505	21,607	10,933	1455	132.2
12	15.12	15.0228	29,095	14,405	1937	134.9
13	15.09	14.694	28,307	13,629	1927	143.9
14	14.93	14.4159	21,620	11,143	1500	131.2
15	15.16	14.7084	31,766	15,489	2160	141.2
16	14.93	14.4853	28,989	13,982	2001	134.7
17	14.94	14.4886	20,277	11,392	1399	132.0
18	14.91	14.6117	19,443	13,768	1331	127.1
19	15.26	15.0599	24,199	11,005	1607	128.9
20	15.05	14.6017	28,896	13,945	1979	137.9
21	15.06	14.6583	28,431	14,572	1940	135.1
22	15.18	14.8258	28,303	15,295	1909	128.2
23	14.87	14.8802	31,997	16,611	2150	138.4
24	14.92	15.1536	30,846	10,768	2036	131.1
25	14.81	14.5661	16,903	91,43	1160	125.7

Table 3.1 Experimental data of the specimens corresponding to the fiber direction

Mean, standard deviation and coefficient of variation values for Young's modulus E_1 are summarized in Table 3.2.

	Young's modulus	Ultimate strength	Ultimate strain	Ultimate load
	E_1 (GPa)	MPa	Micro strain	Newtons
Mean	135.036	1855	13382	27250
Standard Deviation	5.43	300	1937	4423
C.O.V.	4.02	16.19	14.47	16.23

Table 3.2 Mean, Standard Deviation and Coefficient of Variation values of E_1, Ultimate strength, Ultimate strain and Failure load in the fiber direction.

From Table 3.2, one can see that there is more variation in the strength values than the corresponding Young's modulus values.

3.3.6 Tensile Testing Data of Unidirectional Laminate (transverse direction)

Tables 3.3 and 3.4 list the experimental results for specimens with loading in the transverse direction. An effort has been made to control the specimen geometry in the required dimensions.

Sl. no.	Width	Failure load	Failure Strength	Ultimate Strain	Ultimate Strain	Young's modulus	ν_{21}	ν_{12} See the note
	mm	Newtons	MPa	Transverse dir.	Fiber direction	E_2		below **
				Micro strain	Micro strain	(GPa)		
1	24.92	2,485	49.98	6063	-103	8.4	0.0179	0.281
2	25.27	2.889	57.40	7123	-100	8.1	0.0169	0.295
3	24.99	1,648	32.96	4134	-52	8.6	0.0161	0.265
4	25.04	2,561	51.79	6451	-88	8.2	0.0131	0.218
5	25.02	2,740	55.42	6035	-99	9.5	0.0181	0.273
6	25.04	2,871	57.56	6774	-82	8.8	0.0166	0.271
7	25.03	3,261	65.24	7700	-128	8.5	0.0178	0.287
8	25.01	2,623	52.41	6644	-65	7.9	0.0154	0.259
9	25.01	3,681	73.67	9969	-134	7.4	0.0141	0.246
10	25.00	2,661	53.20	7102	-102	7.4	0.0167	0.307
11	25.02	2,240	44.89	5679	-66	7.9	0.0157	0.263
12	24.89	3,192	65.77	8347	-107	8.1	0.0126	0.209
13	25.00	3,040	60.66	8006	-103	7.6	0.0144	0.273
14	25.07	3,023	60.20	7590	-116	7.8	0.0181	0.304
15	24.92	3,033	60.75	7843	-111	8.3	0.0157	0.267
16	25.23	3,009	59.94	7245	-112	8.4	0.0178	0.285
17	25.03	2,892	57.60	7529	-92	7.7	0.0135	0.231
18	24.62	2,451	49.94	5851	-105	8.4	0.0173	0.262
19	25.19	3,375	67.90	8255	-130	8.4	0.0162	0.249
20	25.01	1,972	39.41	4582	-68	8.7	0.019	0.301
21	25.24	3,005	60.15	7452	-92	8.2	0.0156	0.257
22	25.08	3,330	67.14	8103	-119	8.6	0.0173	0.258
23	24.81	3,271	66.34	8216	-123	8.1	0.0149	0.255
24	24.71	2,830	57.04	7185	-116	8.0	0.0157	0.257
25	24.77	3,547	71.81	8860	-135	8.1	0.0148	0.229

** $\nu_{12} = E_1 * \nu_{21}/E_2$

Table 3.3 Experimental results of specimens corresponding to transverse direction

	E_2	ν_{12}	ν_{21}	Strength	Failure strain	Max. strain	Failure
				Transverse direction	Transverse direction	Fiber direction	load
	GPa			MPa	Micro strain	Micro Strain	Newtons
Mean	8.204	0.26415	0.0161	57.57	7150	102	2749.8
Std. dev	0.465	0.02536	0.0017	9.57	1297.10	22.39	742.04
C.O.V.	5.67	9.6	10.54	16.62	18.14	21.98	26.98

Table 3.4 Mean, Standard Deviation and Coefficient of Variation values of E_2, minor and major Poisson ratios, Ultimate strength, Ultimate strain and Failure load in the transverse direction.

From Table 3.4, one can see that there is more variation in the strength values and Poisson ratios than the corresponding Young's modulus values.

3.3.8 Tensile Testing Data of $[\pm 45]_{4s}$ Laminate

Tables 3.5 and 3.6 list the experimental results for specimens with $[\pm 45]_{4s}$ configuration. An effort has also been made to control the specimen geometry in the required dimensions.

Sl.	Width	Area	Failure load	Shear strength	Ultimate strength	Shear modulus
no.	W	A	$[\pm 45]_{4s}$ laminate		$[\pm 45]_{4s}$ laminate	G_{12}
	mm	mm^2	Newtons	MPa	MPa	GPa
1	25.01	50.237	12,187	121.10	242.20	4.3
2	24.99	50.413	12,566	124.63	249.26	4.4
3	25.07	50.266	13,197	131.00	262.00	4.2
4	25.14	50.339	12,464	123.80	247.60	4.4
5	24.94	49.922	13,245	133.00	266.00	4.2
6	24.79	49.656	12,906	130.00	260.00	4.4
7	24.37	48.876	11,930	122.00	244.00	4.3
8	24.94	49.955	12,930	129.00	258.00	4.2
9	25.06	50.339	13,061	129.70	259.40	4.4
10	24.88	49.833	12,758	128.00	256.00	4.2
11	25.22	50.583	13,530	133.70	267.40	4.1
12	25.07	49.981	12,638	126.42	252.84	4.2
13	25.03	49.868	13,368	134.00	268.00	4.2
14	24.66	49.231	12,896	130.97	261.94	4.1
15	25.14	50.245	13,151	130.87	261.74	4.1
16	25.08	49.903	12,214	122.37	244.74	4.2
17	25.12	50.347	12,141	120.57	241.14	4.0
18	25.08	50.559	12,382	122.45	244.90	4.0
19	25.02	50.313	12,662	125.72	251.44	3.9
20	25.01	50.152	12,996	125.57	251.14	3.9
21	25.13	50.443	12,686	125.74	251.48	4.0
22	25.26	50.384	13,320	132.18	264.36	3.8
23	25.08	50.559	12,996	128.52	257.04	4.3
24	24.71	49.733	11,514	115.75	231.50	4.2
25	25.08	50.033	12,272	122.64	245.28	4.3

Note: Strain data until failure of strain gage were recorded.

Table 3.5 Experimental results of specimens with $[\pm 45]_{4s}$ configuration

	Shear modulus	Shear	Failure load	Failure strength of
	G_{12}	Strength	$[\pm 45]_{4s}$ laminate	$[\pm 45]_{4s}$ laminate
	GPa	MPa	Newtons	MPa
Mean	4.172	126.78	12720.4	253.57
Std. Dev.	0.167	4.72	494.72	9.45
C.O.V.	4.006	3.72	3.88	3.72

Table 3.6 Mean, Standard Deviation and Coefficient of Variation values of Shear modulus, Shear strength, Ultimate strength and Failure load of $[\pm 45]_{4s}$ laminate

Mean, standard deviation and coefficient of variation values of all engineering material properties of NCT-301 graphite epoxy material are now summarized in Table 3.7.

	E_1	E_2	ν_{21}	ν_{12}	G_{12}
	GPa	GPa			GPa
Mean	135.036	8.204	0.016052	0.26415	4.172
Standard Deviation	5.43	0.465	0.001692	0.02536	0.1671
C.O.V.	4.02	5.67	10.54	9.6	4.006

Table 3.7 Mean, Standard deviation and Coefficient of variation values of engineering material properties of NCT-301 Graphite/Epoxy material

From Tables 3.2, 3.4 and 3.6, one can see that there is less variation in the modulus values E_1, E_2 and G_{12} than the failure strength and strain in fiber and transverse directions. This is because the modulus is a global property, whereas the ultimate strength and strain are more

local. As ν_{12} and ν_{21} are obtained from the graph of ϵ_{xi} and ϵ_{yi} there is more variation in their values. Again by looking at the values of E_1 (135.04 GPa) and E_2 (8.204 GPa) one can see how much anisotropic the material is!

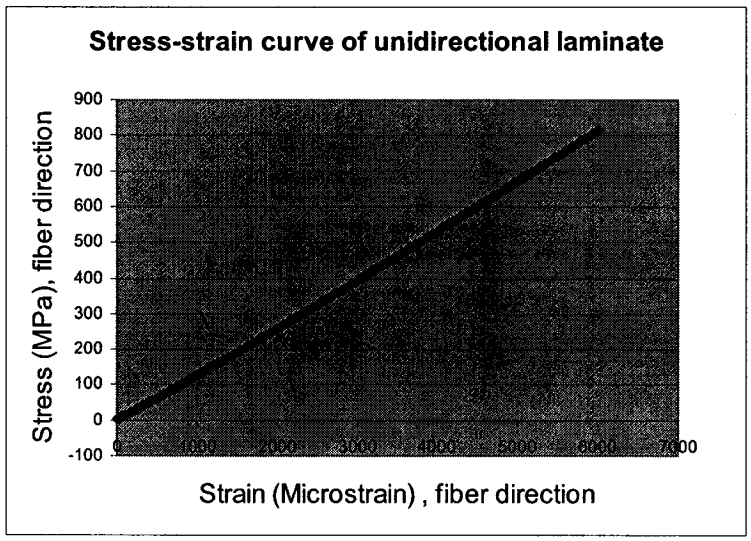

Figure 3.9 Stress–strain curve of unidirectional specimen (fiber direction) $[O]_8$ under tensile load

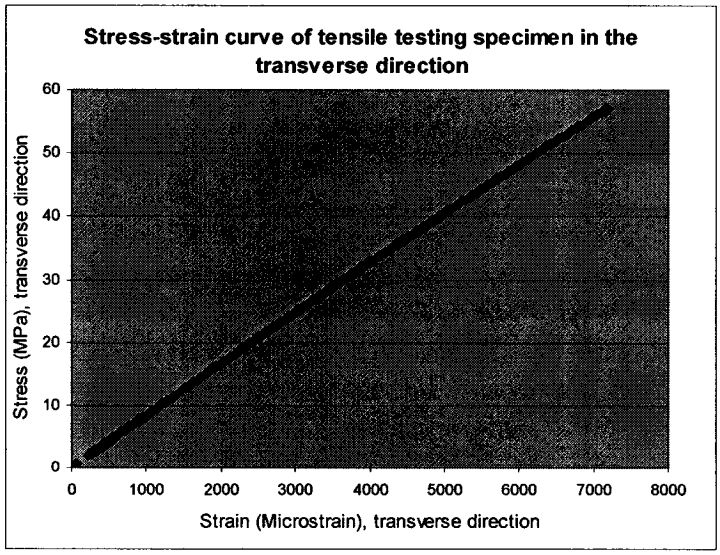

Figure 3.10 Stress–strain curve of unidirectional specimen (transverse direction) $[90]_{16}$ under tensile load

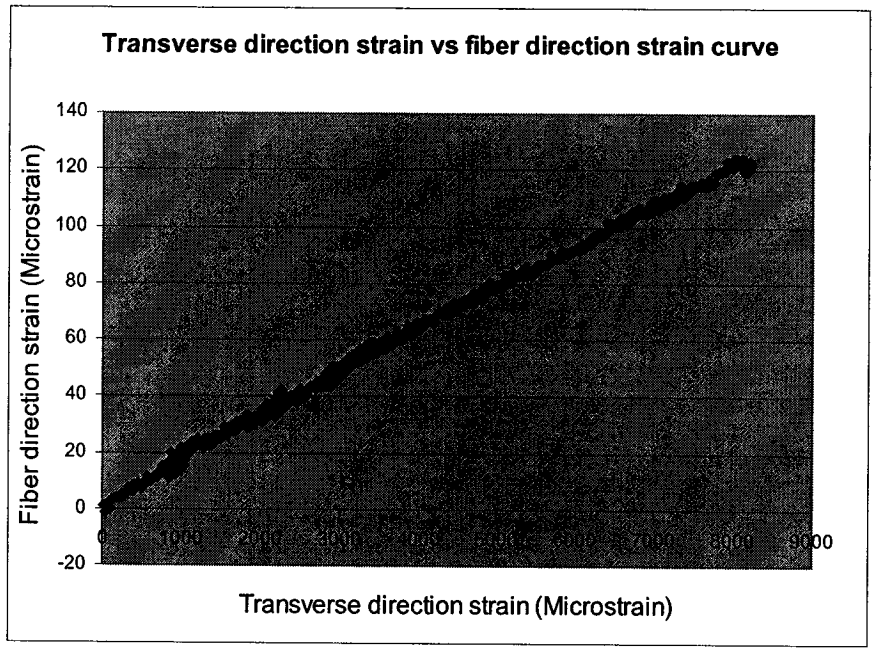

Figure 3.11 Axial strain vs. transverse strain curve of tensile testing specimen in the transverse direction

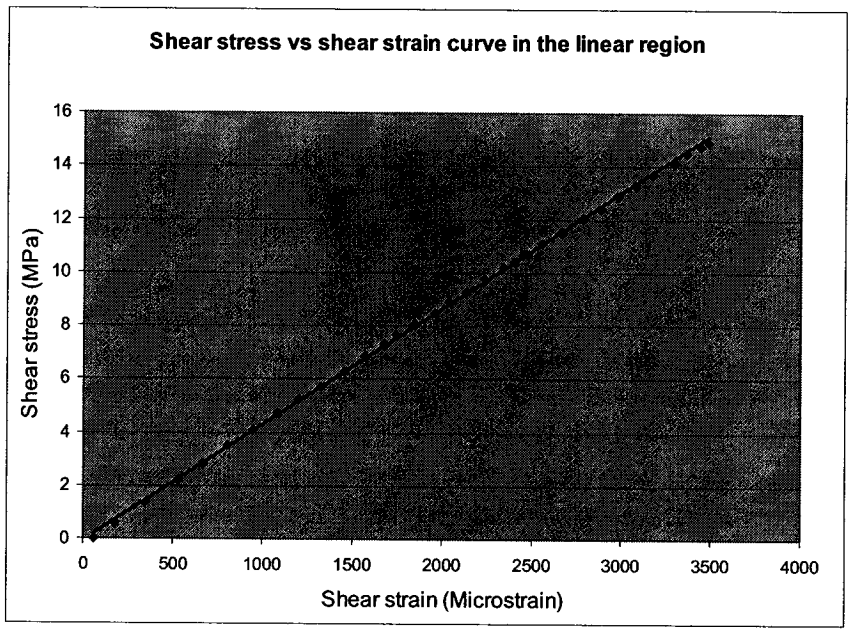

Figure 3.12 Shear stress vs. shear strain curve of $[\pm 45]_{4s}$ specimen under tensile load up to proportional limit

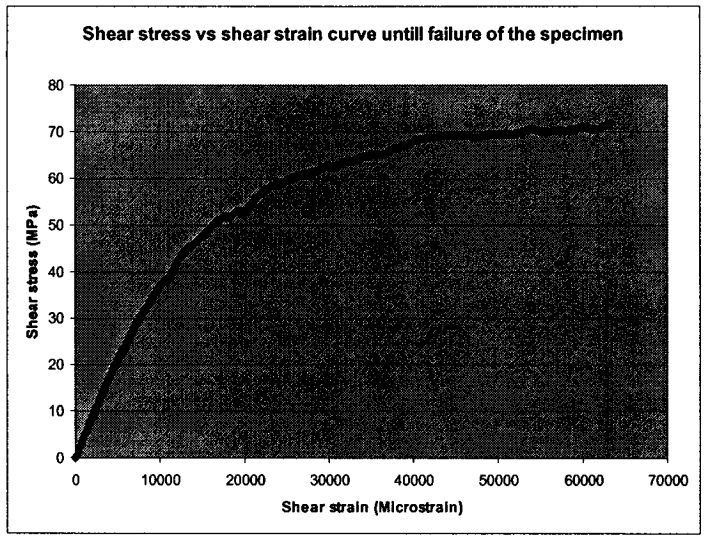

Figure 3.13 Shear stress vs. Shear strain curve of $[\pm 45]_{4s}$ specimen under tensile load, until failure

From Figures 3.9, 3.10 and 3.12, one can see that unidirectional laminates behave elastically (in a practical sense) almost until failure (up to 8000 micro strain), whereas the $[\pm 45]_{4s}$ laminate has a very short elastic range (up to 3000 micro strain). The $[\pm 45]_{4s}$ laminate is almost non-elastic in nature. This is because the failure of these laminates involves more delaminations and matrix cracking rather than fiber breakage. Again from Figure 3.11, one can see that in the transverse direction the response of the laminate in terms of transverse direction strain and the fiber direction strain is not consistently linear and there is little bit of scatter in data points.

Material property values used to analyze for the stress concentration and reliability of laminate with a hole of diameter 5.1 mm are taken from reference [3] and are given in Table 3.8.

NCT-301 material that is tested in the present work differs from that of NCT-301 material tested in reference [3]. There is a continuous development of the material by the manufacturer. So properties of the material also change

accordingly with the development of the material. Material properties data of NCT-301 given in Table 3.8 were tested in 1998. So there was a need for testing the recently manufactured NCT-301 material. If we analyze the test data given in Tables 3.7 and 3.8, we will see the improvement in the material properties of recently manufactured NCT-301.

	E_1	E_2	ν_{21}	ν_{12}	G_{12}
	GPa	GPa			GPa
Mean	113.9	7.985	0.020	0.29	3.130
Standard Deviation	4.578	0.452	.0021	0.0278	0.125
C.O.V.	4.02	5.67	10.54	9.6	4.006

Table 3.8 Mean, Standard deviation and Coefficient of variation of engineering constants of NCT-301 Graphite/Epoxy material [3]

3.4 Photographs of the Specimens before and after Failure

Photographs of all the tested specimens before and after failure, test setup and the MTS machine used to do the test are taken using a digital camera. These photographs will help us to understand the failure modes of different specimens under tensile load.

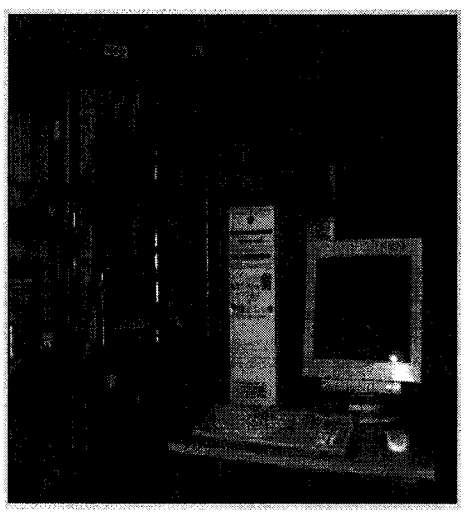

a) Experimental Setup of MTS machine

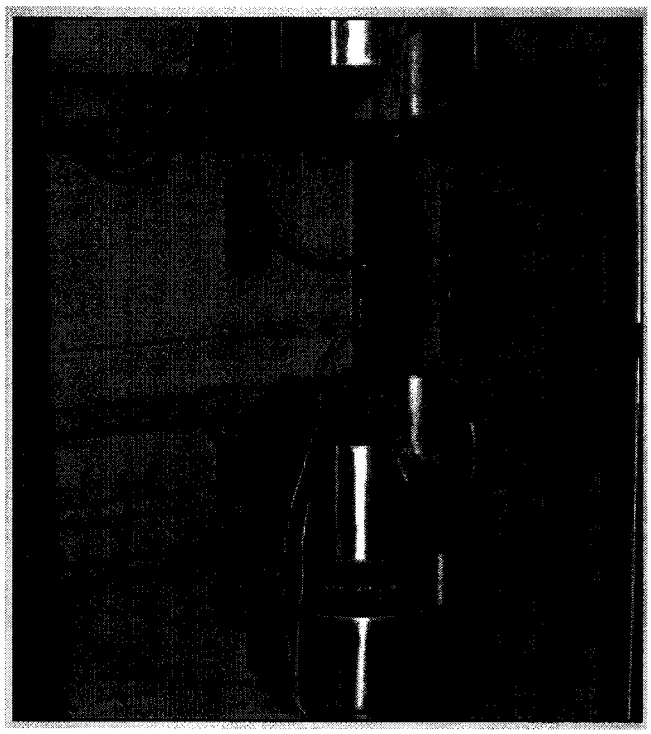

b) E_2 specimen (with strain gage) under tensile load in the MTS machine.

Figure 3.14 MTS machine used to do the tensile test

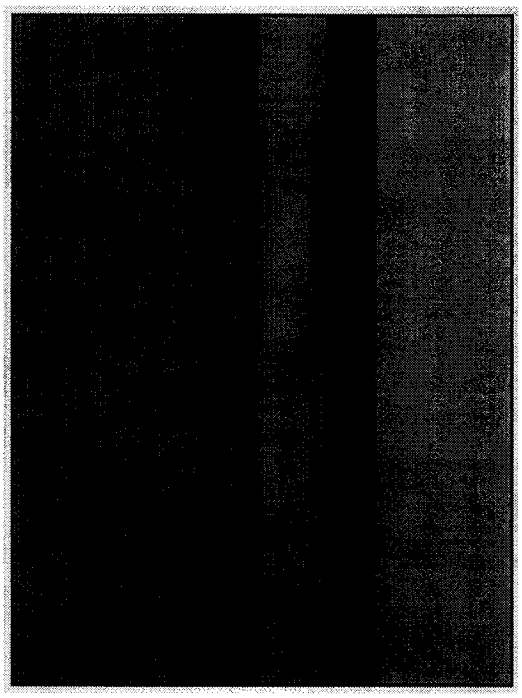

a) E_1 specimen before and after failure

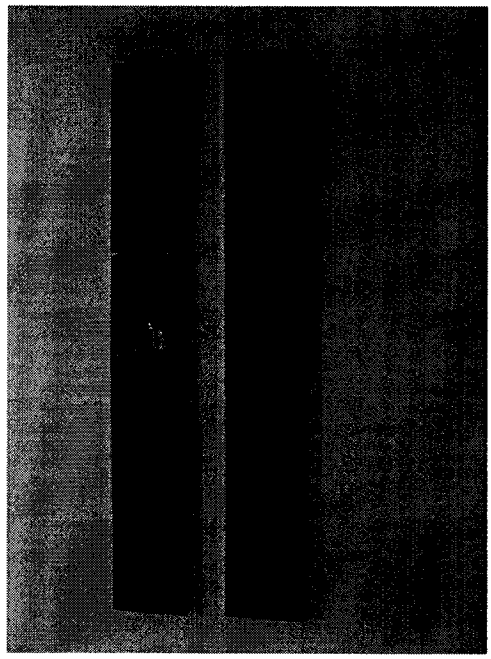

b) E_2 specimen before and after failure

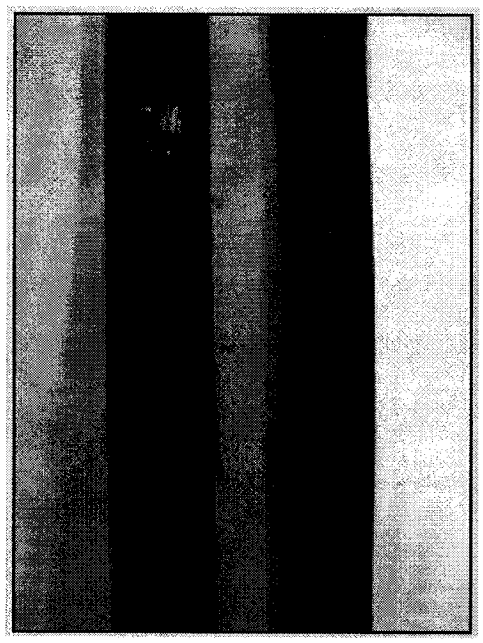

c) G_{12} specimen before and after failure

Figure 3.15 The typical pictures of E_1, E_2 and G_{12} specimens before and after failure

From Figure 3.15(a), one can make out that failure of the unidirectional laminate (E_1 specimen) in the fiber direction takes place all over the laminate by fiber breakage and splitting. This is due to the dominance of fiber in the loading direction.

From Figure 3.15(b), one can also make out that failure of the unidirectional laminate (E_2 specimen) in the transverse direction takes place in a direction perpendicular to the loading near the middle of the specimen. This is due to the dominance of matrix in the loading direction.

From Figure 3.15(c), one can make out that $[\pm 45]_{4s}$ laminate (G_{12} specimen) fails in two directions that are at $+45^0$ and -45^0 with the direction of loading. Failure begins with the matrix cracking followed by the delamination of 45^0 and -45^0 fibers in both the directions, because this laminate is dominated by both fiber and matrix.

3.5 Micro structural Study of the Specimens

Before taking specimens from laminates, they are checked for defects, such as delamination and voids. Laminates with such defects are not considered for testing. These defects are developed as a result of uneven rolling while laying up the plies, poor vacuum bagging, and improper pressurization in furnace during curing and so on.

To observe these defects, a micro structural study is conducted. At least one specimen from each laminate is observed under the microscope. The specimen is cut in the middle along the width to see the cross section of the specimen under the microscope. As the face of the cross section is quite small (1 or 2 mm), for the preparation of specimen, the region

of interest is immersed in a special plastic bowl with resin. Then the resin along with the specimen is cured, giving a bigger part for surface finishing work.

Now the surface generated is polished with the grinding operation. Initially it is treated with 200 grit SiC paper and subsequently with SiC papers that have 300, 400, 600, 800 and 1200 grit levels. It is to be noted at this point that, while grinding the specimen, care is taken to maintain a perfect horizontal surface. Specimens made in this way are put under an optical microscope fitted with a video camera. Microscopic images of the specimens are taken by using Clemex Vision software, which is connected to optical microscope.

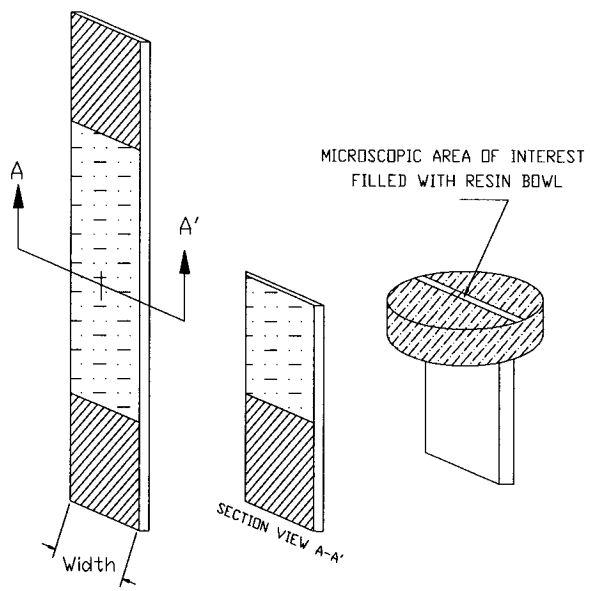

Figure 3.16 Microscopic Specimen for study

One thing to be noted here is that under the optical microscope carbon fibers are shown in bright white color and matrix (that is resin) is shown in grey color. Again a part of the cross section is shown in the microscopic picture to clearly show the image because if the whole cross section is covered image becomes blurred and it becomes hard to explain the defects.

Microscopic image of E_1 specimen before failure is given in Figure 3.17. Specimen is completely separated in tiny fibers after failure. So the microscopic image after failure is not shown.

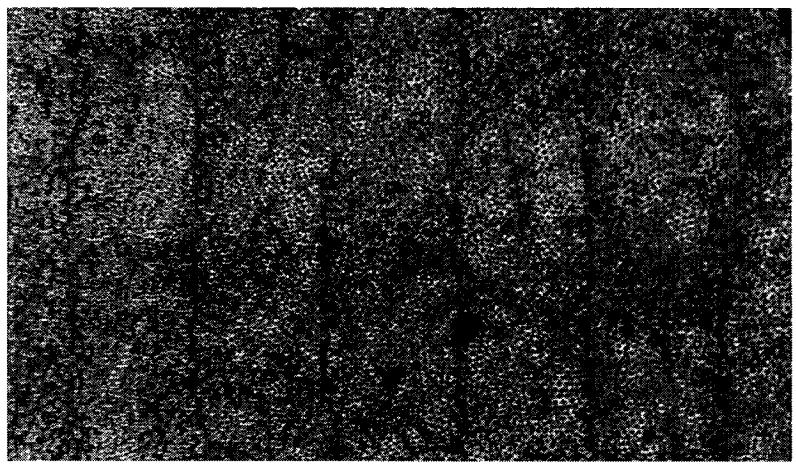

Figure 3.17 A typical image of E_1 $[0_8]$ specimen, before failure, observed under a microscope (magnification 100X)

In Figure 3.17 few voids with average of 5-10 microns are seen. Again they are negligible compared to the dimensions of the specimen and are not considered in calculating the modulus E_1.

Microscopic images of E_2 specimen before and after failure are shown in Figures 3.18 and 3.19.

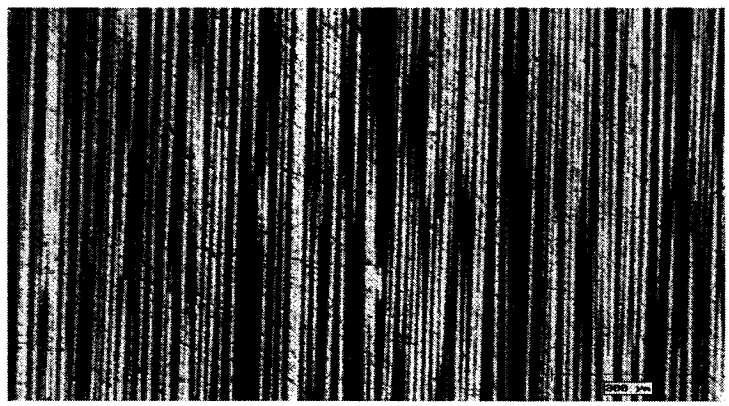

90 90 90 90 90

Figure 3.18 A typical image of E_2 $[90]_{16}$ specimen, before failure observed under a microscope (magnification 100X)

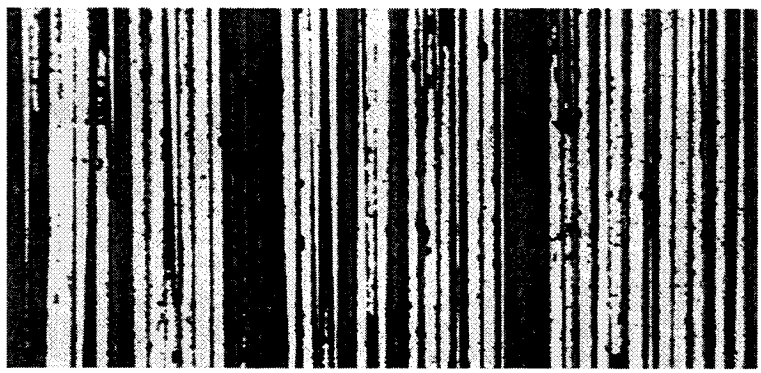

90 90 90 90 90

Figure 3.19 A typical image of E_2 $[90]_{16}$ specimen, after failure observed under a microscope (magnification 100X)

No significant defects are found in this specimen before failure. From Figure 3.19, one can interpret that specimens of this type are failed by matrix cracking because more grey area is found on the failed specimen.

Microscopic images of G_{12} specimen before and after failure are shown in Figures 3.20 and 3.21.

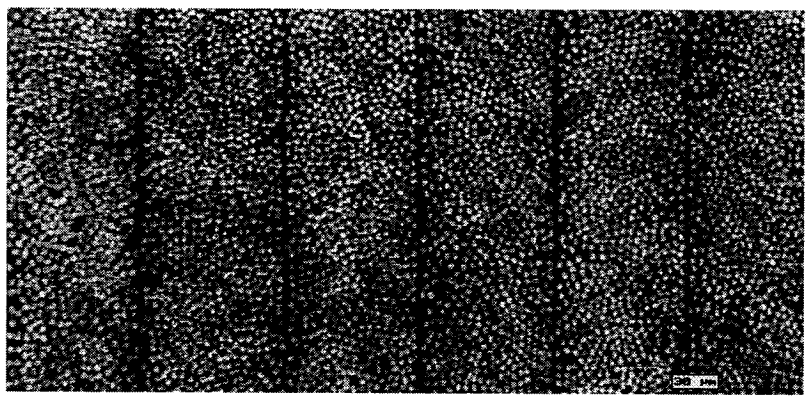

45 -45 45 -45 45 -45

Figure 3.20 A typical image of G_{12} $[\pm 45]_{4s}$ specimen, before failure observed under a microscope (magnification 100X)

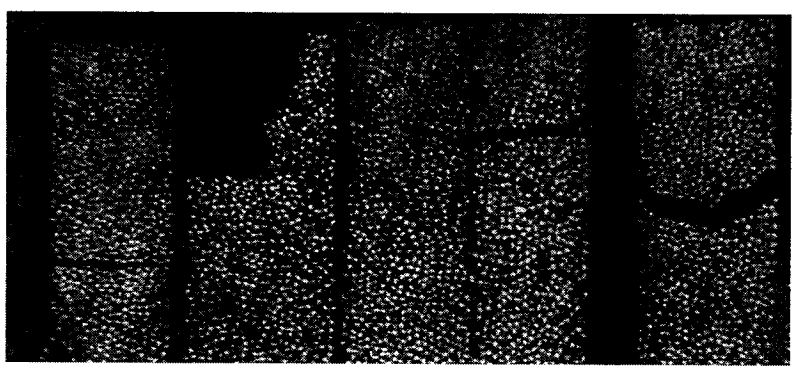

45 -45 45 -45 45

Figure 3.21 A typical image of G_{12} $[\pm 45]_{4s}$ specimen, after failure observed under a microscope (magnification 100X)

In Figure 3.20, no defects are found in the specimen. From Figure 3.21, one can interpret that specimen of this type failed by matrix cracking, delamination and fiber breakage.

3.6 Experiments on Notched and Un-notched Specimens to Determine Tensile Strength

Stress concentration is a fundamental and very important issue in structures. In most cases of practical application, they are the origin of failure. These problems are much more complicated for anisotropic laminates than for isotropic plates, because of the directional anisotropy.

Stress concentration in a structure can be caused by many reasons such as, cutouts or openings, voids and damage due to material fabrication, bolted joints, riveted joints and other mechanical joints etc. In practice, drilling operation in the composite laminates inevitably produces imperfections around holes; also the problem of hole being offset from the desired co-ordinates is encountered. All these in turn increase the stress concentration. Because of the above mentioned reasons, a study of stress concentration at the hole boundary and the stress distribution at a distance from the hole edge for different hole sizes in finite elastic plate subjected to uniform uniaxial load has been conducted. Information about stress concentration factors for different hole sizes provide the designer with useful worst-case information regarding the influence of the uncertainty in the hole shape and location on the resulting stress concentration factor.

Again knowing the stress concentration and stress distribution over the entire structure is not adequate enough to obtain safer design of composite structure. We need to know at

what conditions of stress and strength the structure will fail. A failure criterion can be developed based on the result of a micro-mechanics analysis or a macro-mechanics analysis. A micro-mechanics failure criterion could be useful for the design and material improvements of uni-directional lamina or laminates whereas a macro-mechanics (or lamina-based) failure criterion is essential for structural design and improvements. In composite materials, it is virtually impossible to know exactly the inhomogeneity in each constituent and the distributions and locations of the fibers. These are the main reasons for deviation in data in addition to human error and machine misalignment. Therefore it is more logical and reasonable to use a macroscopic, rather than a microscopic, failure criterion for structural applications [2].

For the present work, two widely accepted failure criteria, point stress criterion and average stress criterion, are considered. Both the criteria indicate that structures will fail if the stress either average or point(normal stress in the loading direction), reaches the un-notched strength of the laminate at certain distance form the hole edge along the axis perpendicular to the loading direction. This distance is named as characteristic length.

Experiments are conducted on notched specimens with different hole sizes to get the characteristic lengths and notched strengths of the laminate. 25 specimens for each hole size are tested to get the characteristic lengths that are required for stochastic analysis to get average and point stresses.

Brief description of the two failure criteria are given below:

3.6.1 Point Stress Criterion

Point stress failure criterion assumes [55] that failure occurs when the stress , σ_y , at some distance d_o away from the hole is equal to or greater than the un-notched strength of the laminate. A pictorial representation is shown in Figure 3.22.

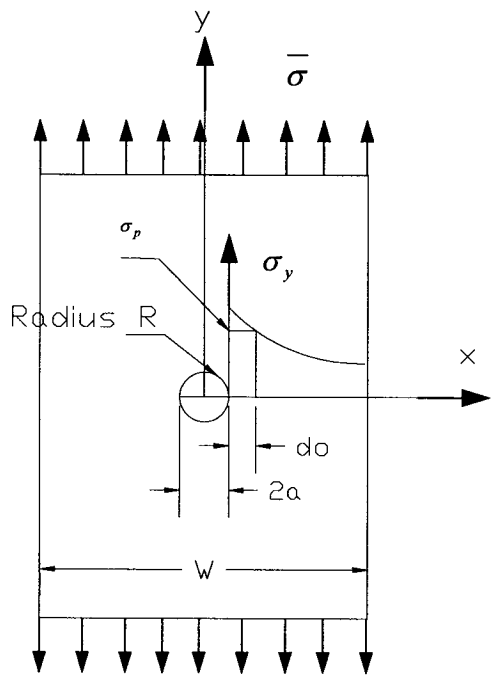

Figure 3.22 Graphical representation of point stress criterion

Mathematically it can be written as,

$$\sigma_y (x,0) \mid_{x = R + do} = \sigma_o \qquad (3.1)$$

where σ_o is the un-notched strength of the laminate and R is the radius of the hole.

For infinite orthotropic plate containing a circular hole, the approximate solution of stress distribution [1] along the axis perpendicular to the loading direction is :

$$\sigma_y(x,0)=\frac{\bar{\sigma}}{2}\left\{2+\left(\frac{R}{x}\right)^2+3\left(\frac{R}{x}\right)^4-\left(K_T^{\alpha}-3\right)\left[5\left(\frac{R}{x}\right)^6-7\left(\frac{R}{x}\right)^8\right]\right\} \qquad (3.2)$$

where $\bar{\sigma}$ is the stress applied at infinity and σ_y (x,0) is the normal stress with origin at the center of the hole.

$$K_T^{\infty} = 1 + \sqrt{\frac{2}{A_{22}}\left[\sqrt{A_{11}A_{22}} - A_{12} + \frac{A_{11}A_{22} - A_{12}^2}{2A_{66}}\right]} \tag{3.3}$$

where K_T^{∞} denotes the stress concentration factor at the edge of the hole of an infinite plate.

A_{ij}, i,j = 1,2,6 are the components of the in-plane stiffness matrix with 1 and 2 directions being parallel and transverse to the loading direction, respectively.

Now by substituting equation (3.2) into equation (3.1) and replacing $\bar{\sigma}$ and σ_y (x,0) by σ_o and σ_N , we obtain

$$\frac{\sigma_N}{\sigma_o} = \frac{2}{2 + \xi_1^2 + 3\xi_1^4 - (K_T^{\infty} - 3)(5\xi_1^6 - 7\xi_1^8)} \tag{3.4}$$

where $\xi_1 = \frac{R}{R + d_0}$ and σ_N is the ultimate strength of the notched laminate.

3.6.2 Average Stress Criterion

In this criterion instead of considering the stress at a point , it considers the average stress over a characteristic length. In other words, this criterion assumes that failure occurs when the average stress , σ_y over some distance , a_o away from the hole edge is equal or greater than the strength of the un-notched laminate.

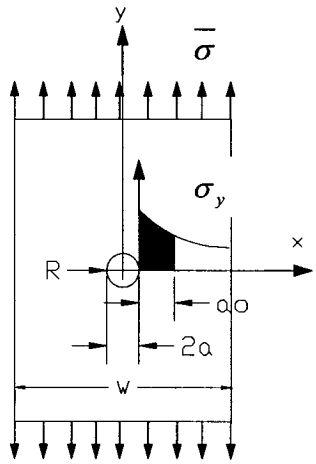

Figure 3.23 Graphical representation of average stress criterion

Mathematically it can be expressed as follows

$$\frac{1}{a_o}\int_{R}^{R+a_0}\sigma_y(x,o)dx = \sigma_o \tag{3.5}$$

In the case of orthotropic plate containing a hole the solution is obtained by substituting equation (3.2) into equation (3.5)

$$\frac{\sigma_N}{\sigma_o} = \frac{2(1-\xi_2)}{2-\xi_2^2-\xi_2^4+(K_T^\alpha-3)(\xi_2^6-\xi_2^8)} \tag{3.6}$$

where $\xi_2 = \dfrac{R}{R+a_0}$ and σ_N is the ultimate strength of the notched laminate.

K_T^α is same as in equation (3.3).

The point stress criterion and the average stress criterion both contain two unknowns , i.e., the un-notched strength , σ_o , and the characteristic length, d_o or a_o. These unknowns are determined experimentally. The procedure is to first obtain a set of un-notched and notched

strengths from experiment. Then substitute these data either in equation (3.4) or equation (3.6) and solve for d_o or a_o.

3.6.3 Dimensions of Notched and Un-notched Cross-Ply Specimen

Symmetric cross-ply laminate is one of the best laminate configurations commonly used by the designer for different structural applications. Due to that reason, cross-ply laminate configuration is chosen for the present thesis work. As there is no ASTM or other standards for testing of the cross-ply notched specimen, we refer to the works of Tan S.C. [2] and Shashank M. Venugopal [3] for specimen configurations and geometry, who have conducted studies on plates with circular hole for different laminate configurations. Accordingly they have come to a conclusion that, the ratio of the diameter to width of the plate should lie within 0 to 0.4. Otherwise, the stress concentration factor tends to deviate from the exact value for regions away from the hole. Based on this consideration, we have set the dimensions of the coupon as : length = 270 mm, gage length = 180mm, width = 37.9 mm, thickness = 2.00 mm and the configuration of the laminate is $[0/90]_{4s}$. Holes of diameter 5.1 mm, 6.35 mm and 7.54 mm are considered for the present study.

Reliability study on hole diameter 5.1 mm is conducted by taking all the related experimental data from reference [3]. Among them notched strength, un-notched strength, characteristic length and material property values are included.

In the present work, experiments are conducted on $[0/90]_{4s}$ cross-ply specimens with hole sizes 6.35 mm and 7.54 mm and on un-notched specimens of the same dimensions. 25 specimens of each of the three types are tested on the MTS machine (100 KN capacity) to get the notched strength and finally characteristic length values for all the specimens are calculated. Trial tests are conducted for each new type of specimen before doing the real

test, to find out suitable test parameters like grip pressure , loading method, need of tabs , data acquisition, etc. For our application notched and un-notched specimens are loaded respectively at 25 lb/s (111.2 Newtons/sec.) and 50lb/s (222.4 Newtons/sec.). Load and displacement data are recorded in a computer automatically at every 0.5 sec interval till failure. No end tabs are used; instead double sided sand paper is used for gripping the specimen, during the tensile test to avoid slippage.

Specimens are made in the same way by using autoclave as described in Section 3.2. Drilling is performed to prepare the notched specimen. The center point of the specimen is located and using the center punch a mark is made at the desired point. A wooden back-up is used to protect the specimen from damage during the drilling operation. Specimen is held properly with two clamps on both sides, so that it could not move during the drilling operation that is shown in Figure 3.24.

Using the nitride coated HSS drill bit, without coolant, drilling is done on the specimen.

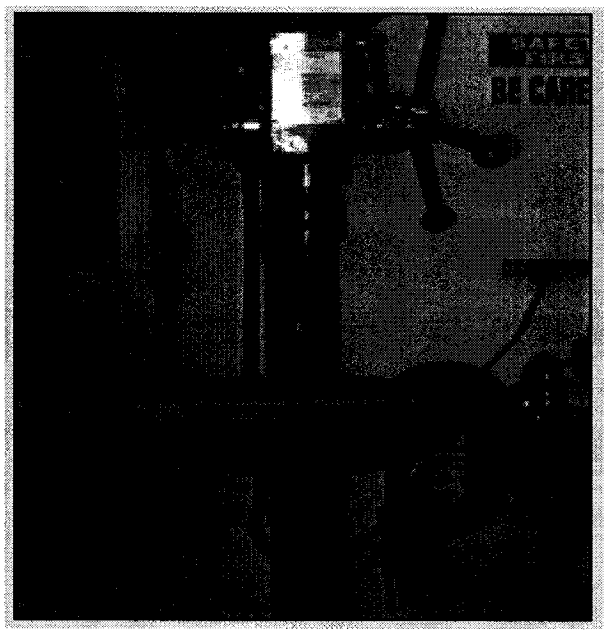

Figure 3.24 Drilling machine (used to make hole in the specimen)

3.6.4 Tensile Testing Data of $[0/90]_{4s}$ Specimens with a Hole of Nominal Size 7.54 mm at the center

Five flat laminates of size 12"x12" are made to get all the 25 specimens. Specimens are tested in the MTS machine at a loading rate of 25lb/sec.Test results are summarized in Table 3.9 and a typical load vs. displacement curve is shown in Figure 3.25.

Spec. No.	Length	Width	Hole diameter	Failure load	Failure Strength	Failure displacement
	mm	mm	mm	Newtons	MPa	mm
1	269.49	38.04	7.52	35467	590.19	2.07
2	269.49	37.92	7.52	34464	569.69	1.98
3	269.49	37.54	7.52	32986	547.48	1.77
4	269.49	37.79	7.52	35147	583.48	2.11
5	270.93	37.80	7.52	33875	560.20	1.78
6	269.49	37.70	7.52	34988	581.98	2.13
7	269.49	37.77	7.52	34657	573.99	1.84
8	269.49	37.82	7.52	36891	608.46	1.89
9	270.27	38.02	7.52	35281	575.49	1.76
10	269.49	37.83	7.52	35236	583.59	2.04
11	270.64	37.73	7.53	36842	608.85	1.92
12	269.98	37.79	7.52	34495	572.65	2.10
13	270.64	38.00	7.52	36628	599.65	1.93
14	270.64	37.69	7.52	34595	574.77	1.91
15	270.64	37.77	7.52	33734	557.03	2.07
16	270.64	37.65	7.52	35915	582.60	1.95
17	270.64	37.84	7.52	35412	586.91	1.84
18	270.64	37.73	7.54	33137	544.09	2.01
19	270.69	37.30	7.52	35464	589.83	2.07
20	270.08	37.49	7.52	35498	598.21	1.77
21	269.49	37.76	7.52	33438	537.29	2.01
22	270.93	37.80	7.52	33744	556.64	1.77
23	270.93	37.72	7.52	36556	607.66	1.98
24	269.96	37.98	7.52	35102	582.02	1.90
25	269.49	37.47	7.52	33744	554.74	2.07

Table 3.9 Experimental result of $[0/90]_{4s}$ laminate with hole of nominal size 7.54 mm

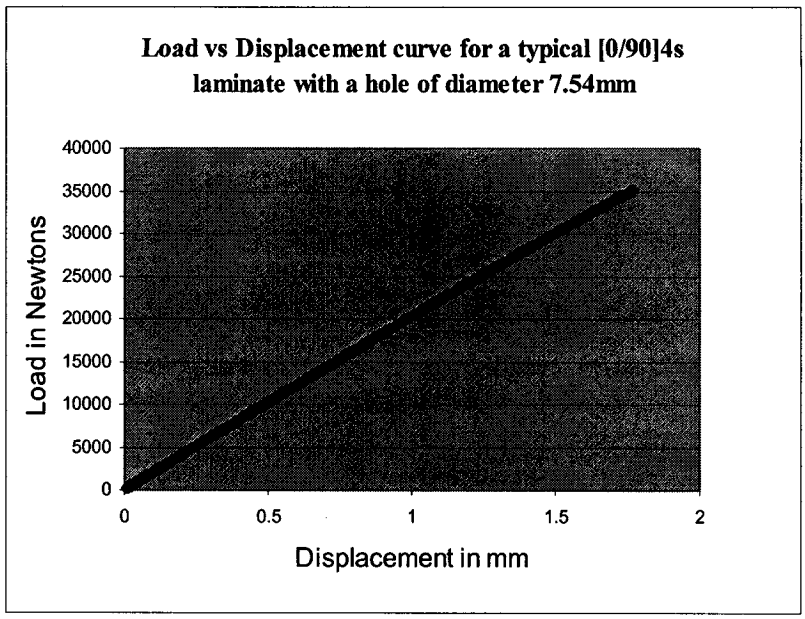

Figure 3.25 A typical load vs. displacement curve for $[0/90]_{4s}$ cross-ply specimen with a hole of diameter 7.54 mm

From Figure 3.25, one can see that $[0/90]_{4s}$ cross-ply laminate with 7.54 mm hole in the center is linear elastic in nature and it can withstand a mean load of 34932 Newtons. From Table 3.9, one can see that most of the specimens elongate more than 2mm before failure.

3.6.5 Tensile Testing Data of $[0/90]_{4s}$ Specimens with a Hole of Nominal Size 6.35 mm at the Center

Five flat laminates of size 12"x12" are made to get all the 25 specimens. Specimens are tested in the MTS machine at a loading rate of 25lb/sec.Test results are summarized in Table 3.10 and a typical load vs.. displacement curve is shown in Figure 3.26. Specimens taken from different laminates showed good consistency in the failure mode and test data.

Spec. No.	Length	Width	Hole Diameter	Failure load	Failure Strength	Displacement at failure
	mm	mm	mm	Newtons	MPa	mm
1	270.30	37.85	6.33	39830	636.68	1.88
2	270.02	37.85	6.33	38024	603.36	1.72
3	270.32	37.87	6.33	35016	551.87	2.03
4	269.64	38.01	6.33	39702	623.88	1.80
5	270.32	37.94	6.34	39726	625.14	1.75
6	270.32	37.90	6.33	38038	601.87	1.92
7	270.32	37.88	6.33	38913	617.11	1.88
8	270.30	37.85	6.35	36694	582.44	1.93
9	269.84	37.49	6.33	38906	630.80	1.84
10	270.30	37.78	6.33	36639	583.45	1.87
11	270.30	37.92	6.33	38776	621.70	1.99
12	270.30	37.87	6.33	37101	596.09	1.97
13	269.88	37.98	6.33	38651	609.68	1.92
14	270.32	37.91	6.35	37597	596.84	1.97
15	270.24	38.06	6.33	38937	603.39	1.92
16	270.32	37.86	6.33	39513	621.00	1.83
17	270.32	37.90	6.33	38403	606.70	1.81
18	269.88	37.83	6.33	37965	597.94	1.83
19	269.88	38.04	6.33	36039	567.69	1.89
20	270.3	37.45	6.33	36574	586.76	1.95
21	269.88	37.89	6.33	36432	572.04	1.82
22	269.88	37.73	6.33	37780	597.22	1.98
23	270.41	38.02	6.33	38706	620.19	1.89
24	270.32	37.75	6.33	38221	608.64	1.83
25	270.24	38.10	6.33	38245	595.44	1.94

Table 3.10 Experimental result of $[0/90]_{4s}$ laminate with a hole of nominal size 6.35 mm

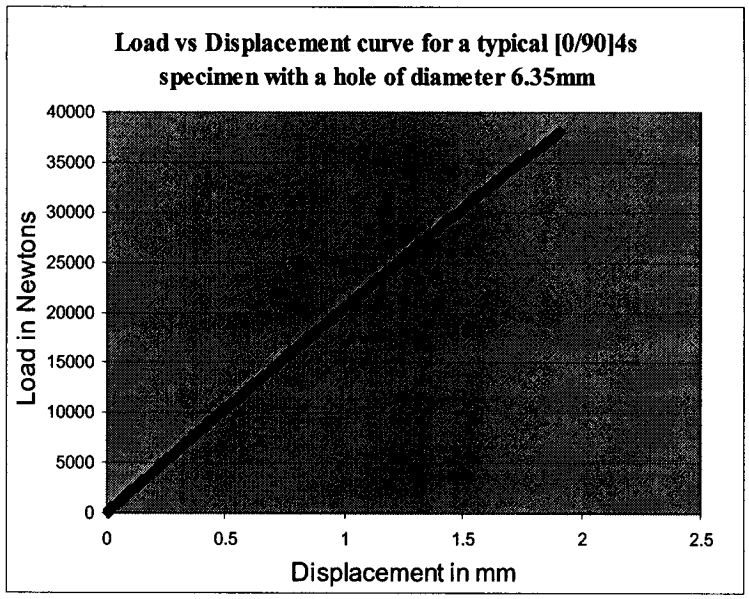

Figure 3. 26 A typical load vs. displacement curve for $[0/90]_{4s}$ cross-ply specimen with a hole of diameter 6.35 mm

From Figure 3.26, one can see that $[0/90]_{4s}$ cross-ply laminate with 6.35 mm hole in the center is almost linear elastic in nature and it can withstand a mean load of 38017 Newtons. From Table 3.10, one can also see that most of the specimens elongate less than 2mm before failure, whereas Table 3.9 shows that most of the laminates with 7.54 mm hole elongate more than 2mm with lesser failure load. This implies that laminate with a 6.35 mm is stiffer compared to the laminate with a 7.54 mm hole.

3.6.6 Tensile Testing Data of Un-notched Cross-ply Specimen

Five flat laminates of size 12"x12" are made to get all the 25 specimens. Specimens are tested in the MTS machine at a loading rate of 50lb/sec.Test results are summarized in Table 3.11 and a typical load vs. displacement curve is shown in Figure 3.27.

Spec. No.	Width mm	Failure load Newtons	Failure Strength MPa
1	37.35	71792	949.67
2	37.41	78663	1030.75
3	37.39	79067	1032.54
4	37.24	80000	1054.09
5	37.79	76792	989.81
6	37.39	77581	1024.12
7	37.48	75462	986.47
8	37.59	79932	1044.92
9	38.16	76444	988.77
10	37.50	78681	1035.61
11	37.32	78987	1042.61
12	37.26	86562	1186.51
13	37.74	89201	1177.67
14	37.40	85944	1161.76
15	37.91	85469	1138.65
16	37.97	87733	1180.08
17	38.17	83036	1105.96
18	37.40	84521	1146.59
19	38.02	86252	1155.08
20	36.88	85369	1177.41
21	38.54	81193	1071.57
22	37.30	78736	1073.69
23	37.42	83109	1130.84
24	37.21	63711	868.69
25	37.96	78157	1072.36

Table 3.11 Experimental results of $[0/90]_{4s}$ un-notched laminate

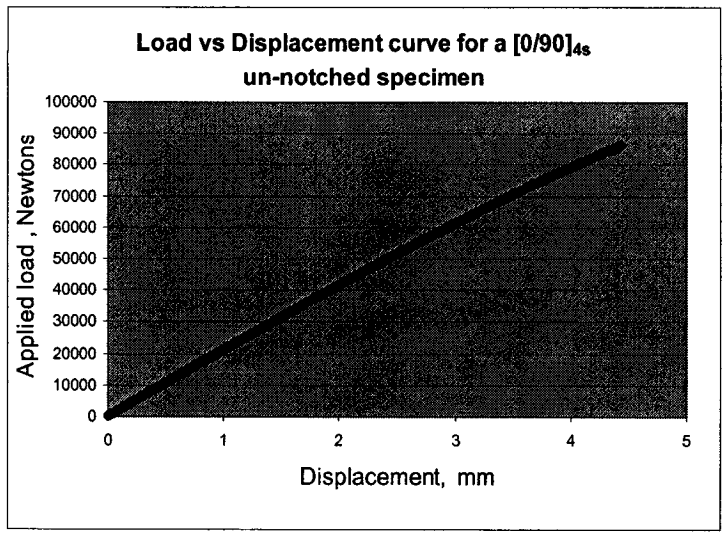

Figure 3. 27 A typical load vs. displacement curve for $[0/90]_{4s}$ cross-ply un-notched specimen

From Figure 3.27, one can see that $[0/90]_{4s}$ un-notched cross-ply specimen can withstand a mean load of 80498 Newtons, which is more than double of the strength of the specimens with a 6.35 mm hole, the value of which is 38017 Newtons.

3.6.7 Tensile Testing Data of $[0/90]_{4s}$Un-notched and Notched Specimens with a Hole of Diameter 5.10 mm

Test data of $[0/90]_{4s}$ cross-ply laminate without a hole and with a hole of diameter 5.1 mm are taken from Shashank [3], who did the test by using the same graphite/epoxy, NCT 301 prepreg material, in 2000, for his M.A.Sc thesis work at Concordia University. These experimental data are used to do the stochastic analysis in the present thesis work to see the effects of different hole sizes on the reliability of the cross-ply laminate. Test data for notched and un-notched specimens are listed in Tables 3.12 and 3.13.

Spec. No.	Width	Hole diameter	Failure load	Failure Strength
	mm	mm	Newtons	MPa
1	37.59	5.08	43890	675.4
2	37.90	5.08	41288	629.3
3	37.78	5.08	41439	634.0
4	36.99	5.08	42631	668.4
5	37.83	5.08	43290	661.3
6	37.96	5.08	41839	636.6
7	37.56	5.08	42178	649.6
8	37.69	5.08	42600	653.5
9	37.66	5.08	40523	622.2
10	37.86	5.08	42035	641.5
11	37.86	5.08	40985	625.5
12	37.92	5.08	39891	607.7
13	37.96	5.08	42195	642.0
14	37.54	5.08	42418	653.7
15	37.83	5.08	43668	667.0
16	37.43	5.08	45474	703.2
17	37.89	5.08	41297	629.7
18	37.96	5.08	42178	641.7
19	38.08	5.08	41261	625.5
20	37.97	5.08	41421	630.0
21	37.09	5.08	41733	652.2
22	37.14	5.08	39713	619.7
23	37.46	5.08	40638	627.9
24	37.24	5.08	42622	663.0
25	37.66	5.08	43049	661.0

Table 3.12 Test data of the $[0/90]_{4s}$ specimens with a hole of diameter 5.1 mm [3]

Spec. No.	Width	Failure load	Failure Strength
	mm	Newtons	MPa
1	38.35	69352	904.20
2	37.53	61959	825.50
3	37.70	63143	837.40
4	37.27	70535	946.30
5	37.83	67342	890.10
6	37.68	62386	827.80
7	37.72	71679	950.10
8	37.65	69993	929.50
9	37.72	74014	981.10
10	37.45	74294	991.90
11	37.74	72212	956.70
12	37.68	71714	951.60
13	37.16	71163	957.50
14	37.73	73191	969.90
15	37.30	73418	984.10
16	37.66	73342	973.70
17	37.83	79258	1047.6
18	37.84	70313	929.10
19	37.47	77604	1035.5
20	37.75	73760	977.00
21	37.26	57845	776.20
22	36.75	74681	1016.1
23	38.12	74143	972.50
24	38.39	75068	977.70
25	37.42	78404	1047.60

Table 3.13 Test data of un-notched $[0/90]_{4s}$ cross-ply specimens [3]

Mean, standard deviation and coefficient of variation values of all the experimental data for notched and un-notched specimens are summarized in Table 3.14.

Hole size	Specimen without hole	Mean Failure load	Mean ultimate strength	Std. dev. of ultimate strength	C.O.V. of ultimate strength	Mean displacement at failure
mm		Newtons	MPa	MPa	%	mm
	Un-notched specimen	80496	1073.40	82.34	7.67	4.6794
5.10		42009	644.80	21.35	3.31	Not given in reference
6.35		38017	602.32	20.59	3.42	1.8864
7.54		34932	577.10	20.13	3.49	1.9468

Table 3.14 Mean, standard dev. and coefficient of variation values of failure load and ultimate strength of notched and un-notched specimens

From Table 3.14, one can see that variation of ultimate strength from mean for the laminate without hole is 7.67% which is almost two times the variation for the laminate with a hole for all 3 hole sizes that are 3.31%, 3.42% and 3.49%. From these results, one can conclude that for the case of plate with hole there is stress concentration, which is localized in a small region around hole, which leads to failure. So the failure region is small compared to the entire plate. But for the case of plate without a hole, the failure region is the entire structure which leads to more variation in the ultimate strength.

In Figure 3.28, ratio of notched and un-notched strength of the laminates is plotted against the hole width ratio to get an overview of the notch size effects on the strength of the laminate.

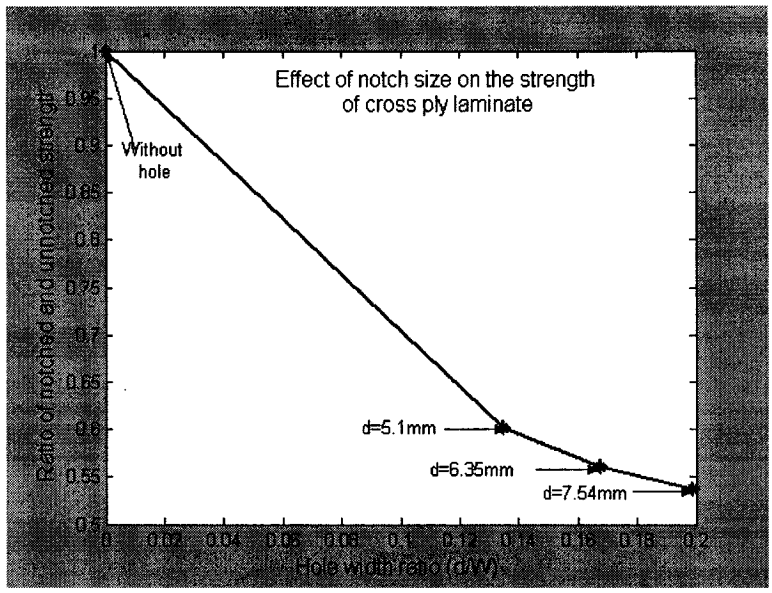

Figure 3.28 Effect of hole size on the strength of $[0/90]_{4s}$ cross-ply specimen

From Figure 3.28, one can see that strength decreases drastically from that of a plate without hole to that of a plate with a hole of size 5.1 mm. This is due to higher stress concentration for smaller hole. As the hole size increases from 5.1 mm to 6.35 mm and further to 7.54 mm the decrease of strength is less sharp than before. This is because stress concentration factor is comparatively small for larger hole than the smaller hole.

3.6.8 Tensile Testing Data of $[\pm 45]_{4s}$ Laminate with a Hole of Nominal Size 6.35 mm in the center

Specimens of this type are tested to verify the results of the MATLAB® program with the reference [11]. Displacements obtained from these experiments are checked with the MATLAB® results. Experimental data of these laminates are listed in Table 3.15 and a typical load vs. displacement curve is shown in Figure 3.29.

Spec. No.	Width mm	Hole dia. mm	Failure load Newtons	Failure Strength MPa	Displac-ement at 3000 N mm	Displac-ement at failure mm
1	37.86	6.35	17041	269.33	0.5379	22.05
2	37.60	6.35	16865	269.71	0.5414	21.44
3	37.83	6.35	16948	268.52	0.5355	22.74
Mean value of all three specimens			16952	269.18	0.5382	22.07

Table 3.15 Experimental results of $[\pm 45]_{4s}$ laminate with a hole of nominal size 6.35 mm

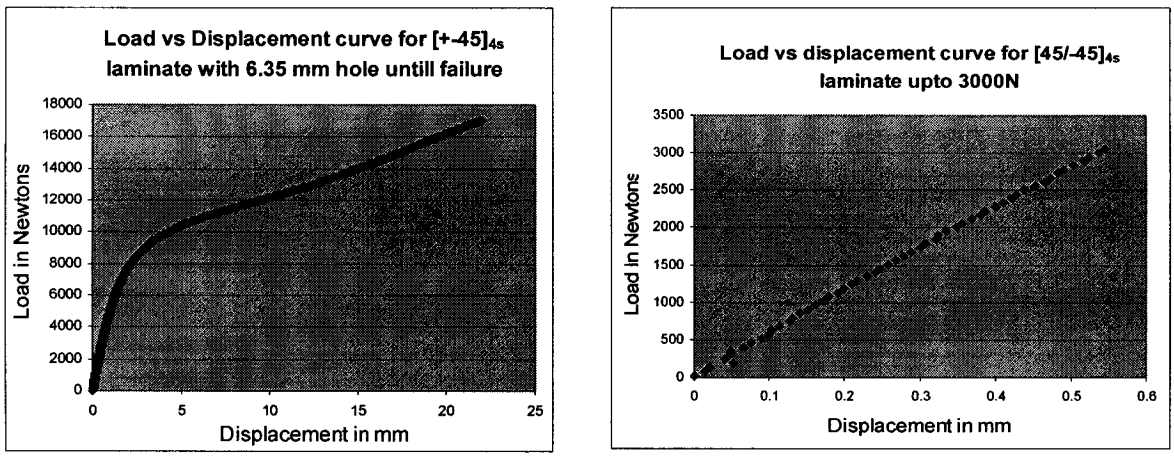

Figure 3.29 Load vs. displacement curve for a typical $[\pm 45]_{4s}$ specimen

From Tables 3.14 and 3.15 one can see that strength of $[\pm 45]_{4s}$ laminate with a hole of 6.35 mm diameter is 269.18 MPa, whereas the $[0/90]_{4s}$ laminate with the same geometric configuration has the strength of 602.32 MPa, which is 2.24 times more than that of the $[\pm 45]_{4s}$ laminate. That is because $[0/90]_{4s}$ laminate is mainly fiber dominated whereas the other one is matrix dominated.

From Figure 3.29, one can also see that $[\pm 45]_{4s}$ laminate is mostly non-linear in nature. Only for a very small region up to 3000 Newtons it is almost linear. Finite element formulation in the present work is based on linear elastic analysis. That is the basis for choosing the analysis load as 3000 Newtons, after that load the laminate is non-linear.

One more thing to be noticed here is that displacement of $[0/90]_{4s}$ laminate with a mean load of 38017 Newtons at the time of failure is 1.8864 mm, whereas $[\pm 45]_{4s}$ laminate displaced up to 22.07 mm with a mean failure load of 16952 Newtons. That is because failure of this laminate involves more delamination than any other laminate.

3.7 Photographs of the Notched Specimens before and after Failure

Photographs of each of the different types of the tested notched specimens, before and after failure with test setup are taken. These photographs will help us to understand the failure modes of different notched specimens under tensile load in the MTS machine.

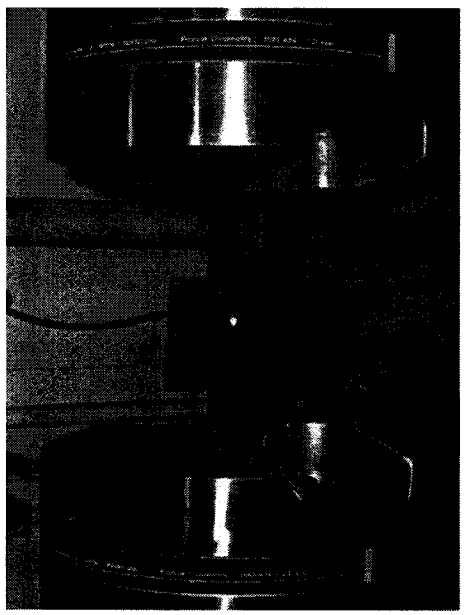

a) $[0/90]_{4s}$ cross-ply specimen with a hole of diameter 6.35 mm before failure in MTS machine

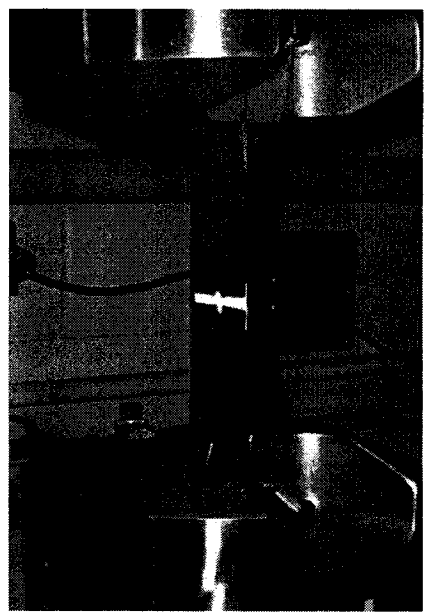

b) $[0/90]_{4s}$ cross-ply specimen with a hole of diameter 6.35 mm after failure in MTS machine

Figure 3.30 Experimental set up of $[090]_{4s}$ specimen with a hole

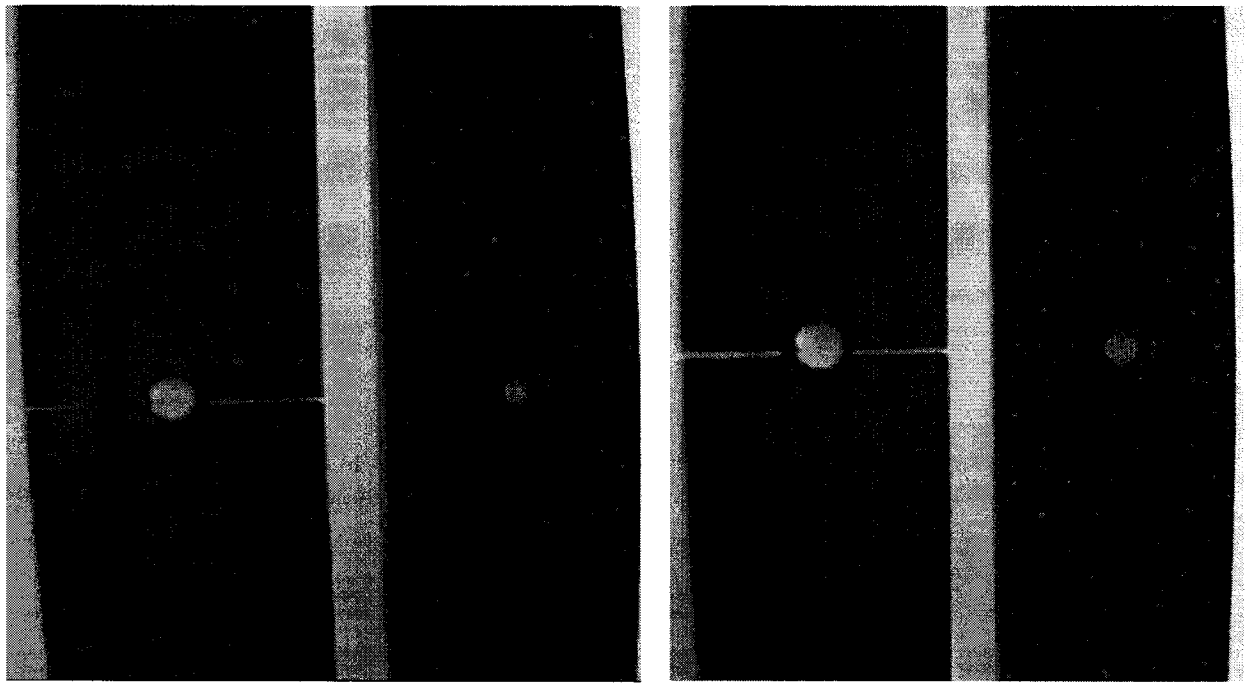

a) Typical failure of a $[0/90]_{4s}$ cross-ply specimen with a hole of diameter 6.35 mm before and after failure.

b) Typical failure of a $[0/90]_{4s}$ cross-ply specimen with a hole of diameter 7.54 mm before and after failure.

Figure 3.31 Pictures of notched specimen before and after failure

From Figure 3.31, one can make out that the failure of $[0/90]_{4s}$ cross-ply laminates with hole sizes of 6.35 mm and 7.54 mm take place in a direction perpendicular to the loading and across the circular cutout. This is due to the presence of 90^0 ply in the laminate configuration. Failure begins with the matrix cracking followed by fiber breakage.

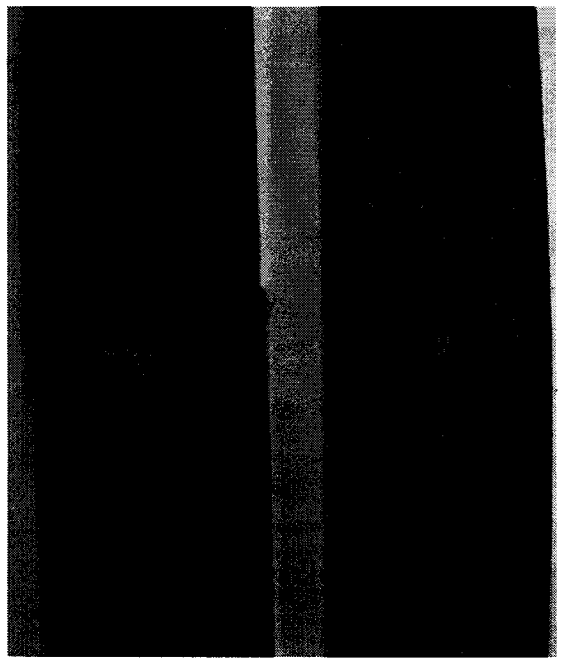

Figure 3.32 A typical picture of a $[\pm 45]_{4s}$ specimen with a hole of diameter 6.35 mm before and after failure

From Figure 3.32, one can make out that $[\pm 45]_{4s}$ laminate with a hole of 6.35 mm fails in two directions that are at 45^0 and -45^0 with the direction of loading and across the circular cutout. Failure begins with the matrix cracking followed by delamination of 45^0 and -45^0 fibers in both the directions.

3.8 Micro Structural Study of Notched Specimen

In the same way as described in Section 3.5, a micro structural study is conducted on notched specimens. Here the region of interest is the hole periphery. Due to the drilling operation on the specimen, the region near the hole is more vulnerable to damage. So specimens are cut along the width in the middle of the hole and prepared in the same way as described earlier. These things are shown more clearly in Figure 3.33. After that the cross section near the edge of the hole is focused under the microscope and the image of the specimen is taken by a camera attached with the microscope.

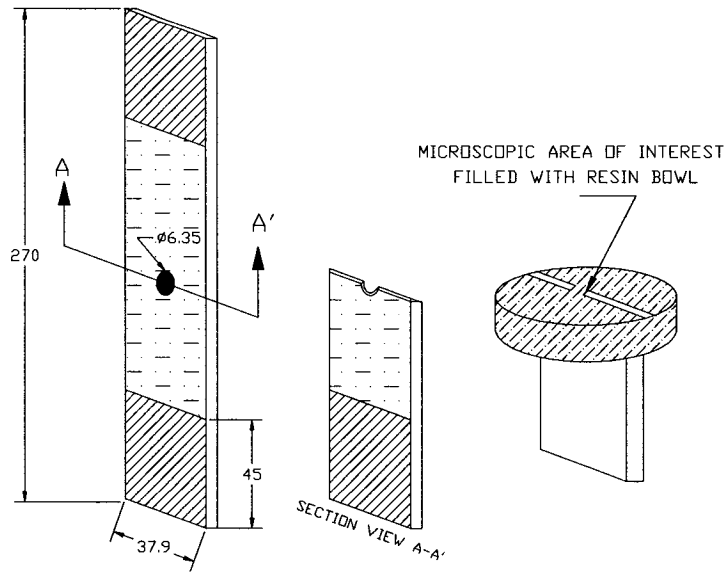

Figure 3. 33 Notched specimen for microscopic study

In Figures 3.34, 3.35 and 3.36, typical microscopic images of un-notched $[0/90]_{4s}$ specimen before failure and specimens with 6.35 mm hole before and after failure are shown. A magnification value of 100X is used in the microscope to see the images of all the notched specimens.

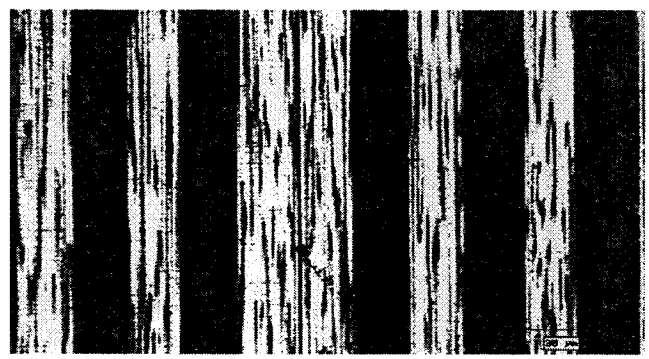

90 0 90 0 90 90 0 90 0 90 0

Figure 3.34 A typical image of $[0/90]_{4s}$ specimen without hole observed under a microscope

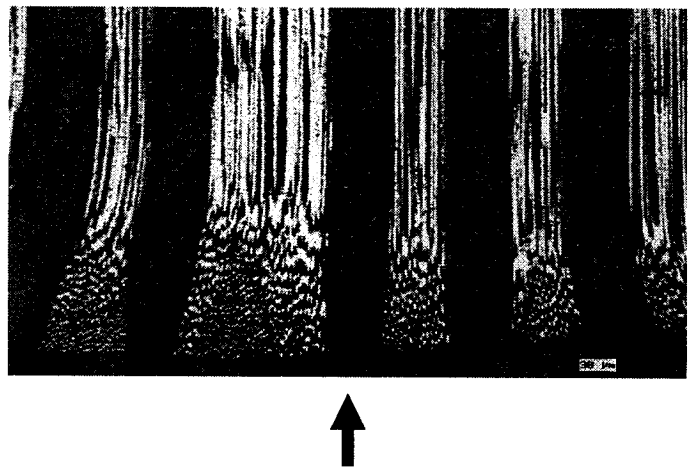

Figure 3.35 A typical image of a $[0/90]_{4s}$ specimen with a hole of diameter 6.35 mm before failure, observed under a microscope (arrow mark indicates the hole edge)

Figure 3.36 A typical image of $[0/90]_{4s}$ specimen with a hole of diameter 6.35 mm after failure, observed under a microscope (arrow mark indicates the hole edge)

Microscopic image of $[0/90]_{4s}$ cross-ply specimen without hole is given in Figure 3.34. No significant defects are found on the image. Layers of 0^0 and 90^0 fibers are arranged in a good shape almost at equal distance from each other.

In Figures 3.35 and 3.36, $[0/90]_{4s}$ cross-ply specimens with a hole of 6.35 mm before and after failure are shown. From Figure 3.35, one can make out that some of the 0^0 and 90^0 fibers are reshaped and few 900 fibers are broken at the hole edge due to the drilling operation but fibers in the 0^0 layers are not broken. As the load is mainly carried by the 0^0

fiber, the damage of the 90^0 fiber will not affect much the strength of the laminate. Again a damage area of approximately 50 microns x 30 microns is negligible compared to the dimensions of the laminate. From Figure 3.36, one can make out that a typical failure occurred due to matrix cracking in the 90^0 layer followed by fiber breakage in the 0^0 layer. In Figures 3.37 and 3.38, typical microscopic images of notched $[0/90]_{4s}$ specimens with a hole of 7.54 mm diameter, before and after failure are shown.

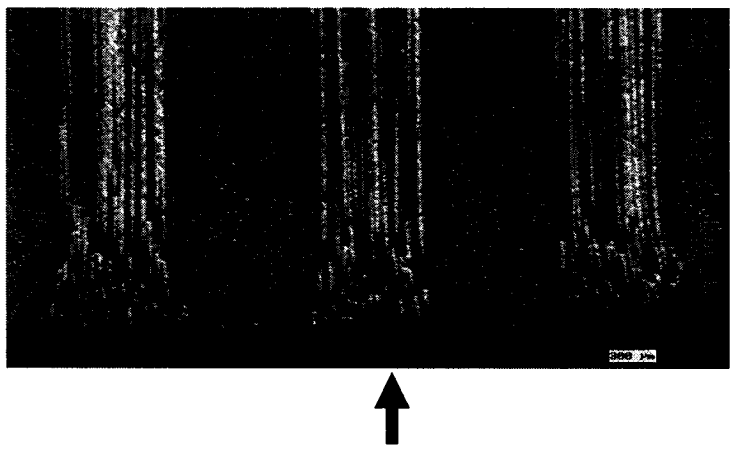

Figure 3.37 A typical image of [0/90]4s specimen with a hole of diameter 7.54 mm before failure, observed under a microscope (arrow mark indicates the hole edge)

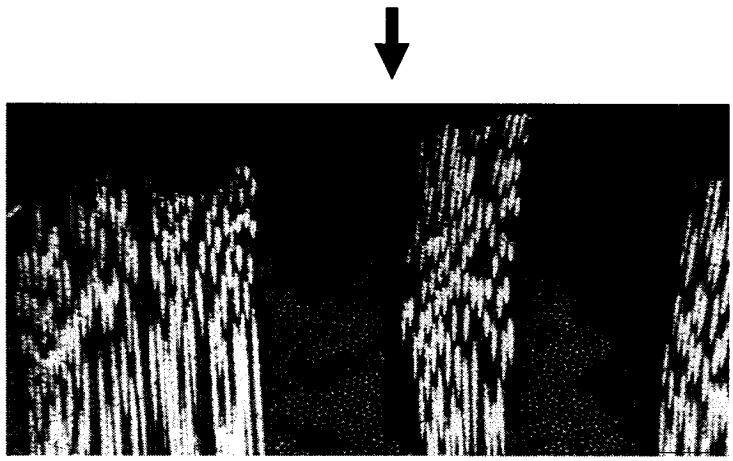

Figure 3.38 A typical image of [0/90]4s specimen with a hole of diameter 7.54 mm after failure, observed under a microscope (arrow mark indicates the hole edge)

From Figures 3.37 and 3.38, one can see that same thing that is found for hole of diameter 6.35 mm, has happened for the case of 7.54 mm.

3.9 Characteristic Length (CHLEN) Calculation

As mentioned in Sections 3.6.1 and 3.6.2, in order to find out the characteristic length value of a laminate, a set of un-notched and notched strength values have to be found out. Table 3.11 lists the experimental strength values of un-notched specimens. Tables 3.9 and 3.10, list the ultimate strength values obtained experimentally for specimens with hole sizes of 7.54 mm and 6.35 mm respectively. Characteristic lengths d_o and a_o are found out by using equations (3.4) and (3.6). For example from Table 3.10, considering specimen number 20, the ultimate strength value for a notched laminate of hole size 6.35 mm is 586.7MPa. Now from Table 3.11, for specimen number 7, the ultimate strength value for an un-notched laminate is 986.47MPa. These values are used in equations (3.4) and (3.6) respectively to obtain the corresponding value of characteristic lengths d_o and a_o. A similar procedure is adopted for the hole size 7.54 mm also. Sub-routine aodo_calculation.m given in appendix–D is used to calculate the value of all the characteristic lengths for 25 specimens each with different hole size.

Characteristic length values obtained using point stress criterion are listed in Table 3.16 and their mean, standard deviation and coefficient of variation values are listed in Table 3.17. Characteristic length values listed in the 2nd column of Table 3.16 for the hole size of 5.1 mm are calculated by using the data taken from reference [3]. So, at this point CHLEN values for hole diameter 5.1 mm will not be compared with the CHLEN values obtained for

hole diameter 6.35 mm and 7.54 mm. Rather CHLEN values obtained for hole diameter 6.35 mm and 7.54 mm will be compared.

Sl. No.	d_o for hole size 5.10 mm	d_o for hole size 6.35 mm	d_o for hole size 7.54 mm
	mm	mm	mm
1	1.1500	0.8980	0.9270
2	1.2320	0.8460	0.9060
3	1.2030	0.7190	0.8430
4	0.9820	0.9690	1.0080
5	1.1310	0.9820	0.9450
6	1.2720	0.8530	0.9520
7	0.9070	0.8720	0.9940
8	1.2000	0.7740	0.9190
9	0.8780	1.0030	0.9950
10	0.8050	0.7890	0.9380
11	0.8230	0.8760	1.0010
12	0.8440	0.5960	0.6590
13	0.8690	0.6810	0.7860
14	0.8790	0.6720	0.7490
15	0.8900	0.7090	0.8540
16	0.7860	0.8310	0.8800
17	0.7470	0.7530	0.8440
18	0.9290	0.6890	0.7210
19	0.7070	0.7330	0.7900
20	0.7750	0.6950	0.7830
21	1.62100	1.0740	1.1180
22	0.6940	0.7710	0.8800
23	0.8020	0.7520	0.8620
24	0.8910	0.6760	0.6910
25	0.7500	0.7690	0.8530

Table 3.16 Values of characteristic length d_o, obtained using point stress criterion

Hole diameter	Mean d_o	Std. Dev. value of d_o	C.O.V.	Maximum value of d_o	Minimum value of d_o
mm	mm	mm	%	mm	mm
5.10	0.9507	0.2230	23.46	1.6210	0.6940
6.35	0.7993	0.1193	14.93	1.0740	0.5960
7.54	0.8759	0.1096	12.51	1.1180	0.6590

Table 3.17 Statistics of characteristic length d_o for different hole sizes

From Table 3.17, one can see that mean CHLEN value for hole diameter 7.54 mm is greater than that of hole diameter 6.35 mm. This implies that more area near hole is damaged by bigger hole than the smaller hole.

Characteristic length values obtained using average stress criterion are listed in Table 3.18 and their mean, standard deviation and coefficient of variation values are listed in Table 3.19. As described before for point stress criterion, characteristic length values listed in the 2nd column of Table 3.18 for the hole size of 5.10 mm are taken from reference [3]. So, at this point CHLEN values for hole diameter 5.10 mm will not be compared with the CHLEN values obtained for hole diameter 6.35 mm and 7.54 mm. Rather CHLEN values obtained for hole diameter 6.35 mm and 7.54 mm will be compared.

Sl. No.	a_o for hole size 5.10 mm	a_o for hole size 6.35 mm	a_o for hole size 7.54 mm
	mm	mm	mm
1	6.39	3.54	3.34
2	7.04	3.21	3.21
3	6.80	2.46	2.86
4	5.02	4.02	3.83
5	6.23	4.11	3.44
6	7.34	3.25	3.49
7	4.42	3.37	3.74
8	4.93	2.77	3.28
9	3.37	4.25	3.75
10	3.60	2.86	3.40
11	3.74	3.40	3.79
12	3.45	1.83	1.95
13	4.10	2.25	2.56
14	4.18	2.20	2.37
15	4.27	2.40	2.92
16	5.51	3.11	3.06
17	2.82	2.65	2.86
18	4.59	2.30	2.24
19	2.87	2.53	2.58
20	3.57	2.33	2.54
21	2.24	4.75	4.55
22	3.57	2.75	3.06
23	3.58	2.64	2.96
24	4.28	2.23	2.10
25	3.31	2.74	2.91

Table 3.18 Values of characteristic length a_o, obtained using average stress criterion.

Hole size mm	Mean of a_o mm	Std. dev. of a_o mm	C.O.V. %	Maximum Value of a_o mm	Minimum Value of a_o mm
5.10	4.440	1.3920	31.35	7.34	2.24
6.35	2.958	0.7357	24.87	4.75	1.83
7.54	3.0716	0.6144	20.00	4.55	1.95

Table 3.19 Statistics of characteristic length a_o for different hole sizes

From Table 3.17, one can see that mean CHLEN value for hole diameter 7.54 mm is greater than that of hole diameter 6.35 mm. This implies the same meaning as of point stress criterion that more area near hole is damaged by bigger hole than the smaller hole. Again from Tables 3.17 and 3.19, one can see that CHLEN values obtained by average stress criterion are always differ by a great number from that of point stress criterion for all the hole sizes. The reason for that is, average stress criterion considers the stresses over a region near hole and averaged those stresses, whereas point stress criterion considers stress at a point near hole.

It is to be noted here that the ratio $\frac{\sigma_N}{\sigma_o}$ (ultimate strength value of a notched laminate to ultimate strength value of a un-notched laminate) on the left hand side of the equations (3.4) and (3.6) is very sensitive when used to calculate the value of characteristic length for any laminate. The values of d_o and a_o depend mainly on the experimental results, obtained from the testing of notched and un-notched laminates.

It is important to highlight that the values of characteristic length obtained are based on different combinations of ultimate strength values of notched laminates and ultimate strength values of un-notched laminates obtained experimentally. This means to say that, the notched laminate numbered 1 in Table 3.9 need not be considered together with the un-notched laminate numbered 1 in Table 3.11 to find out the value of characteristic length. In certain situations, it is observed that considering a similar pair of laminates in Tables 3.9 and 3.11 may result in a higher value of characteristic length, which is irrelevant to other values of characteristic length of the same group.

3.10 Conclusions and Discussions

In Section 3.3 tests are conducted on three different types of specimens with uniform cross section to get the material properties of a lamina (layer of prepreg) that will be used in the stochastic analysis. The experimental values of mean, standard deviation and coefficient of variation of Young's modulus, Poisson's ratio and shear modulus are listed in Table 3.7.

In Sections 3.4 and 3.7 photographs of the tested specimens before and after failure are taken to explain the failure mode. In Sections 3.5 and 3.8 micro structural studies on uniform and notched specimens are described respectively to explain the micro structure of matrix and fiber, before and after failure.

In Section 3.6 tests are conducted on notched specimens with hole diameter of 6.35 mm and 7.54 mm and also on un-notched specimens to determine the ultimate strength. Notched and un-notched strength values with failure displacements are summarized in Table 3.14. In Figure 3.28, how the strength of notched laminate changes with d/W (hole diameter to width) ratio is shown. From that graph one can conclude that the differences

between the strength values corresponding to larger hole sizes are smaller compared to that corresponding to the smaller hole sizes.

Notched and un-notched strength values obtained from Tables 3.9, 3.10 and 3.11 are used to calculate the characteristic lengths a_o and d_o, by using average stress criterion and point stress criterion.

The value of characteristic length thus obtained will be used to conduct the stochastic finite element analysis for controlled and uncontrolled hole laminates in Chapter 4, to obtain mean and standard deviation values of average and point stress values and finally to calculate the reliability.

CHAPTER 4

STOCHASTIC ANALYSIS OF NOTCHED COMPOSITE LAMINATES

4.1 Introduction

Simulation process is employed in the present work because of the randomness in the stress distribution, which is attributed to the stochastic material and geometric properties of the composite laminate. Variations in the material properties occur due to the variations in the fiber properties, matrices and interfaces, fiber orientation, fiber volume fraction and ply thickness, etc. Theses variations are quite unavoidable and most of them are induced during manufacturing. Although composite materials have attractive features, such as high ratios of strength-to-weight and stiffness-to-weight, they are easily damaged when they are machined. A typical damage is delamination, which can occur when fiber reinforced composite laminates are drilled. This in turn creates an irregularity around the circumference of the hole and hence a geometric variation results. Because of the above stated unpredictable variations, a study on stress distribution near the hole boundary of the laminate is conducted.

The MATLAB® program developed in Chapter 2 will be capable of handling the probabilistic distributions of these variations and can calculate the stresses over each laminate, with an addition of a subroutine AVGSTR.m and after suitable modifications in the main program MODIFYSTIFPS.m which is given in Appendix-C. The generalized program thus developed is capable of accepting any laminate configuration, geometry

and number of laminates to be analyzed. In the present Chapter, two stress parameters, point stress and average stress, which are considered to be the prime design parameters, are calculated. Sections 5.2 and 5.3 are completely devoted to the calculation of point stress and average stress values over laminates. Subroutine AVGSTR.m achieves the objectives by calculating the point stress and average stress value for each and every laminate and stores them automatically in a MATLAB® file. Simultaneously the maximum stress and displacement (at the loading boundary) developed in the laminate due to the application of loading are also calculated and stored in the same file.

Considering practical situations, two categories of notched laminates are analyzed:

(1) Controlled hole laminate (CHL)

(2) Un-controlled hole laminate (UCHL)

In controlled hole laminate analysis, it is assumed that geometric variation in the hole boundary and eccentricity of the hole from the center of the laminate do not exist, and only the stochastic variation in material properties are considered. Whereas in the un-controlled hole laminate analysis, all the above mentioned variations are considered, which happen in most practical situations. Accordingly for the un-controlled hole laminates, appropriate equations are taken from reference [34], which express the imperfections around the hole boundary in the form of an equation. Using the Gaussian random value generating function, the center position of the hole within the laminate is varied. An acceptable tolerance for the eccentricity of the hole from the central co-ordinates is fixed. These equations are described in Section 4.4. First-order auto regressive model or Markov model is employed, to bring in the stochastic variation of the

material properties, which has been discussed in Section 2.4.1 of Chapter 2 and used in the flowchart in Figure 2.8.

In the present work, an extensive study on $[0/90]_{4s}$ cross-ply laminate with length 180 mm, width 37.9 mm and thickness 2 mm under uniaxial load with three different hole sizes, i.e. 5.10 mm, 6.35 mm and 7.54 mm is carried out. Controlled and un-controlled hole laminate analysis is done on all the three hole sizes.

Simulation is performed over a number of laminates, adequate provisions are made in the program to calculate the point and average stresses for each and every laminate. Simulation is carried out, till the fluctuations in the point and average stress parameter values culminate. Standard deviation and hence the co-efficient of variation are calculated based on the mean value obtained.

4.2 Calculation of Average Stress and Point stress Parameters

From the MATLAB® program stresses are calculated at Gauss points of each element. Nodal stresses in turn are found out by using the Gauss point stresses that contribute to the corresponding nodes. Distribution of nodes in the laminate near hole edge A to the plate boundary B, along x axis are shown in Figure 4.1 and more details were given in Figure 2.4. There are 15 nodes in the finite element mesh along line AB. Stress distribution curve (stress profile) along line AB is represented by a 10^{th} order polynomial, which is given below

$$\sigma_y(x)=b_0+b_1x+b_2x^2+b_3x^3+b_4x^4+b_5x^5+b_6x^6+b_7x^7+b_8x^8+b_9x^9+b_{10}x^{10} \qquad (4.1)$$

The coefficients b_i, i=0,1,...10 of the polynomial equation 4.1 are calculated by using a MATLAB® function named POLYFIT.m, which utilizes the nodal stress values, the

nodal distance values along X axis from hole edge and order of polynomial as its input. Stress profile obtained by polynomial function will be used to calculate the average and point stresses by equations 3.1 and 3.5.

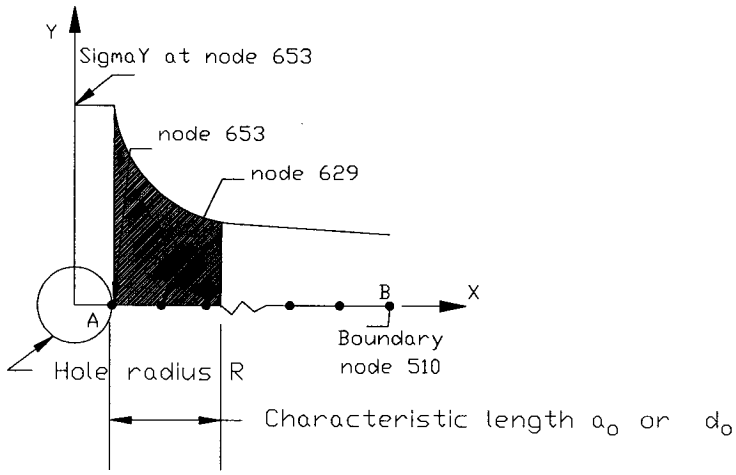

Figure 4.1 Node numbering and stress profile near hole, which will be used to calculate the average and point stresses.

Stress profiles obtained by both 10th order polynomial and by actual data are shown in Figure 4.2.

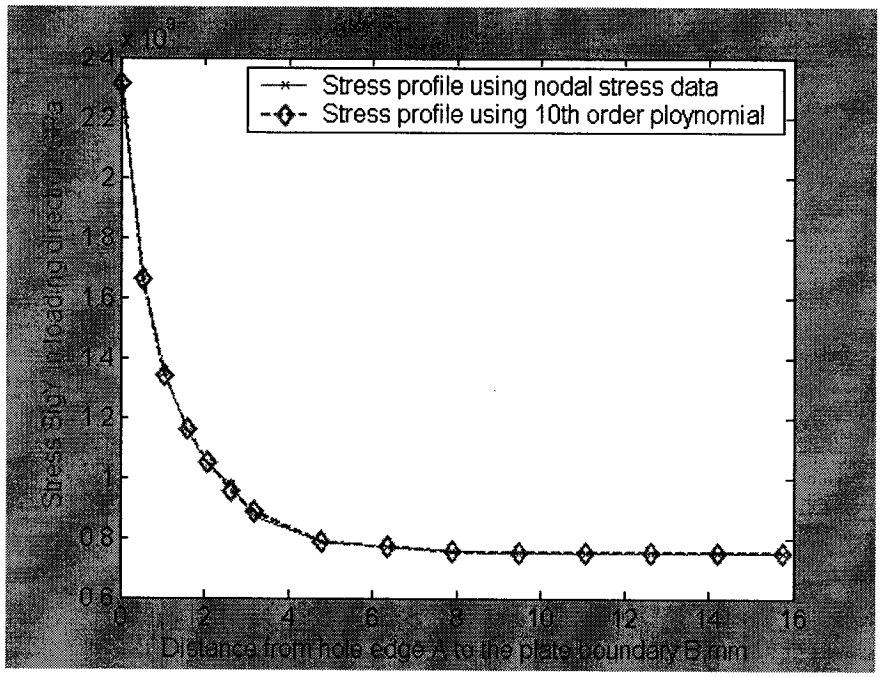

Figure 4.2 Comparison of stress profiles obtained by curve fitting of the 10^{th} order polynomial function and the actual data

From Figure 4.2, one can see that assumption of 10^{th} order polynomial function to describe the stress profile near hole edge A to plate boundary B is quite justified, as it is almost overlapping the curve of actual data of the stresses obtained by the analysis of the laminate.

4.3 Category I: Controlled Hole Laminate (CHL) Analysis

In the controlled hole laminate, only the spatial material properties are varying, while the geometric properties and values of characteristic lengths are held constant. Fluctuations in the material properties are expressed using stochastic processes as explained in Chapter 2. Analysis is performed on a laminate having a width of 37.9mm, length 180mm, ply thickness of 0.125mm and with a hole of diameter 7.54 mm. Finite element mesh utilized for the laminate analysis is shown in Figure 2.3. The material properties are taken from the testing of NCT-301 prepreg that are listed in Table 3.7. The mean ultimate

tensile load at which specimen fails as recorded from the tensile testing experiment of $[0/90]_{4s}$ notched coupons is used for the simulation. Accordingly, a uniformly distributed load of 1.1542 MN/m is applied on the laminate in the direction parallel to y-axis. The influence of the number of simulations, within the range of 1 to 300 on the probabilistic moments i.e. the mean value and variance and hence the standard deviation of the average stress (σ_{avg}) and point stress (σ_p) parameters has been studied. The variations in the mean values and standard deviation values with the number of simulations for the two parameters have been presented in Figures 4.3.a - 4.3.d.

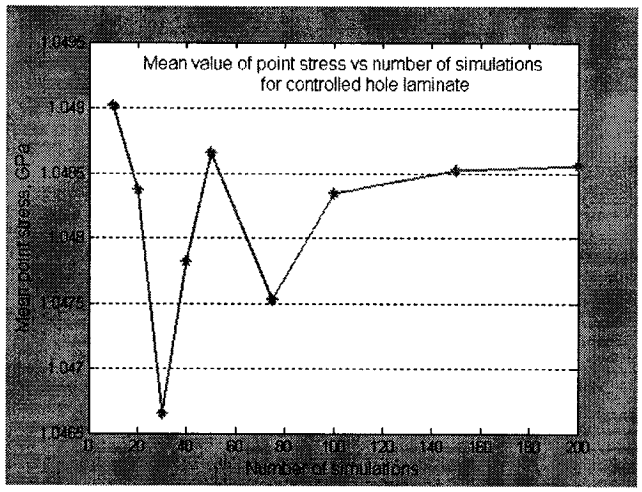

(a)

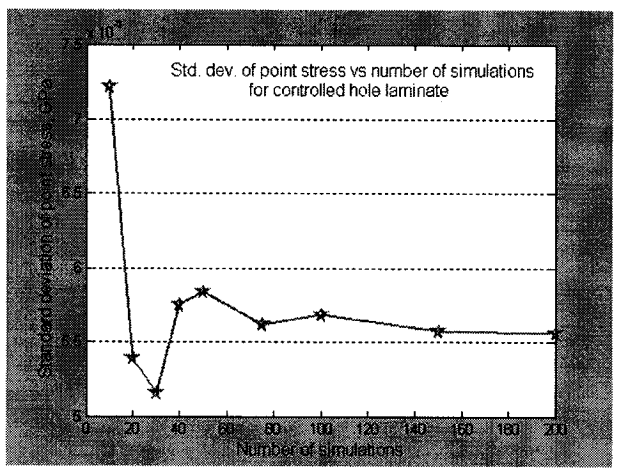

(b)

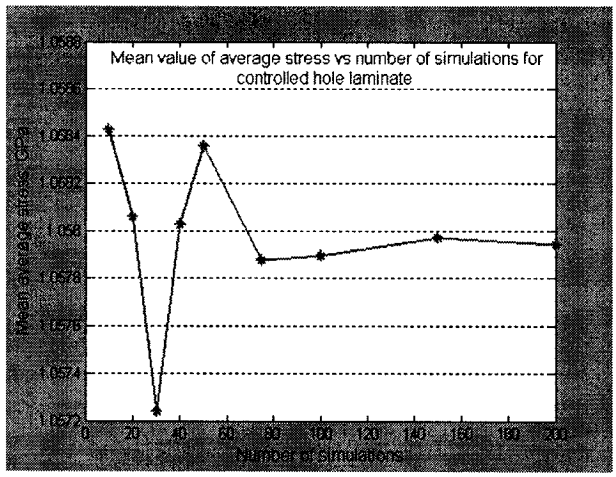

(c)

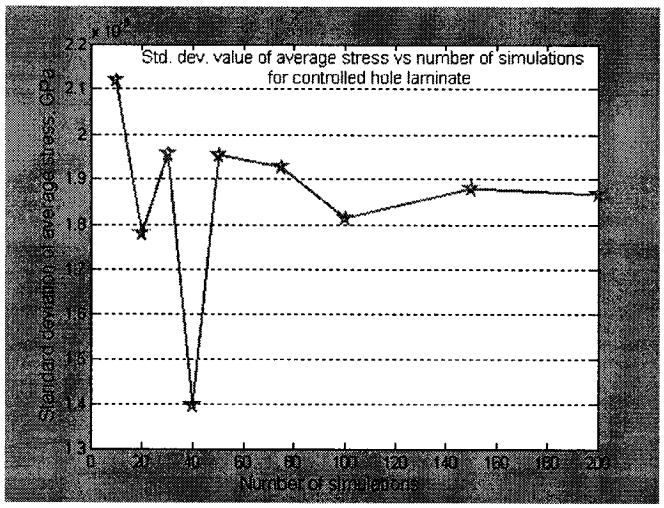

(d)

Figure 4.3 Stochastic simulation of $[0/90]_{4s}$ controlled hole laminate with 7.54 mm hole subjected to uniaxial load: (a) Mean values of point stress, (b) Std. dev. values of point stress, (c) Mean values of average stress and (d) Std. dev. values of average stress

Simulation is carried out on a controlled hole laminate subjected to uniaxial load. Our main aim is to see that the mean value of any stress parameter does not change with further increase in the number of simulations. It is observed that after 150 simulations the

mean value of point stress converges almost to a constant value of 1.04856 GPa. In the first 100 simulations, fluctuation is high, but as the number of simulations approaches 200 a steady state mean point stress value is achieved. This implies that a minimum of 200 laminates need to be simulated to achieve a mean point stress value for controlled hole laminate. Corresponding standard deviation values also have same variation in the first 150 simulations and attain a constant value at 200 simulations. This can be observed from Figure 4.3.b.

The average stress curve in Figure 4.3.c gains a steady state after 200 simulations and the corresponding mean average stress value is 1.05797 GPa. Accordingly, the standard deviation value for average stress parameter almost reaches a constant value at about 200 simulations as can be seen from Figure 4.3.d. The initial variation of values in the first 150 simulations can be attributed to the stochastic variation in the material properties induced by using the Markov correlation model. Comparing the mean point stress and mean average stress curves from Figures 4.3.a and 4.3.c respectively, it is clear that, both trajectories almost follow the same path. A similar observation can be made when a comparison is sought between the standard deviation of average stress curve and standard deviation of point stress curve as shown in Figures 4.3.b and 4.3.d.

4.4 Category II : Un-controlled Hole Laminate (UCHL) Analysis

Practically it is impossible to achieve a perfect circular hole in the structure at the desired coordinates during the manufacturing process. Thus it calls for an analysis to check for the change in the mean value of average and point stresses over the characteristic length. In the present Section un-controlled hole laminate analysis will be performed by varying material properties, geometry of the hole and also the characteristic length (by Gaussian

random variation). Mean value of maximum stress at the hole edge will also be checked. Based on reference [34], hypotrochoid variation in the hole shape in Cartesian coordinates is considered and the equation for variation is given by:

$$x = R(\cos\alpha + \psi\cos\rho\alpha), y = R(\sin\alpha - \psi\sin\rho\alpha) \tag{4.2}$$

where the value of ρ is 7 (a non-negative integer), $\psi = 0.01$ and $0 < (\rho\Psi) < 1$. These two parameters describe the irregularity in the hole shape. Here α is the angle at which a node is created on the circle while developing a finite element mesh. Maximum tolerance for eccentricity of the hole is of the order of $\left(\frac{1}{20}\right)^{th}$ of an inch [3]. Gaussian random variables are generated and these values control the movement of the hole depending on the number of the nodes associated with the hole. Modifications in the circular opening are reflected in subroutines HOLE_UNCERTAINITY.m and GLOB_COORD.m. Change of circular shape of the hole due to hypotrochoid variation is shown in Figure 4.4.

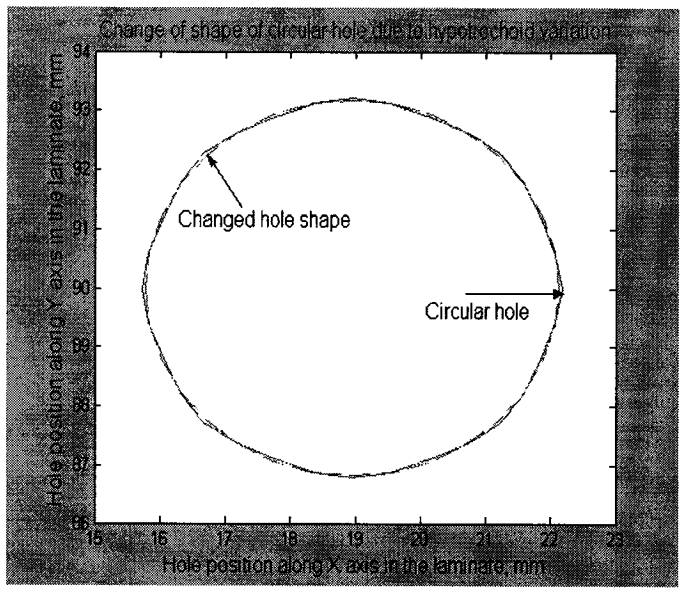

Figure 4.4 Shape change of circular hole due to hypotrochoid variation

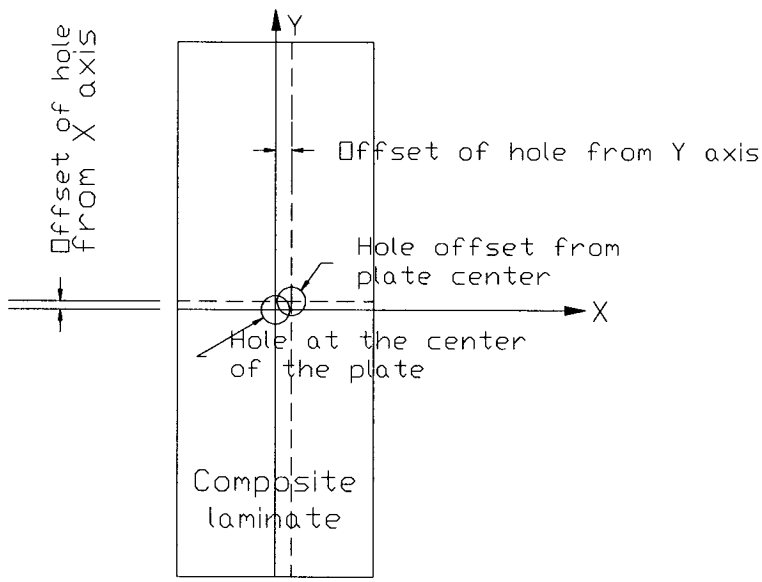

Figure 4.5 Eccentricity of the hole from plate center

Eccentricity of the hole from plate center is clearly shown in Figure 4.5. It is to be noted that, in the case of uncontrolled circular opening, as the hole location is not fixed, the value of characteristic length ceases to remain constant. Assuming the variation in the characteristic length to follow a Gaussian distribution, a series of values are generated for the characteristic lengths a_o and d_o using the subroutine DISAODO.m in the MATLAB® program. Sub-routine DISAODO.m in turn uses a MATLAB® sub-function:

$$[R] = a_2 + (a_1 - a_2) * rand(m,n) \tag{4.3}$$

where 'rand' is the sub-function, 'a_1' and 'a_2' are the maximum and minimum limits of the value of characteristic length respectively, m is the number of rows of Gaussian random numbers to be generatced and 'n' is the number of columns to be realized. In the present case 'm' is assigned a value equal to the number of laminates to be analyzed and 'n=1', giving matrix [R] a dimension (m*n).

In order to compare the behavior of an un-controlled hole laminate with that of a controlled hole laminate, the plate geometry, hole size, boundary conditions and application of load are kept same as that for a controlled hole laminate. But it is to be noticed, that the finite element mesh close to the hole boundary assumes new co-ordinate values based on the tolerance value set. Referring to Tables 3.16 and 3.18, it is clear that the value of characteristic lengths a_o and d_o will not remain constant all the time. MATLAB® program developed generates as many values of characteristic length as the number of simulations and these values are based on the Gaussian distribution method. Figures 4.6 and 4.7 show the Gaussian distribution curves for the values of characteristic lengths a_o and d_o for hole diameter 7.54 mm. Following distribution is achieved by supplying values from the Tables 3.16 and 3.18. It can be noticed that the curve in Figure 4.6 has a minimum value of 0.6590 mm and maximum of 1.1180 mm as can be made out from Table 3.16.

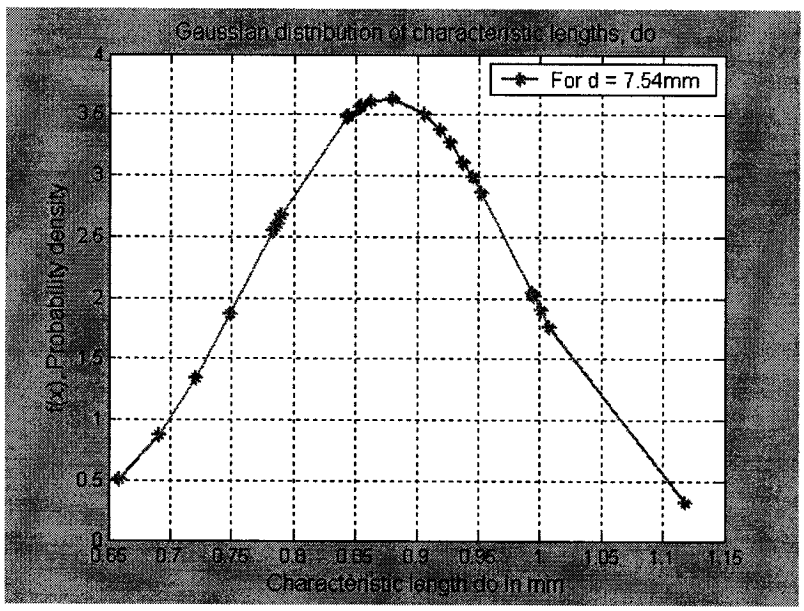

Figure 4.6 Gaussian distribution curve for the value of characteristic length d_o for hole diameter of 7.54 mm.

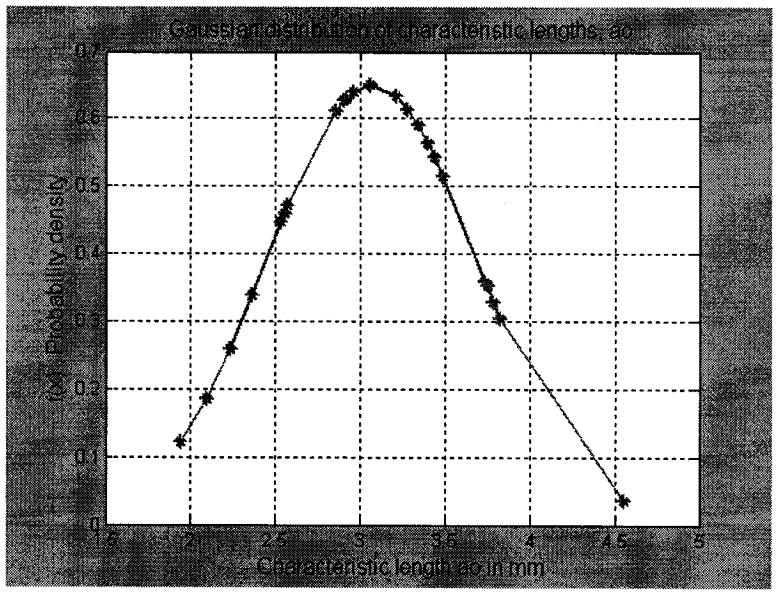

Figure 4.7 Gaussian distribution curve for the value of characteristic length a_o for hole diameter of 7.54 mm.

Maintaining similar condition as expressed for controlled hole laminate with hole diameter 7.54 mm, simulation is carried out to achieve mean point and average stress values for the uncontrolled hole laminate. The corresponding plots are shown in Figures 4.8.a - 4.8.d.

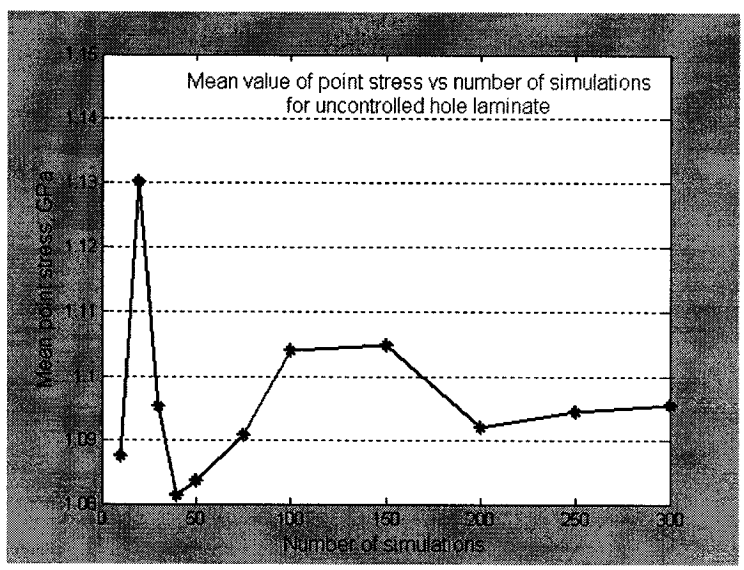

(a)

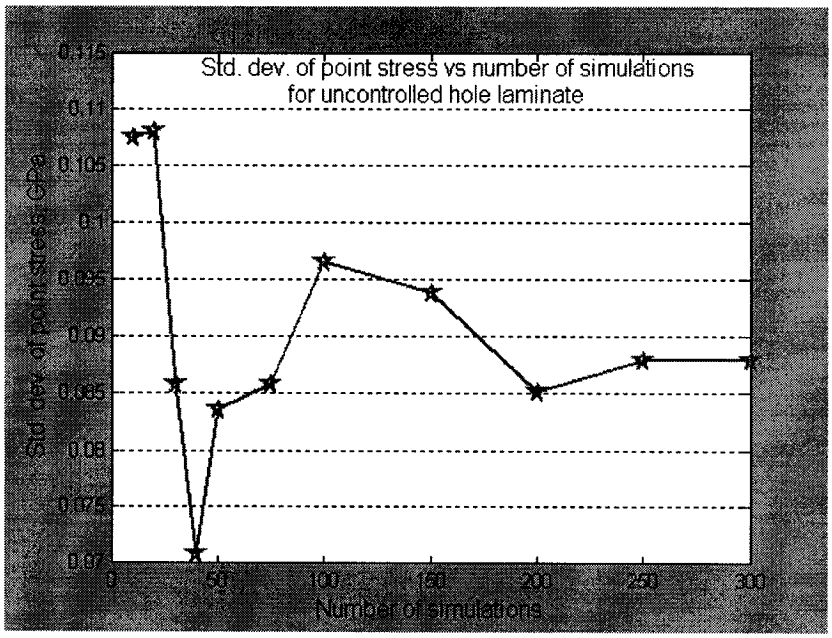
Std. dev. of point stress vs number of simulations
for uncontrolled hole laminate
Std dev. of point stress, GPa
Number of simulations
0.115
0.11
0.105
0.1
0.095
0.09
0.085
0.08
0.075
0.07
0
50
100
150
200
250
300

(b)

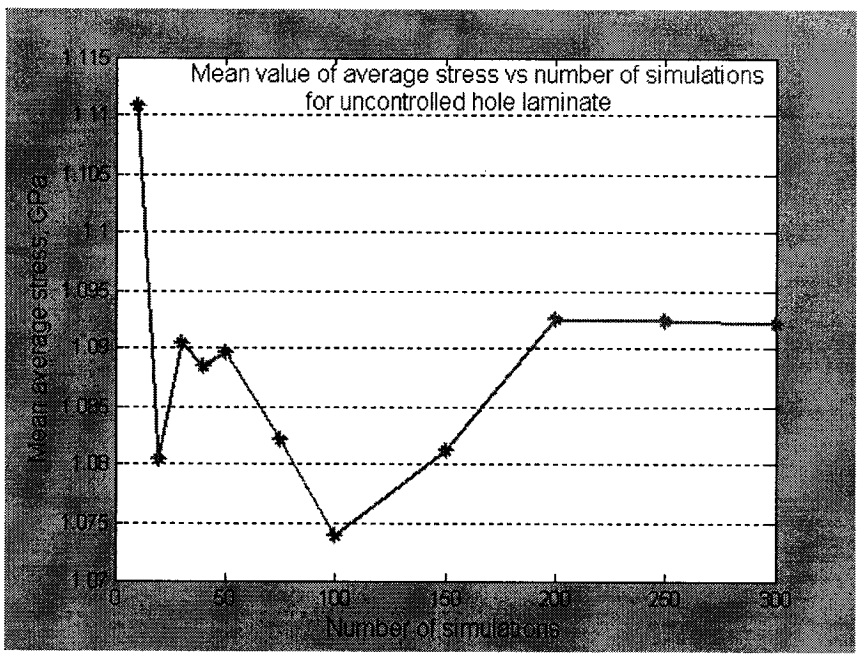
Mean value of average stress vs number of simulations
for uncontrolled hole laminate
Mean average stress, GPa
Number of simulations
1.115
1.11
1.105
1.1
1.095
1.09
1.085
1.08
1.075
1.07
0
50
100
150
200
250
300

(c)

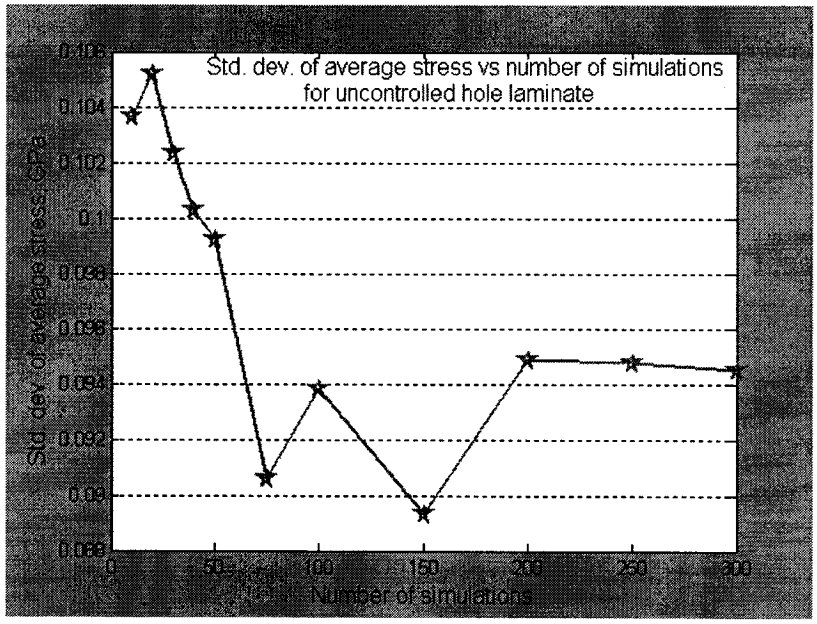

(d)

Figure 4.8 Stochastic simulation of $[0/90]_{4s}$ un-controlled hole laminate with 7.54 mm hole subjected to uniaxial load: (a) Mean values of point stress, (b) Std. dev. values of point stress, (c) Mean values of average stress and (d) Std. dev. values of average stress.

It is observed that after 300 simulations the mean value of point stress converges almost to a constant value of 1.09635 GPa. In the first 150 simulations, fluctuation is high, but as the number of simulations approaches 300 a steady state mean point stress value is achieved. This implies that a minimum of 300 laminates need to be simulated to achieve a mean point stress value for uncontrolled hole laminate. Corresponding standard deviation value also has same variation in the first 150 simulations and attains a constant value at 300 simulations. This can be observed from Figure 4.3.b. Similarly the mean value of average stress converges almost to a value of 1.09121 GPa after 300 simulations. Same thing happens for standard deviation value of average stress. Point stress reaches a

stable state near 250 simulations whereas average stress reaches near 200 simulations. This is because point stress is calculated at a point in the stress profile, whereas the average stress is calculated by averaging the stresses over a region in the stress profile.

4.5 Comparative Study of Stress Parameters Obtained using Controlled and Uncontrolled Hole Laminate Conditions

In Sections 4.3 and 4.4, simulations on controlled and uncontrolled hole laminate were conducted in detail respectively, and we have determined the total number of simulations that will be required to obtain the mean stress parameters without fluctuations. Both the cases, laminate configurations, geometry, loading parameters and boundary conditions are kept the same and in addition, the hole shape, hole eccentricity and changes in characteristic lengths are included in uncontrolled hole laminate. The amount of variation the uncontrolled hole laminate would generate on the stress parameters can be observed from Tables 4.1 and 4.2 highlighting the mean values of point and average stresses.

Type of hole	No. of simulat-ions	Uniformly distributed load	Mean value of point stress	Std. dev. value of point stress	C.O.V. of point stress
		MN/m	GPa	MPa	%
Controlled	200	1.1542	1.05034	5.073	0.483
Uncontrolled	300	1.1542	1.09435	87.97	8.03

Table 4.1 Mean, Standard dev. and Coefficient of variation values of point stress parameters for controlled and uncontrolled hole laminates for hole size of 7.54 mm

Type of hole	No. of simulat -ions	Uniformly distributed load	Mean value of average stress	Std. dev. value of average stress	C.O.V. of average stress
		MN/m	GPa	MPa	%
Controlled	200	1.1542	1.05878	1.889	0.178
Uncontrolled	300	1.1542	1.09252	94.76	8.67

Table 4.2 Mean, Standard dev. and Coefficient of variation values of average stress parameters for controlled and uncontrolled hole laminates for hole size of 7.54 mm

From Tables 4.1 and 4.2, one can also see that both point and average stress parameters for controlled hole laminate reach a stable value at 200 simulations, whereas uncontrolled hole laminate takes 300 simulations. Because in controlled hole laminate only the stochastic variation of material properties are considered. But in uncontrolled hole laminate stochastic variation of material properties, variations in the value of characteristic length and geometry of the hole are considered, all these together contribute to the prolonged and non-uniform variation in pattern and hence lead to more number of simulations.

On comparing the mean value of point stress for controlled and uncontrolled hole laminates with hole size of 7.54 mm, an increase of about 44 MPa in the later case can be observed. Again from Table 4.2, one can see that average stress for uncontrolled hole laminate increases by an amount of 33.74 MPa from that of controlled hole. In the case of standard dev. values of point stress, we will see for controlled hole the value is 5.073 MPa and for uncontrolled hole it is 87.97 MPa. Similarly, standard dev. values of average

stress for controlled hole laminate is 1.889 MPa and for uncontrolled hole laminate is 94.76 MPa. It may be noted here that there is a difference between the mean values and between the standard deviation values of the point stress.

The cause for increase in the mean point and average stress values for uncontrolled hole laminate can be reasoned as follows; when the circular opening moves closer to the laminate edge, in the process of maintaining a uniform stress distribution along the axis perpendicular to the loading direction, a higher stress value is attained near the hole edge. This is explained in Figures 4.9 and 4.10 respectively.

It is of utmost importance to consider the extra stress developed while designing the laminates. The increase in the mean value of stresses achieved through simulation, accounts for only one hole driven in the laminate. But in practical applications, series of holes would be driven to have a good fixity of the parts in union. In such conditions depending on the arrangement of holes, a multiplied effect of the severity in stress may be expected.

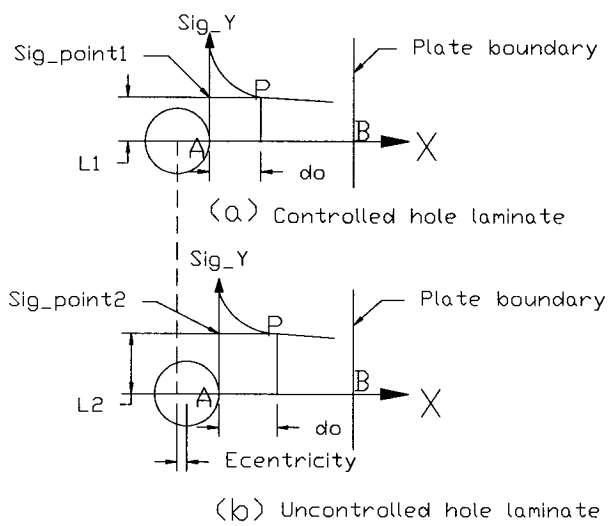

Figure 4.9 Increase of point stress due to hole eccentricity

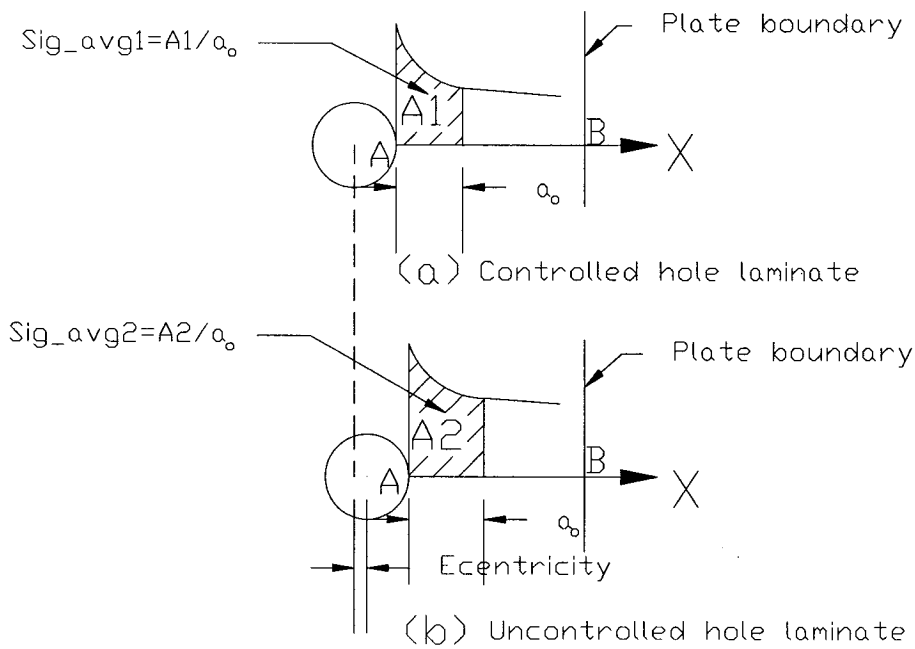

Figure 4.10 Increase of average stress due to hole eccentricity

As expressed in Section 4.4, the value of characteristic length in uncontrolled hole laminate is changing as per the Gaussian distribution. When compared with a fixed value of characteristic length of the controlled hole laminate, a higher, lower or a similar value of the characteristic length is expected in uncontrolled hole laminate during the simulation. Considering the same values of characteristic lengths a_o and d_o for controlled and uncontrolled hole laminates, it is clear from Figures 4.9 and 4.10 that due to the eccentricity of the hole, the region of higher stress is larger in uncontrolled hole laminate, from hole edge A to the plate boundary B. For that reason, in Figure 4.9 the point stress at a point P, at a characteristic length distance d_o away from hole edge A for controlled hole laminate is L1, which is less than L2, of the corresponding value for the uncontrolled hole laminate. Similarly, from Figure 4.10 for average stress criterion, one

can see that area under integration for controlled hole laminate A1 is less than the corresponding area for the uncontrolled hole laminate A2 for same characteristic length value a_0.

4.6 Effect of Hole Size on Stress Concentration Factor (SCF)

Stress concentration factor will help us to understand the behavior of $[0/90]_{4s}$ composite laminate for different hole sizes. Thus simulation is carried out on laminates with three different hole sizes that are tested in Chapter 3. For analysis, plate geometry and boundary condition for the three different hole sizes are kept the same as that corresponding to their experimental coupon size. Uniformly distributed load applied at the top boundary for different hole sizes are taken from the corresponding failure load of the notched specimen which is given in Table 3.14. Experimental values of material properties are used for the stochastic analysis. Stress concentration factor (SCF) values for various nodes from hole edge A to plate boundary B are calculated and plotted against the corresponding nodal distances for three hole sizes in Figure 4.11. SCF values at hole edge are listed in Table 4.3.

Hole Size	Hole width ratio(d/W)	Uniformly distributed load	Number of simulations	Stress concentration factor at hole edge (SCF)
mm	mm/mm	MN/m		
5.10	0.1346	1.2896	200	4.54
6.35	0.1675	1.2054	200	4.48
7.54	0.1989	1.1542	200	4.40

Table 4.3 Stress concentration factor for different hole sizes for controlled hole laminate

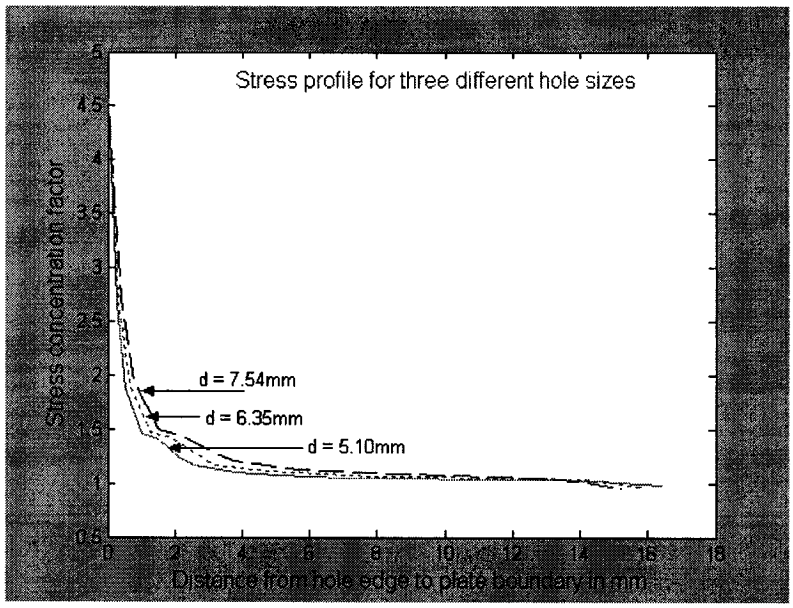

Figure 4. 11 Stress concentration profile in a $[0/90]_{4s}$ laminate with three different hole sizes under uniaxial load for controlled hole laminate

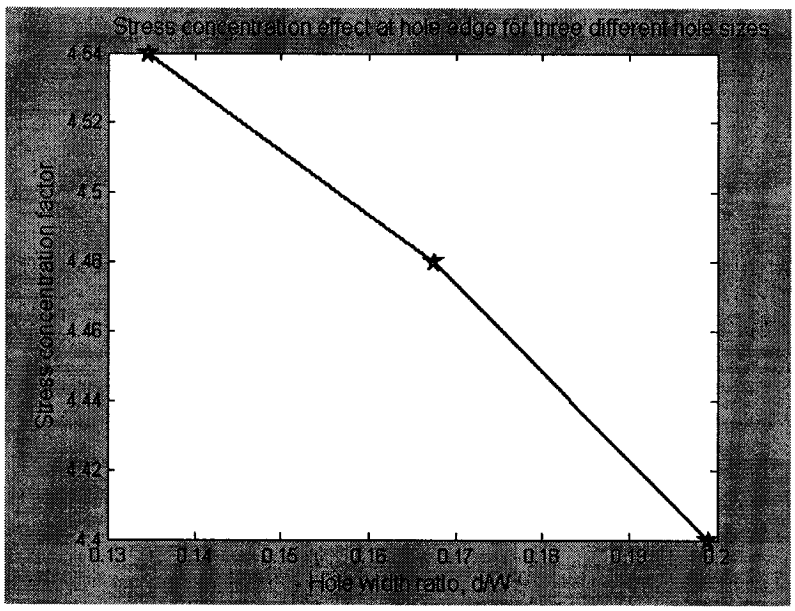

Figure 4.12 Effect of hole sizes on stress concentration factor

From Figure 4.11, one can see that stress concentration factor for all three hole sizes are very high for a small region that is less than 1mm from the hole edge and within this

region it decreases very sharply, after that it decreases slowly and diminishes near the plate boundary. At the plate end or after two radius distances from hole edge it is almost one; that means there is no more stress concentration. Again from Figure 4.12 and Table 4.3, one can see that stress concentration factor at the hole edge decreases from 4.54 to 4.40 with the increase of d/W ratio. The values of d are 5.1 mm, 6.35 mm and 7.54 mm respectively, whereas W is kept constant at 37.9mm. From Figure 4.11, it is seen that for a small region just after the hole edge, SCF value is higher for larger hole (7.54 mm) than the smaller hole (5.1 mm).

This enables us to draw the conclusion that more area near the hole is under a higher stress for a larger hole than for the smaller hole even though the SCF value at hole edge is higher for a smaller hole. This is a very important observation that will help us to explain the reason for higher average and point stress values for larger hole as in Section 4.7.

For this reason when designing composite laminate with hole, considering only the SCF is not adequate enough.

4.7 Effect of Hole Size on Point and Average Stress Parameters

To see the effect of different hole sizes on the average and point stress parameters all the geometric and boundary conditions of the laminate adopted in Section 4.6 are considered. In addition the characteristic length values for point and average stress criteria are varied for different hole sizes corresponding to their calculated values listed in Tables 3.17 and 3.19. For hole sizes 6.35 mm and 7.54 mm, mean characteristic length value of the two hole sizes are considered. Simulation is done for both controlled and uncontrolled hole laminates and the results are put in Tables 4.4 and 4.5 and in Figures 4.13 to 4.16.

Hole size	Hole width ratio (d/W)	Un-notched strength	Uniformly distrib-uted load	Mean value of point stress	Std. dev. value of point stress	Mean value of average stress	Std. dev. value of average stress
mm		GPa	MN/m	GPa	MPa	GPa	MPa
5.10	0.135	0.9462	1.2896	0.91538	5.24	0.91807	1.603
6.35	0.168	1.073	1.2054	1.03977	5.84	1.04348	1.773
7.54	0.199	1.073	1.1542	1.05034	5.07	1.05878	1.889

Table 4.4 Point and average stress parameters for controlled hole laminate for different hole sizes

Hole size	Hole width ratio (d/W)	Un-notched strength	Uniformly distrib-uted load	Mean value of point stress	Std. dev. value of point stress	Mean value of average stress	Std. dev. value of average stress
mm		GPa	MN/m	GPa	MPa	GPa	MPa
5.10	0.135	0.9462	1.2896	0.91648	50.88	0.94525	88.40
6.35	0.168	1.073	1.2054	1.04501	82.64	1.07239	97.44
7.54	0.199	1.073	1.1542	1.09435	87.97	1.09252	94.76

Table 4.5 Point and average stress parameters for un-controlled hole laminate for different hole sizes

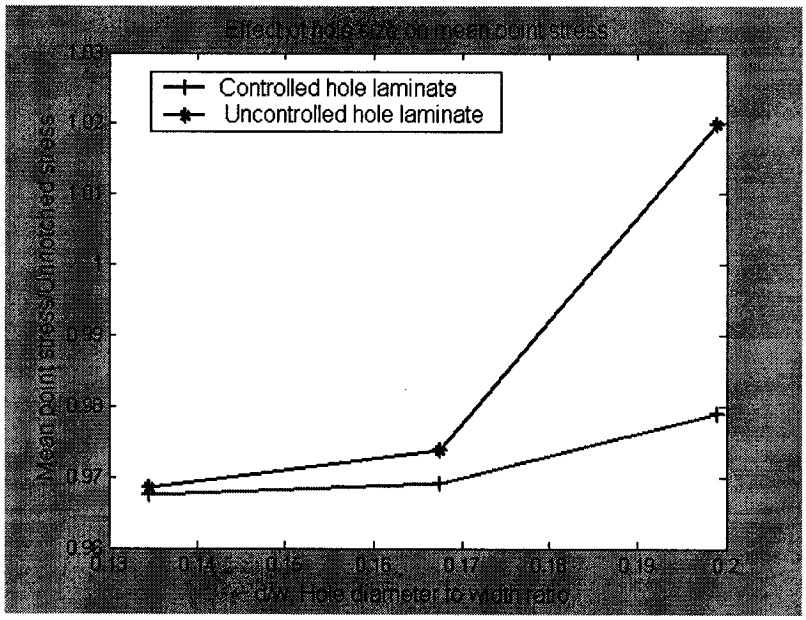

Figure 4.13 Effect of hole size on mean point stress for controlled and uncontrolled hole laminates

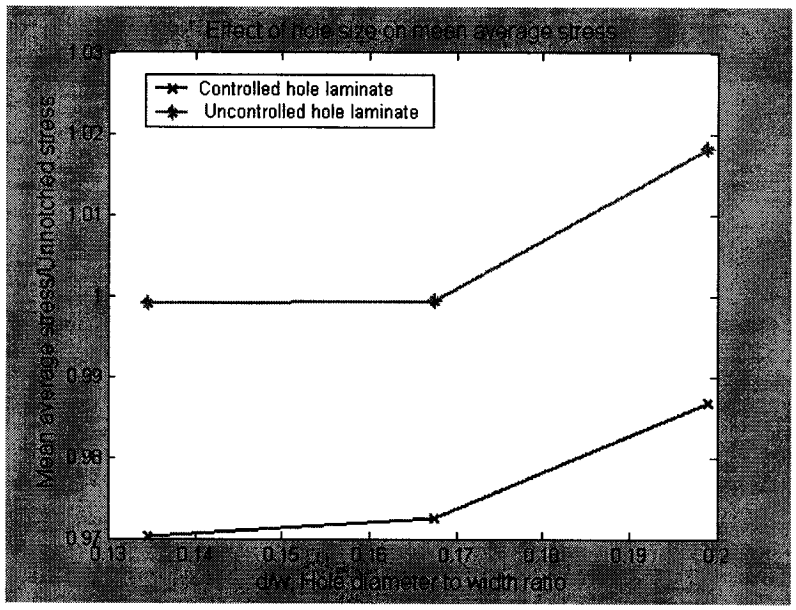

Figure 4.14 Effect of hole size on mean average stress for controlled and uncontrolled hole laminates

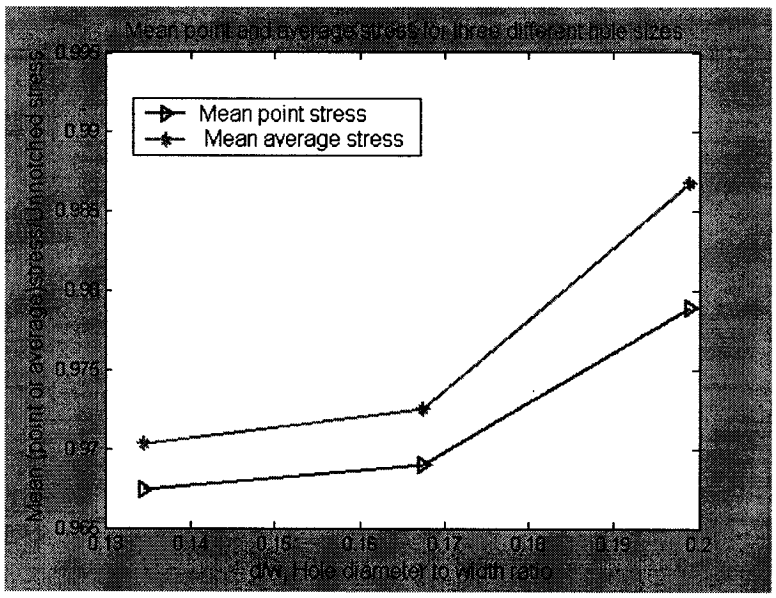

Figure 4.15 Effect of hole size on the mean point and average stress for controlled hole laminates

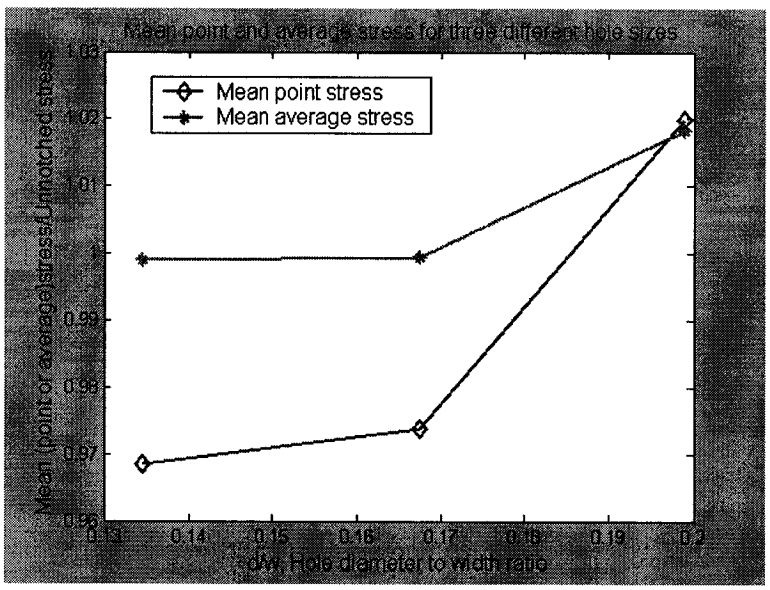

Figure 4.16 Effect of hole size on the mean point and average stress for uncontrolled hole laminates

From Table 4.4 and Figure 4.15, one can see that both mean point and average stress values increase with the increase of d/W ratio or simply with the increase of hole size for

controlled hole laminate. It increases slowly from d/w ratio of 0.1346 to 0.1675 and sharply from 0.1675 to 0.1989. Mean average stress is always higher than the mean point stress for all the hole sizes. Similarly, from Table 4.5 and Figure 4.16, it is seen that both mean point and average stress values increase with the increase of d/W ratio for uncontrolled hole laminate. It increases slowly from d/W ratio of 0.1346 to 0.1675 and sharply from 0.1675 to 0.1989. Mean average stress is higher until d/W=0.1675, after that mean point stress starts to increase rapidly and it exceeds mean average stress at d/W=0.1989.

The reason for increase in mean point stress with the increase of d/W ratio is due to the fact that the stress curve for larger hole stays above the smaller hole, which is shown in Figure 4.11, which leads to the higher value of point stress for larger hole than the smaller hole for the same characteristic length. Similarly from Tables 4.4 and 4.5 and Figure 4.14, one can see that mean average stress for both controlled and uncontrolled hole laminates increases with d/W ratio. The reason for this is, that the area under the stress profile for larger hole is bigger than that of smaller hole for the same characteristic length, which is explained in Figures 4.10 and 4.11.

If we focus on Figure 4.15, we will see that mean average stress for CHL is always larger than mean point stress for all d/W ratios. Figure 4.16 shows that until d/W=0.1675, mean average stress is larger than mean point stress, after that mean point stress has a sharp increase and almost reaches the same value of mean average stress, the values are 1.09435 GPa and 1.09252 GPa respectively.

One very important thing to be noticed in all the four Figures from 4.13 to 4.16, is that mean point and average stress values for both CHL and UCHL cases have a very small

increase for d/W ratio values of 0.1346 to 0.1675 (or hole size from 5.10 mm to 6.35 mm) and after that it has a very sharp increase.

So, if a notched $[0/90]_{4s}$ cross-ply composite laminate with d/W ratio greater than 0.1675 has to be used, the designer should be careful about the extra stresses developed due to larger hole.

CHAPTER 5

RELIABILTY ANALYSIS OF NOTCHED COMPOSITE LAMINATES

5.1 Introduction

Composite laminates can develop local failures or exhibit local damage such as matrix cracking, fiber breakage, fiber–matrix debond and delamination which necessitates the reliable design of laminates based on probabilistic approach. It is shown in chapter 4 that the stresses near the hole boundary increase significantly with the increase of hole size. Thus it becomes necessary to choose the optimum hole size that could be used for the safer operation of the structure. At the same time decision has to be taken about the reliability of the laminate for worthiness of intended application. *"**Reliability** [64] is defined as the probability that a component or device or system will achieve a specified life without failure under a given loading".*

It is to be noted here that in order to evaluate the reliability of any structure, two parameters are required, for instance, one representing the strength and the other representing the stress developed due to the external loading. In the present case, point (σ_{point}) and average (σ_{avg}) stresses of a notched laminate are used as parameters for evaluating the probabilistic reliability of orthotropic laminates with respect to strength (σ_o) of corresponding un-notched laminate.

5.2 Strength Distribution of Composite Laminates

The analysis and design of composite structures require the input of reliable experimental data. One of the major objectives of testing composite material is the determination of un-notched and notched laminate strength values and hence, the exact distribution of characteristic length data for different notch sizes.

Probability distribution arises from experiments where the outcome is subject to chance. The nature of the experiment dictates which probability distribution may be appropriate for modeling the resulting outcomes. In the present work, the Gaussian distribution method is used to generate probability density function (PDF) for the stress parameters and hence to calculate the reliability. Probability density function is the basic tool for codifying and communicating uncertainty about the value of a continuously varying variable. This information together with the distribution of the point (σ_{point}) and average (σ_{avg}) stresses obtained using the stochastic finite element analysis can then be used to determine the reliability of the laminate.

5.3 Stress Distribution in Notched Laminate

The main purpose of stochastic analysis when both the parameters i.e. point/average stress and the strength of un-notched laminate are involved, is to determine the reliability considering both the distributions which are known at a critical location in the component. The distributions followed by each of these representatives might be quite different from each other and they can be represented as

$$F_1 = A\left(\mu_{\sigma_{point/avg}}, S_{\sigma_{point/avg}}\right) \quad \text{and} \quad F_2 = B\left(\mu_{\sigma_o}, S_{\sigma_o}\right) \tag{5.1}$$

in which A and B represent the two different distributions followed by ($\sigma_{point/avg}$) and the (σ_o) respectively.

5.4 Gaussian Distribution

The Gaussian distribution is one of the best known and widely used two-parameter distribution. It is also known as the normal distribution. It is an approximation to the distribution of values of a characteristic. The exact shape of the normal distribution depends on the mean and the standard deviation values of the distribution. The standard deviation is a measure of spread and indicates the amount of departure of the values from the mean. All normal distributions are symmetric and have bell shaped density curves with a single peak and tails that go to infinity at both ends. The probability density function of the normal distribution is given by [65]

$$f(t) = \frac{1}{s\sqrt{2\pi}} \exp\left[-\frac{(t-\mu)^2}{2s^2}\right]; \quad -\infty < t < +\infty \tag{5.2}$$

where,

μ is the mean value

s is the standard deviation

Here, we have two populations, one is strength and the other one is stress. If we assume that both are normally distributed, there is a possibility that the forward tail of the stress distribution may overlap the backward tail of the strength distribution and the result is some failures. To determine the reliability, we combine the two populations and compute the corresponding standardized variable Z_R, which is given by [67]

$$Z_R = \frac{\mu}{s} = \frac{\mu_{\sigma_o} - \mu_{\sigma_{point/avg}}}{\sqrt{s_{\sigma_o}{}^2 + s^2{}_{\sigma_{point/avg}}}} \tag{5.3}$$

where

μ_{σ_o} is the mean value of the strength of the un-notched laminate, $\mu_{point/avg}$ is the mean value of point or average stress of a notched laminate, s_{σ_o} is the standard deviation value of the strength of the un-notched laminate and $s_{\sigma\ point/avg}$ is the standard deviation value of the point or average stress of a notched laminate.

Reliability of a system can be defined as the probability of success and we have

$$R_s = 1 - P_f \tag{5.4}$$

where, P_f is the probability of failure, which can be calculated by obtaining the value corresponding to the value of Z_R from appendix K of reference [65], that is the area under the normal distribution curve corresponding to the combined population. Thus, we are able to quantify system reliability in terms of a number that lies between zero and one.

5.5 Reliability Calculation

In this chapter, $[0/90]_{4s}$ cross-ply laminates with three different notch sizes are analyzed by subjecting them to uni-axial tension. To have a better understanding of the load bearing capacity of the laminates with the variation of notch sizes, how reliable and safe the design is, laminates are loaded with different values of factor of safety on the ultimate load and stochastic simulations are performed.

5.5.1 Reliability Calculation using Point Stress Criterion

As an example, a laminate with 5.1 mm hole in the center is considered for the stochastic simulation. Both the controlled and uncontrolled hole laminate conditions are analyzed by subjecting them to uni-axial tensile load. Probabilistic parameters such as mean and standard deviation values of point stress parameter considered for the judgment of failure of the laminate are calculated. Section 5.4 provides a detailed description of the calculation of reliability based on the Gaussian distribution method. Proceeding in a similar manner, reliability values are also calculated for the notch sizes of 6.35 mm and 7.54 mm, for both controlled and uncontrolled hole laminate conditions using point stress criterion and are presented in Tables 5.1 to 5.3.

The effect of decreasing the factor of safety on the area of interference, obtained by superposition of distribution curves of point stress and un-notched laminate strength is shown pictorially in Figures 5.1 and 5.2. The distribution curves developed for the two stress parameters with the factor of safety values of 1.2 and 1.3 are also shown respectively in Figures 5.1 and 5.2, for an uncontrolled hole laminate with hole size of 5.1 mm.

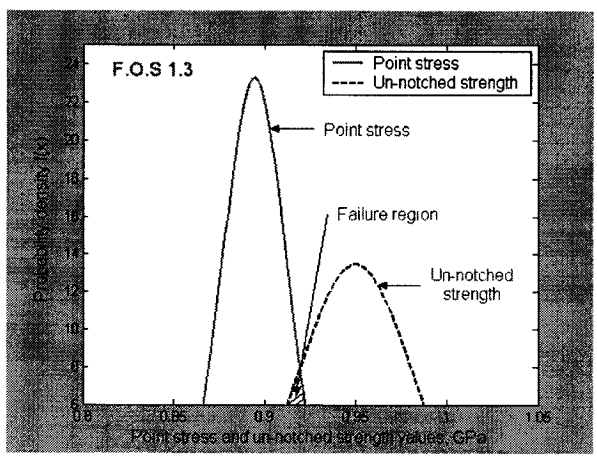

Figure 5.1 Area of interference at a factor of safety of 1.3 on the ultimate load

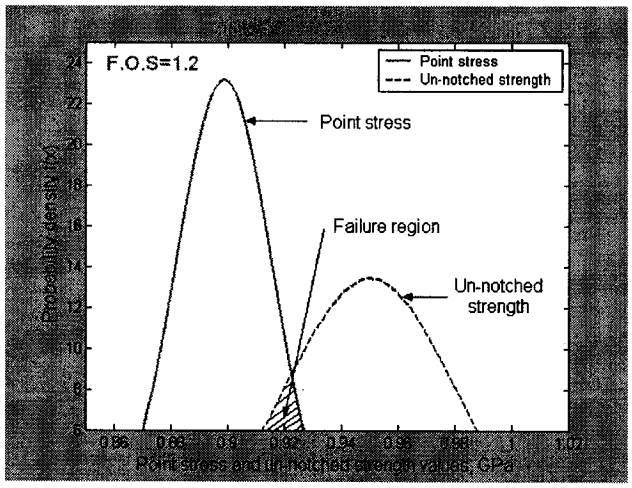

Figure 5.2 Area of interference at a factor of safety of 1.2 on the ultimate load

From Figures 5.1 and 5.2, one can see that for a factor of safety of 1.3 on the ultimate load, the area of interference between the two stress parameters is less than the area of interference when factor of safety is 1.20. Thus by increasing the factor of safety, it is possible to make the area of interference to be close to zero, thus preventing the failure that might be caused while in use. Increase of factor of safety decreases the amount of applied load which in turn decreases the mean point stress and possibly standard deviation values of point stress that causes the distribution curve of point stress to be shifted towards left from un-notched strength distribution curve. This shifting of point stress curve to the left reduces the area of interference thus decreasing the chance of failure. Same thing happens for the average stress too.

Tables 5.1 to 5.3, list the reliability values associated with the different notch sizes for controlled and uncontrolled hole laminates with the variation of factor of safety by point stress criterion. In these Tables R_{point}, μ_{point} and S_{point} respectively refers to reliability, mean stress and standard deviation of stress values obtained using point stress criterion.

Factor of safety (F.O.S.)	Load (MN/m)	Controlled hole laminate			Un-controlled hole laminate		
		μ_{point} GPa	s_{point} GPa	R_{point} %	μ_{point} GPa	s_{point} GPa	R_{point} %
1.00	1.289	0.9154	0.0052	67.00	0.9165	0.0509	63.44
1.05	1.228	0.8718	0.0050	84.28	0.8728	0.0485	80.57
1.10	1.172	0.8322	0.0048	94.84	0.8332	0.0463	91.15
1.15	1.121	0.7960	0.0046	97.80	0.7969	0.0442	96.45
1.20	1.074	0.7628	0.0044	99.56	0.7637	0.0424	98.71
1.45	0.889	0.6313	0.0036	≈100.00	0.6321	0.0351	≈100

Table 5.1 Reliability values of laminate with hole diameter 5.10 mm obtained using point stress criterion

Factor of safety (F.O.S.)	Load (MN/m)	Controlled Hole laminate			Un-controlled hole laminate		
		μ_{point} GPa	s_{point} GPa	R_{point} %	μ_{point} GPa	s_{point} GPa	R_{point} %
1.00	1.205	1.0398	0.0058	65.63	1.0450	0.0826	59.48
1.05	1.148	0.9903	0.0056	84.13	0.9952	0.0787	75.26
1.10	1.096	0.9452	0.0053	93.90	0.9500	0.0751	86.43
1.15	1.048	0.9041	0.0051	97.75	0.9087	0.0719	93.32
1.20	1.004	0.8665	0.0049	99.38	0.8708	0.0689	96.99
1.45	0.8331	0.7171	0.0040	≈100.00	0.7207	0.0570	99.98

Table 5.2 Reliability values of laminate with hole diameter 6.35 mm obtained using point stress criterion

Factor of safety (F.O.S.)	Load (MN/m)	Controlled Hole laminate			Un-controlled hole laminate		
		μ_{point} GPa	s_{point} GPa	R_{point} %	μ_{point} GPa	s_{point} GPa	R_{point} %
1.00	1.154	1.0503	0.0051	60.82	1.0943	0.0880	43.02
1.05	1.099	1.0003	0.0048	81.09	1.0422	0.0838	60.33
1.10	1.049	0.9549	0.0046	92.40	0.9949	0.080	75.18
1.15	1.004	0.9133	0.0044	97.35	0.9516	0.0765	85.99
1.20	0.9618	0.8753	0.0042	99.19	0.9120	0.0733	92.79
1.45	0.7690	0.7244	0.0035	≈100.00	0.7547	0.0607	99.91

Table 5.3 Reliability values of laminate with hole diameter 7.54 mm obtained using point stress criterion

From Tables 5.1 to 5.3, one can see that reliability values obtained using point stress criterion for all the three notch sizes increase with the increase of factor of safety for both the CHL and UCHL conditions. This is because applying FOS on the ultimate load reduces the stresses and hence increases the reliability. For all the cases reliability values increase very rapidly from FOS value 1.0 to 1.2, after that increases very slowly. For example, in Table 5.3 for UCHL case, one can see that when FOS value increases from 1.0 to 1.2, reliability value jumped from 43.02% to 92.79%, an increase of almost 50%, but for further increase of FOS value from 1.20 to 1.45 reliability value increases to 99.91%, that is, it increases only by 7%. From these reliability Tables, one can conclude that in designing notched laminates, if someone intends to achieve very high reliability, he/she has to use bigger FOS value, which ultimately increases the cost of the design. By

using proper FOS value on the ultimate load, one can optimize the design cost for the intended reliability.

Change of reliability with F.O.S values and notch sizes, for both the controlled and uncontrolled hole laminate conditions is shown in Figures 5.3 and 5.4 respectively.

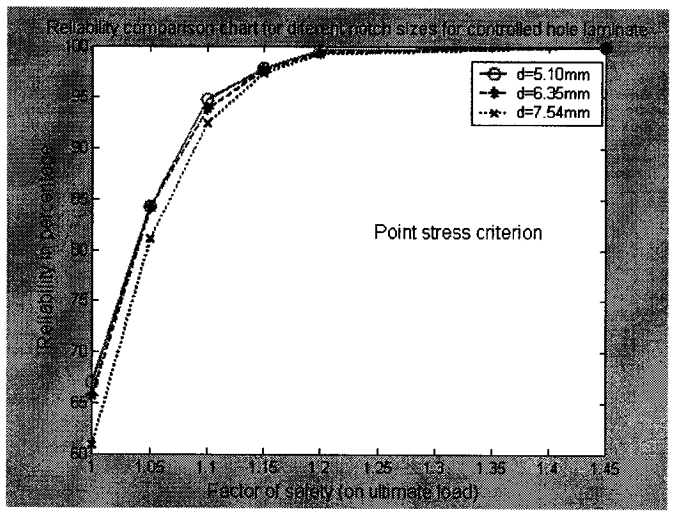

Figure 5.3 Plot of reliability curves for controlled hole laminate using point stress criterion

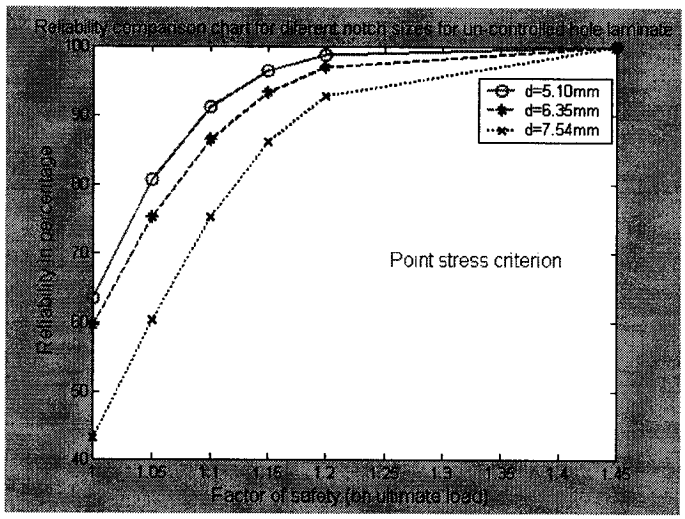

Figure 5.4 Plot of reliability curves for un-controlled hole laminate using point stress criterion

From Figures 5.3 and 5.4, one can see that for both the CHL and UCHL cases reliability curves follow the same pattern for different notch sizes with FOS values. Again the reliability curves for notch sizes 5.1 mm and 6.35 mm are very close to each other, whereas the curve for 7.54 mm is significantly apart from the other two with lesser reliability. This implies that reliability decreases significantly when the notch size increases from certain critical value, in this case it is 6.35 mm.

5.5.2 Reliability Calculation Using Average Stress Criterion

Stochastic simulations are performed on laminates with three different notch sizes by applying FOS value on their ultimate load, and the corresponding average stress parameters and reliability values are calculated in the (same) manner that is described in Section 5.5.1 for point stress criterion. Reliability values for all the three notch sizes are listed in Tables 5.4 to 5.6.

Factor of safety	Load (MN/m)	Controlled Hole laminate			Un-controlled hole laminate		
		μ_{avg} GPa	s_{avg} GPa	R_{avg} %	μ_{avg} GPa	s_{avg} GPa	R_{avg} %
1.00	1.289	0.918	0.0016	65.63	0.9453	0.0884	50.30
1.05	1.228	0.874	0.0016	84.79	0.9002	0.0842	66.28
1.10	1.172	0.835	0.0015	94.48	0.8593	0.0804	79.28
1.15	1.121	0.798	0.0014	98.28	0.8220	0.0769	88.41
1.20	1.074	0.765	0.0014	99.52	0.7877	0.0737	94.06
1.45	0.889	0.633	0.0011	≈100	0.6519	0.0610	99.92

Table 5.4 Reliability values of laminate with hole diameter 5.10 mm obtained using average stress criterion

Factor of safety (F.O.S.)	Load (MN/m)	Controlled Hole laminate			Un-controlled hole laminate		
		μ_{avg} GPa	s_{avg} GPa	R_{avg} %	μ_{avg} GPa	s_{avg} GPa	R_{avg} %
1.00	1.205	1.0435	0.0018	63.98	1.0724	0.0974	50.10
1.05	1.148	0.9938	0.0017	83.19	1.0213	0.0928	66.14
1.10	1.096	0.9486	0.0016	93.45	0.9749	0.0886	78.84
1.15	1.048	0.9074	0.0015	97.78	0.9325	0.0847	88.28
1.20	1.004	0.8696	0.0015	99.32	0.8937	0.0812	93.94
1.45	0.8331	0.7196	0.0012	≈100.00	0.7396	0.0672	99.91

Table 5.5 Reliability values of laminate with hole diameter 6.35 mm obtained using average stress criterion

From Tables 5.4 to 5.6, one can see that reliability values increase significantly for all the notch sizes from FOS value 1.0 to 1.2, but after that increases very slowly. As for example, in Table 5.3 for UCHL case, one can see that when FOS value increases from 1.0 to 1.2, reliability value jumped from 43.84% to 92.99%, i.e. it increases by almost 49%, but for further increase of FOS value from 1.20 to 1.45 reliability value increases to 99.88%, i.e. it increases only by 7%. If we want to increase the reliability value to (close to) 100%, we have to increase the FOS value to 1.61. Only 0.12% increase of reliability requires 11% increase of FOS value. So, designing notched laminates considering higher reliability always involves higher FOS value, which in turn increases the design cost. One can even achieve the reliability of more than 90% with a FOS value of 1.2 on the ultimate load, which can reduce the design cost significantly.

Factor of safety (F.O.S.)	Load (MN/m)	Controlled Hole laminate			Un-controlled hole laminate		
		μ_{avg} GPa	s_{avg} GPa	R_{avg} %	μ_{avg} GPa	s_{avg} GPa	R_{avg} %
1.00	1.1542	1.0588	0.0019	56.85	1.0925	0.0948	43.84
1.05	1.0992	1.0084	0.0018	78.37	1.0405	0.0902	60.45
1.10	1.0493	0.9625	0.0017	91.02	0.9932	0.0861	74.86
1.15	1.0037	0.9207	0.0016	96.78	0.9500	0.0824	85.41
1.20	0.9618	0.8823	0.0016	98.97	0.9104	0.0790	92.99
1.45	0.7690	0.7302	0.0013	≈100.00	0.7535	0.0654	99.88

Table 5.6 Reliability values of laminate with hole diameter 7.54 mm obtained using average stress criterion

Reliability values are plotted against corresponding FOS values for three notch sizes for both CHL and UCHL cases in Figures 5.5 and 5.6.

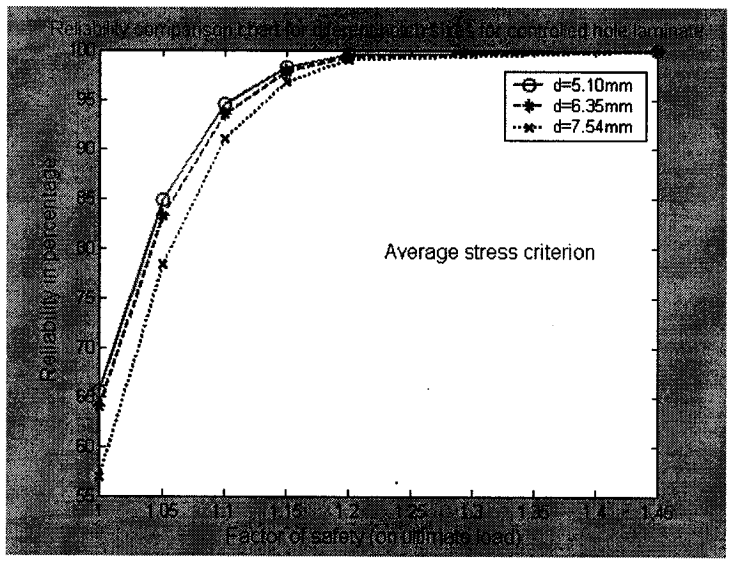

Figure 5.5 Plot of reliability curves for controlled hole laminate using average stress criterion

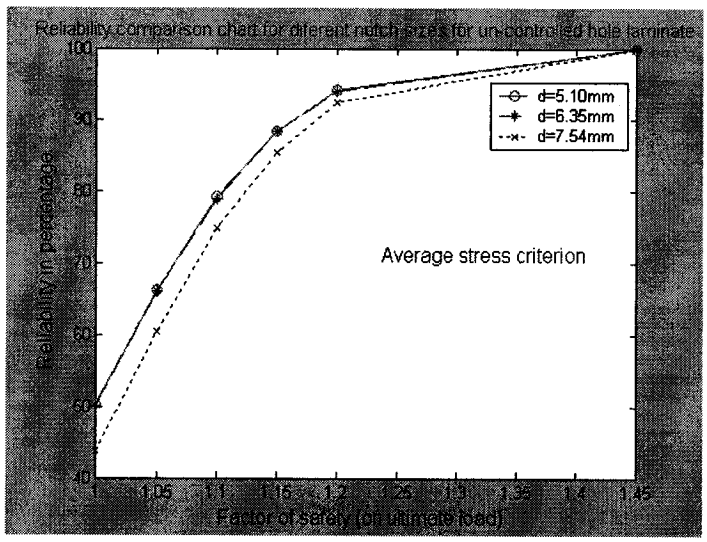

Figure 5.6 Plot of reliability curves for un-controlled hole laminate using average stress criterion

From reliability charts in Figures 5.5 and 5.6, one can see that for all the three notch sizes reliability curves follow the same pattern. Reliability curves for notch sizes of diameter 5.1 mm and 6.35 mm are very close, whereas the reliability curve for notch size 7.54 mm

is distinctively apart from them with significantly lesser reliability. This observation implies the same meaning as of point stress criterion that the reliability value decreases significantly when the notch size increases from certain critical value.

5.6 Effect of Notch size on the Reliability of Cross-ply Composite Laminates

In this Section, an attempt has been made to see the effect of notch size on the reliability of cross-ply laminates and a comparison is also made at the same time on the reliability values obtained using point stress and average stress criteria. The reliability values calculated in Sections 5.5.2 and 5.5.3 for three notch sizes with FOS value of 1.0, using both the point stress criterion and average stress criterion are summarized in Table 5.7.

Hole size	d/W ratio	Reliability values obtained using point stress criterion		Reliability values obtained using average stress criterion	
mm		Controlled hole laminate	Un-controlled hole laminate	Controlled hole laminate	Un-controlled hole laminate
5.10	0.1346	67.00	63.46	65.63	50.40
6.35	0.1675	65.63	59.48	64.02	50.10
7.54	0.1989	60.82	43.02	56.85	43.84

***Note**: All reliability values are in percentage.*

Table 5.7 Change of reliability with the variation of d/W ratio for controlled and un-controlled hole laminates using point and average stress criteria

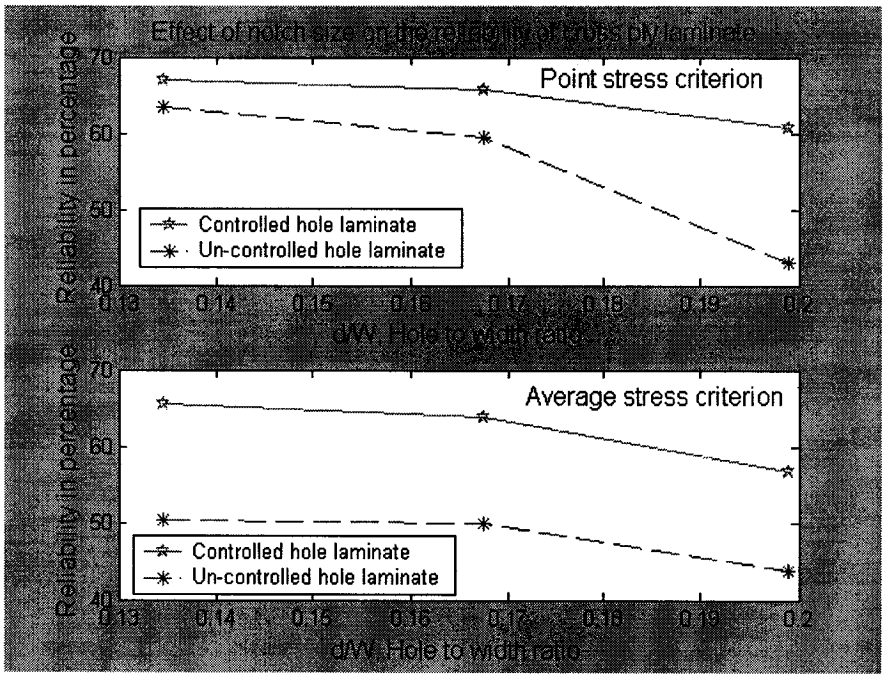

Figure 5.7 Change of reliability with the increase of notch size for both controlled and un-controlled hole laminates

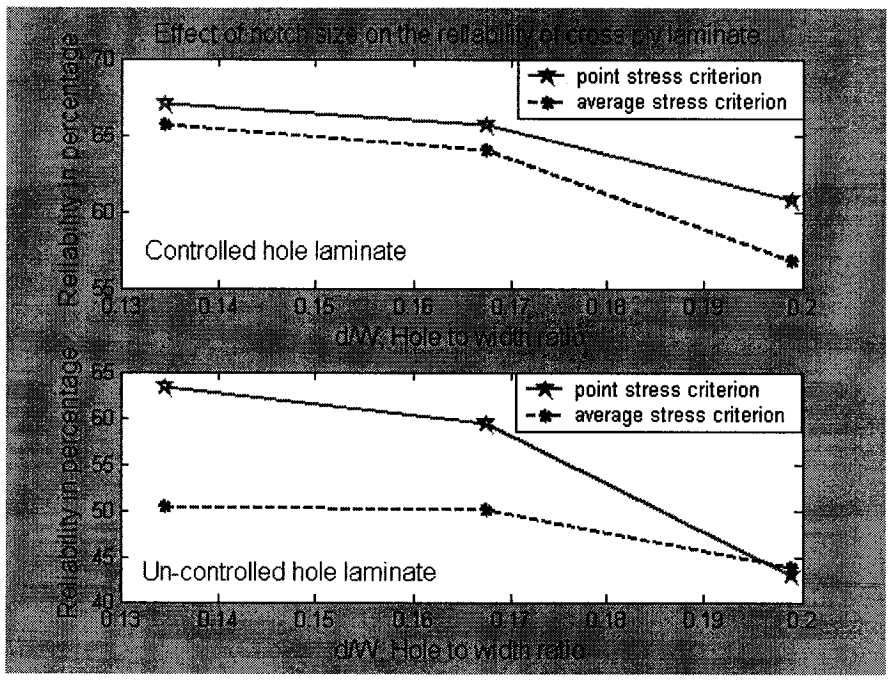

Figure 5.8 Change of reliability with the increase of notch size using point stress criterion and average stress criterion

In Figures 5.7 and 5.8, reliability values are plotted against d/W ratios for controlled and uncontrolled hole laminates using point stress criterion and average stress criterion.

From Table 5.7 and Figure 5.7, one can see that reliability values of uncontrolled hole laminates are always less than that of controlled hole laminates for all d/W ratio values. Thus it is not advisable to consider the ideal controlled hole laminate condition in practical applications subjected to uniaxial tension. The geometry perturbation around the circumference of the hole, eccentricity of the hole from plate center and stochastic variation in the material properties together enhance the stresses around the hole region of the laminate. These in turn increase the probability of failure of the laminate.

Another important observation could be made from Table 5.7 and Figures 5.7 and 5.8 that for all the conditions using both the stress criteria reliability value decreases slowly for d/W ratio change from 0.1346 to 0.1675, but decreases very rapidly from 0.1675 to 0.1989. As for example, one can see in Table 5.7 for average stress criterion and uncontrolled hole laminate condition, when d/W ratio increases from 0.1346 to 0.1675 reliability value decreases from 50.40% to 50.10%, whereas for further increase of d/W ratio to 0.1989 reliability value drastically decreases to 43.84%. So, one should pay more attention in designing laminates with d/W ratio more than 0.1675.

Again from Table 5.7 and Figure 5.8, one can see that reliability values obtained by average stress criterion is always less than that of point stress criterion for both CHL and UCHL cases, except in the case of hole size 7.54 mm in UCHL condition, where the reliability values are almost same that is 43.84% and 43.02% respectively. So, designing the laminate using average stress criterion considering uncontrolled hole laminate will reduce the chance of failure.

5.7 Conclusions and Discussions

In the present chapter a reliability study is conducted on $[0/90]_{4s}$ cross-ply laminate with three different notch sizes using point stress criterion and average stress criterion. A stochastic simulation is carried out on both the controlled and uncontrolled hole laminates subjected to unaxial tension. A safety factor value is assumed on the ultimate load bearing capacity of the laminate and stochastic finite element analysis is carried out. The standardized variable calculation is made using the Gaussian distribution method and hence the reliability is found out. A series of reliability values are obtained by varying the factor of safety value. Following observations are made on both the controlled and uncontrolled hole laminate cases using point stress and average stress criteria.

From Figure 5.7, one can conclude that with the increase of d/W ratio, the uncontrolled hole laminate always provides less reliability as opposed to the controlled hole laminate. Thus while designing the laminates, precautions must be taken to consider this reduction in reliability, which can be solely attributed to the geometric variation around the hole region and to the eccentricity of the hole from the center.

From Figures 5.7 and 5.8, it is observed that if the d/W ratio value exceeds 0.1675, the reliability value drops significantly for both the CHL and UCHL cases. So, attention should be given while designing laminates with bigger notch size, which leads to larger d/W ratio with lesser reliability.

Average stress criterion provides lesser reliability than that of point stress criterion. So, it is recommended to design laminates using average stress criterion considering un-controlled hole condition.

CHAPTER 6

CONCLUSIONS AND RECOMMENDATIONS

In the present thesis work, stress distributions in notched isotropic plate and notched composite laminates with various notch sizes are determined using stochastic finite element method. A MATLAB© program is developed, which reflects the stochastic variation of the material properties and imposes the geometric variation on the laminates. The program is capable of handling any notch sizes of any laminate configurations.

Finite element formulation and the flowcharts of the programs are given in chapter 2, where analysis for number of simulated laminates is performed and the mean values of the nodal stresses are recorded. Program validation is demonstrated by using suitable example problems for both isotropic plate and composite laminates at appropriate stages.

The present work considers $[0/90]_{4s}$ cross-ply configuration to study the effect of notch size on the reliability of the laminates. An extensive experimental investigation is performed in chapter 3 on notched and un-notched coupons subjected to uniaxial tension. Coupons are prepared using NCT-301 graphite/epoxy material. At first experiments are conducted on unidirectional and $[\pm 45]_{4s}$ specimens to determine the stochastic material properties. After that experiments are conducted on $[0/90]_{4s}$ cross-ply laminated coupons to determine the ultimate notched and un-notched strength values. It is observed that strength of laminate decreases more slowly for the larger hole than the smaller hole.

Microscopic specimens are prepared for all types of tensile specimens that are tested and observed under microscope to check for defects and damages. Finally, point stress criterion and average stress criterion are used to calculate the values of characteristic length.

In chapter 4, stochastic simulations are performed on controlled and uncontrolled hole laminates subjected to uniaxial tension for three different notch sizes. The mean and standard deviation values of point and average stress parameters are calculated. It is found that, i) un-controlled hole laminate develops higher stress values due to the presence of the geometric variation in the radius of the hole and eccentricity of the hole from plate center in addition to the stochastic variation of material properties; ii) stresses obtained by average stress criterion for all the three notch sizes are higher than that of the point stress criterion for both the controlled and un-controlled hole laminate conditions; iii) A sudden increase in the stress values are observed for both the stress criteria, when hole-width ratio exceeds 0.1675.

Finally in chapter 5, reliability study is conducted. The Gaussian distribution is used to model the distribution of a set of randomly distributed values. The distribution thus obtained is used to compute the reliability values of cross-ply laminates with three different notch sizes using point stress criterion and average stress criterion. The reliability graphs depicting the variation in the reliability values with the change in the factor of safety on ultimate load and also with hole-width ratio are obtained for both controlled and un-controlled hole laminates.

Following observations are made from the reliability graphs and Tables of chapter 5:

- ❖ Reliability values of the laminates increase sharply with the increase of factor of safety value from 1.0 to 1.2 for all the notch sizes; after that the reliability increases very slowly with further increase of factor of safety value.
- ❖ Un-controlled hole laminate analysis always produces a lower reliability value for all the notch sizes than that of the controlled hole laminate.
- ❖ There is a critical hole-width ratio, that is 0.1675, after which reliability values of the laminates drop significantly.
- ❖ Reliability values obtained using average stress criterion for different hole–width ratios are less than that of the point stress criterion. So a recommendation is made to design laminates using average stress criterion considering uncontrolled hole laminate conditions.

The thesis can be further extended on the following topics, which will constitute the future research work:

- Laminates with notch sizes bigger than 7.54mm could be tested and analyzed to see the effect of bigger hole-width ratios, on the reliability of the composite laminates.
- Analysis can be extended to different types of notch opening shapes in the laminate such as elliptical and rectangular shapes.
- Further testing can be conducted on laminates having different configurations such as quasi isotropic laminate, angle ply laminate, etc.
- A three dimensional model can be developed which offers better features in the analysis and thus helps in arriving at a more accurate result.

References

[1] Fidgeon, E.R., "Impact of Composites on Commercial Aircraft Operations and Maintenance: Benefits and Challenges", Proceedings of Third Canadian International Conference on Composites, Edited by Suong V. Hoa, Andrew Johnston and Johanne Denault, 2001, p.740.

[2] Tan, S.C., "Stress concentrations in Laminated Composites", 1994, Technomic Publishing Company, Lancastar.

[3] Shashank, M.V., "Stochastic mechanics and reliability of composite laminates based on experimental investigation and stochastic FEM", April 2003, M.A.Sc. Thesis, Concordia University.

[4] Hori, M., "Statistical Theory of Effective Electrical, Thermal and Magnetic Properties of Random Heterogeneous Material-II", Journal of Math. Phys., Vol. 14, 1973, p. 1942.

[5] Borr, A., "Stochastic Behavior of Special Materials: The Composite Materials", In Dynamic Motion: Chaotic and Stochastic behavior", Ed.:F Casciati, Springer-Verlag, 1993, p. 171.

[6] Peterson R.E., "Stress concentration design factors", John Willey, New York ,1974.

[7] Lekhnitskii S.G., 1968. Anisotropic plates (translated from the second Russian edition by S.W. Tsai and T. Cheron), New York, NY: Gordon and Breach.

[8] Green A.E., "Stress Systems in Isotropic and allotropic plates", Proceedings of Royal Society of London, Series A, Vol. 184, 1945, p.231.

[9] Greszczuk, L.B. "Stress Concentration and Failure Criteria for Orthotropic and Anisotropic Plates with Circular Openings", Composite Materials: Testing and Design (Second conference), ASTM STP 497, ASTM, 1972, p. 363.

[10] Fischer, L., "How to predict structural behavior of RP laminates", Modern Plastics, 1960, p. 122.

[11] Harold J. Konish and James M. Whitney, "Approximate stresses in an Orthotropic Plate Containing a Circular Hole", Journal of Composite Materials, Vol. 9 (April 1975), p. 157.

[12] Shastry B.P. and Rao G.V., "Effect of fiber orientation on stress concentration in a unidirectional tensile laminate of finite width with a central circular hole", Fiber Science and Technology, Vol.10, 1977, p.151.

[13] Lucking W.M., Hoa S.V. and Sankar T.S., "The effect of geometry on interlaminar stresses of $[0/90]_{4s}$ composite laminates with circular holes", Journal of Composite Materials, Vol. 17, March 1984, p.188.

[14] Dana J.R., "Three-dimensional finite element analysis of thick laminated composites–Including interlaminar and boundary effects near circular holes", Ph.D. thesis, Virginia Polytechnique Institute and State University, August 1973.

[15] Harn F., "Notched strength of $[0_2/\pm\theta]_s$ graphite /epoxy laminates with various hole sizes", Ph.D. thesis, The university of Texas at Arlington, 1997.

[16] Pipes R.B. and Pagano N.J., "Interlaminar stresses in composite laminates under uniform axial extension", Journal of Composite Materials, Vol. 4, October 1970, p.538.

[17] Whitney J.M., "The effect of boundary conditions on the response of laminated

composites", Journal of Composite Materials, Vol. 4, April 1970, p.192.

[18] Puppo A.H. and Evensen H.A., "Interlaminar shear in laminated composites under generalized plane stress", Journal of Composite Materials, Vol. 4, April 1970, p.204.

[19] Rybicki E.F., "Approximate three dimensional solutions for symmetric laminates under in-plane loading", Journal of Composite Materials, Vol. 9, April 1975, p.33.

[20] Tang S., "A boundary layer theory--Part II: Extension of laminated finite strip", Journal of Composite Materials, Vol. 9, April 1975, p.42.

[21] Chan W.S. and Ochoa O.O, "Delamination characterization of Laminates under tension, bending and torsion loads", Computational Mechanics, Vol. 6, 1990, p.393.

[22] Shah D.K. and W.S. Chan "Delamination characterization around hole in laminates with softening strips", Journal of Aerospace Engineering,Vol.6, No. 2, April 1993, p.199.

[23] Hufenbach, W., Schafer, M and Hermann, A.S., "Calculation of the stress and displacement field of anisotropic plates with elliptical hole", Ingenier-Archive, Vol. 60, 1990, p.507.

[24] Daoust, J and Hoa S.V., "An analytical solution for anisotropic plates containing triangular holes", Computers and Structures, Vol. 19, 1991, p.107.

[25] Ugadgaonkar, V.G. and Rao, D.K.N., "Stress distribution around triangular holes in anisotropic plates", Computers and Structures, Vol. 45(3), 1993, p. 171.

[26] Theocaris, P.S. and perou, J., "Stress distributions and intensities at corners of

equilateral triangular holes", International Journal of Fracture, Vol.31, 1986, p. 271.

[27] Theocaris, P.S. and perou, J., "From the rectangular hole to the ideal crack", International Journal of Solids and Structures, Vol. 25(3), 1989, p. 213.

[28] Tan, S.C., "Laminated composites containing an elliptical opening. I. Approximate stress analysis and fracture models", Journal of Composite Materials, Vol. 21(10), 1987, p. 925.

[29] Tan, S.C., "Finite–width correction factors for anisotropic plate containing a central opening", Journal of Composite Materials, Vol. 22(11), 1988, p. 1080.

[30] Tan, S.C., "Mixed-mode fracture of notched unidirectional and off-axis laminates under tensile loading", Journal of Composite Materials, Vol. 23(11), 1988, p. 1082.

[31] Lin, J. and Ueng, C.E.S., "Stresses in laminated composites containing two elliptical holes", Composite Structures, Vol. 7, Elsevier Applied Science, London, Chapter 2, 1987, p. 1.

[32] Xu , X. W. and Yue , T. M. and Man , H. C. , "Stress analysis of finite composite laminate with multiple loaded holes", International Journal of Solids and Structures, Vol. 36, Issue 6, February 1999, p. 919.

[33] Rowlands, R.E., Daniel, I.M. and Whiteside , J.B., "Stress and failure analysis of a glass-epoxy composite plate with a circular hole", Experimental Mechanics, Vol. 5, 1973, p. 31.

[34] Givoli, D. and Elishakoff, I., "Stress concentration at a nearly circular hole with uncertain irregularities", Journal of Applied Mechanics, Vol. 59, June 1992, p.

S65.

[35] Pal'mov, V.A., "An elastic plane with hole of random shape", Trudy Leningradskogo Instituta, N. 235(in Russian), 1964.

[36] Lomakin, V.A., "Concentration of stresses near a surface with rapidly oscillating irregularities", (English Translation) Soviet Applied Mechanics, No.2, p.1.

[37] Sayles, R.S., "The profile as a random process", Rough Surfaces, T.R. ed., Longman, London, p-91.

[38] Rosen, B.W., "Tensile failure of fibrous composites", AIAA Journal, Vol.2, No.11, 1964, p.1985.

[39] Zweben, C. "Tensile failure of fiber composite", AIAA Journal, Vol. 6, No. 12, 1968, p. 2325.

[40] Harlow D.G. and Phonix, S.L. "The chain of bundles probability model for the strength of fibrous materials I: Analysis and Conjectures", Journal of Composite Materials, Vol. 12, 1978, p. 195.

[41] Harlow D.G. and Phonix, S.L. "The chain of bundles probability model for the strength of fibrous materials II: A numerical; study of convergence", Journal of Composite Materials, Vol. 12, 1978, p. 314.

[42] Batdorf, S.B., "Tensile strength of unidirectionally reinforced composites-I", Journal of Reinforced Plastics and Composites, Vol.1, 1982, p.153.

[43] Tamuzus, V.P., "Some peculiarities of fracture in heterogeneous materials', Fracture of Composite Materials, Edited by G.C. Sih and V.P. Tamuzus, Martinus Hijhoff, Boston, MA, 1982, p.131.

[44] Yushanov, S.P. and Jhosi, S.P., "Stochastic processes in fiber reinforced

composites", AIAA Journal, Vol. 33, No. 9, 1995, p. 1689.

[45] Stefanou, G. and Papadrakakis, M., "Stochastic finite element analysis of shells with combined random material and geometric properties", Computer Methods in Applied Mechanics and Engineering, Vol. 193, 2004, p. 139.

[46] Falsone, G and Impollonia, N, "A new approach for the stochastic analysis of finite element modeled structures with uncertain parameters", Computer Methods in Applied Mechanics and Engineering, Vol. 191, (2002), p. 5067.

[47] Ghanem, R.G., and R.M. Kruger, R.M., "Numerical solution of spectral stochastic finite element systems", Computer Methods in Applied Mechanics and Engineering, Vol. 129, (1996), p. 289.

[48] Ganesan, R. and Hoa, S.V., "Stochastic finite element analysis of composite structures", CANCAM 95, 15th Canadian Congress of Applied Mechanics, May 95, Victoria, Canada.

[49] Ganesan, R. and Pondugala, L.V.P., "Stochastic J-integral of laminated composites based on an efficient finite element analysis methodology", Advances in Composite Materials and Structures VII, 200, WIT Press, Southampton.

[50] Ganesan, R. and Haque, Z., "Stochastic characteristics of fracture in laminated composites', Proceedings of the Third Joint Canada-Japan Workshop on Composites, Edited by Hoa, S.V., Hamada, H., Lo, J. and Yokoyama, A., 2000, Technomic Publishing Company, Lancaster.

[51] Contreras, N. "The stochastic finite element method", Computers and Structures, Vo. 12, 1980, p. 541.

[52] Vanmarcke, E. and Grigoriu, M., "Stochastic finite element analysis of simple

beams", ASCE, Journal of Engineering Mechanics, Vo. 109, 1983, p.1203.

[53] Yamazaki, F., Shinozuka, M., and Dasgupta, G., "Neumann expansion for stochastic finite element analysis", ASCE Journal of Engineering Mechjanics, Vol. 111, 1985, p. 1335.

[54] Waddoups M.E., Eisenmann J.R. and Kaminski B.E, "Macroscopic fracture mechanics of advanced composite materials", Journal of Composite Materials, Vol.5, October 1971, p.446.

[55] Whitney, J.M and Nuismer, R.J., "Stress fracture criteria for laminated composites containing stress concentrations", Journal of Composite Materials, Vol. 8, July 1974, p.253

[56] Whitney, J.M and Nuismer, R.J., "Uniaxial failure of composite laminates containing stress concentrations", Fracture Mechanics of Composites, ASTM STP 593, 1975, p. 117.

[57] Awerbuch, J. and Madhukar, M., "Notched strength of composite laminates: Predictions and experiments-A review", Journal of Reinforced Plastics and Composites, Vol. 4, Jan 1985, p. 3.

[58] El-Zein, M.S. and Reifsnider, K.L., "The strength prediction of composite laminates containing a circular hole", Journal of Composites Technology and Research, JCTRER, Vol.12, No.1 Spring 1990, p.24.

[59] Timoshenko, S., " Strength of Materials", Third Edition, 1956, D.Van Nostrand Company, N.Y.

[60] Boresi, A.P. and Sidebottom, O.M., "Advanced Mechanics of Materials, Fourth Editon, 1985, John Wiley and Sons, N.Y.

[61] Berthelot, Jean-Marie, "Composite Material, Mechanical Behavior and Structural Analysis", 1999, Springer-Verlag, NY Inc

[60] Hyer, M.W., "Stress analysis of fiber-reinforced composite materials", WCB Mc Graw-Hill, 1998.

[62] ASTM D 3039/D 3039M - 00, "Standard Test Method for Tensile Properties of Polymer Matrix Composite Materials".

[63] ASTM D 3518/D 3518M - 94, "Standard Test Method for In-Plane Shear Response of Polymer Matrix Composite Materials by Tensile Test of a $[\pm 45^0]$ laminate".

[64] Siddal, J.N., "Probabilistic Engineering design: Principles and Applications", 1983, Marcel Dekker, Newyork.

[65] Ramakumar, R. "Engineering Reliability, Fundamentals and Conceptions", 1993, Prentice Hall, Inc., Newjersy.

[66] Cook, R.d., Malkus, D.S. and Plesha,M.E, " Concepts and Applications of Finite Element Analysis",1989, John Wiley & Sons, N.Y.

[67] Timoshenko, S., " Strength of Materials", Third Edition, 1956, D. Van Nostrand Company, N.Y

[68] Reddy, J.N., "An introduction to the finite element method", 1984, McGraw-Hill, New York.

APPENDIX - A

Finite element formulation for isotropic plates

The strain matrix for two dimensional finite element formulations can be written as

$$\{\varepsilon\}^{\{e\}} = \left\{ \frac{\partial u}{\partial x} \quad \frac{\partial u}{\partial y} \quad \left(\frac{\partial u}{\partial y} + \frac{\partial v}{\partial x} \right) \right\}^{T(e)} = [B]^{(e)} \{d\}^{(e)} \tag{A1}$$

in which the $[B]^{(e)}$ matrix relates the element nodal displacements to the element strains and is given by

$$[B]^{(e)} = \begin{bmatrix} \frac{\partial}{\partial x} & 0 \\ 0 & \frac{\partial}{\partial y} \\ \frac{\partial}{\partial y} & \frac{\partial}{\partial x} \end{bmatrix} [N]^{(e)} \tag{A2}$$

The derivatives of the shape functions are expressed in terms of the local coordinates and they can be obtained by using the chain rule of partial differentiation as

$$\begin{aligned} \frac{\partial N_i}{\partial \xi} &= \frac{\partial N_i}{\partial x}\frac{\partial x}{\partial \xi} + \frac{\partial N_i}{\partial y}\frac{\partial y}{\partial \xi} \\ \frac{\partial N_i}{\partial \eta} &= \frac{\partial N_i}{\partial x}\frac{\partial x}{\partial \eta} + \frac{\partial N_i}{\partial y}\frac{\partial y}{\partial \eta} \end{aligned} \tag{A3}$$

The above expressions can be written in the matrix form as

$$\begin{Bmatrix} \frac{\partial N_i^{(e)}}{\partial \xi} \\ \frac{\partial N_i^{(e)}}{\partial \eta} \end{Bmatrix} = \begin{bmatrix} \frac{\partial x}{\partial \xi} & \frac{\partial y}{\partial \xi} \\ \frac{\partial x}{\partial \eta} & \frac{\partial y}{\partial \eta} \end{bmatrix}^{(e)} \begin{Bmatrix} \frac{\partial N_i^{(e)}}{\partial x} \\ \frac{\partial N_i^{(e)}}{\partial y} \end{Bmatrix} \tag{A4}$$

In the above, the matrix relating the derivatives of the shape functions with respect to the local co-ordinates to the derivatives of the shape functions with respect to the global co-ordinates is called the Jacobian matrix of transformation and is denoted by [J]. The Jacobian of transformation can be written as

$$[J] = \begin{bmatrix} J_{11} & J_{12} \\ J_{21} & J_{22} \end{bmatrix} = \begin{bmatrix} \frac{\partial x}{\partial \xi} & \frac{\partial y}{\partial \xi} \\ \frac{\partial x}{\partial \mu} & \frac{\partial y}{\partial \eta} \end{bmatrix}^{(e)} \tag{A4}$$

The components of the Jacobian matrix are calculated using the shape functions and nodal co-ordinates. For example,

$$J_{11} = \frac{\partial x}{\partial \xi} = \sum_{i=1}^{Num.ofnodes} \frac{\partial N_i}{\partial \xi} x_i \tag{A6}$$

APPENDIX – B

Program for the Finite Element Analysis of Notched Isotropic Plate

```
clear all;
close all;
clc;

tic
format long;

%%%%%%%%%%%%%%%%%%%%%%%%%%%%%%%%%%%%%%%%%%%%%%%%%%%%%%%%%%%%%%%%
%%%%%%%%%%%%%%%%%%%%%%%        In the organization of the program
%%%%%%%%%%%%%%%%%%%%%%%%%%%%
%%%%%%%%%%%%%%%%%%%%%%%  LOCAL and GLOBAL variables are referred to by the
%%%%%%%%%%%%%%%%%%%%%%%%%%%%
%%%%%%%%%%%%%%%%%%%%%%%  names so that any variable is given a single name
%%%%%%%%%%%%%%%%%%%%%%%%%%%%
%%%%%%%%%%%%%%%%%%%%%%%      all throughout the program, in order to avoid
%%%%%%%%%%%%%%%%%%%%%%%%%%%%
%%%%%%%%%%%%%%%%%%%%%%%        confusion over variable names
%%%%%%%%%%%%%%%%%%%%%%%%%%%%%%%%%%%%%%%%%%%%%%%%%%%%%%%%%%%%%%%%

dummy=0;      % Used to  pass  dummy variable to I_GETDAT and I_GETARR

nelem=0;
%%%%%%%%%%%%%%%%%%%%%%%%%%%%%%%%%%%%%%%%%%%%%%%%%%%%%%%%%%%%%%%%
ndofn=0;      %                                                   %
nnode=0;      %     Initialize all the relevant variables which are   %
ngaus=0;      %                                                   %
ntype=0;      %     passed to the data functions so that all the relevant   %
nmats=0;      %                                                   %
numnp=0;      %     data is passed back through the same variables.   %
nstre=0;      %                                                   %
nstr1=0;
        %%%%%%%%%%%%%%%%%%%%%%%%%%%%%%%%%%%%%%%%%%%%%%%%%%%%%%%%%%%%%%%%
%%%%%%%%%%%%%%%%%%%%%%%%%%%%%%%%

props = 0;
lnods = 0;
coord = 0;

%%%%%%%%%%%%%%%%%%%%%%   I_GETDAT - Contains relevant scalar variables   %%%%%%%%%%%%%%%%%%%%%%

fprintf('\n RESULTS CORRESPONDS TO TENSILE ANALYSIS FULL ISOTROPIC PLATE, 200
ELEM.\n');


[nelem,ndofn,nnode,ngaus,ntype,nmats,numnp,nstre,nstr1]=I_GETDAT(dummy);

%%%%%%%%%%%%%%%%%%%%%%   I_GETARR - Contains the relevant data in Array from
```

```
[props,lnods,coord] = I_GETARR(dummy);

%%%%%%%%%%%%%%%%%%%%    ESTABLISH THE NODAL CONNECTIVITY
nevab = ndofn*nnode;

[lm,id] = I_ELCON(ndofn,nnode,nelem,numnp,lnods);

for ielem=1:nelem
   matno(ielem)=1.0;
end

globK = zeros(numnp*ndofn);  % Initialize the Global "K" matrix for each element

%%%%%%%%%%%%%%%%%%%%%%%%%%%%%%%%%%%%%%%%%%%%%%%%%%%%%%%%%%%%%%%%%%%%%%%%%%%%%%%
%%%%%%%%%%%%%%%%%%%%    START COMPUTING THE STIFFNESS MATRICES
%%%%%%%%%%%%%%%%%%%%%%%%%%%%%%%%%%%%%%%%%%%%%%%%%%%%%%%%%%%%%%%%%%%%%%%%%%%%%%%

for ielem = 1 : nelem            %  Loop over   nelem

   lprop=matno(ielem);

%%%%%%%%%%%%%%%%%%%%%%%%%%%%%%%%%%%%%%%%%%%%%%%%%%%%%%%%%%%%%%%%%%%%%%%%%%%%%%%
%%%%%%%%%%%  Get the coordinates of each node in the element       %%%%%%%%%%%%%
%%%%%%%%%%%%%%%%%%%%%%%%%%%%%%%%%%%%%%%%%%%%%%%%%%%%%%%%%%%%%%%%%%%%%%%%%%%%%%%

 for inode = 1 : nnode
  lnode = round(abs(lnods(ielem,inode)));
  for idime = 1 : ndofn
   elcod(idime,inode) = coord(lnode,idime);
  end
 end

 shape = zeros(8,1);
 deriv = zeros(2,8);
 xjacm = zeros(2,2);
 cartd = zeros(2,8);
 estif = zeros(nevab,nevab);

 [dmatx] = I_MODPS(props);

 thick= props(lprop,3);

%%%%%%%%%%%%%%%%%%%%%%%%%%%%%%%%%%%%%%%%%%%%%%%%%%%%%%%%%%%%%%%%%%%%%%%%%%%%%%%
%%%%%%%%%%%%%%%%%%%%%%%    Start Gaussian Integration
%%%%%%%%%%%%%%%%%%%%%%%%%%%%%%%%%%%%%%%%%%%%%%%%%%%%%%%%%%%%%%%%%%%%%%%%%%%%%%%

kgasp = 0;   %  Keep track over the gauss points in each element.

[posgp,weigp] = I_GAUSSQ(ngaus);

for igaus = 1 : ngaus              %  Loop over each Gauss point along "Zi" axis
                                   %  i.e., horizontally, starting from left.
for jgaus = 1 : ngaus              %  Loop over each Gauss point along "Eta" axis
                                   %  i.e., vertically, starting from bottom.
kgasp = kgasp + 1;
```

```
%%%%%%%%%%%%%%%%%%%%%%%%%%%%%%%%%%%%%%%%%%%%%%%%%%%%%%%%%%%%%%%%%%%%%%%%%%%%
%%%%%%%%%%        Evaluate the Shape functions, derivatives etc.          %%%%%%%%%%
%%%%%%%%%%%%%%%%%%%%%%%%%%%%%%%%%%%%%%%%%%%%%%%%%%%%%%%%%%%%%%%%%%%%%%%%%%%%

    exisp = posgp(igaus);
    etasp = posgp(jgaus);

    [shape,deriv] = I_SFR2(exisp,etasp);

   [xjacm,djacb,gpcod,cartd]=I_JACOB2(ielem,kgasp,ndofn,nnode,shape,deriv,elcod);

    dvolu = djacb*weigp(igaus)*weigp(jgaus)*thick;  % volume calculation :  t*j*ds*dt

%%%%%%%%%%%%%%%%%%%%%%%%%%%%%%%%%%%%%%%%%%%%%%%%%%%%%%%%%%%%%%%%%%%%%%%%%%%%
%%%%%%%%%%%%%    Evaluate the 'B' matrix and 'DB' matrices
%%%%%%%%%%%%%%%%%%%%%%%%%%%%%%%%%%%%%%%%%%%%%%%%%%%%%%%%%%%%%%%%%%%%%%%%%%%%

[bmatx] = I_BMATPS(nnode,cartd);
[dbmat] = I_DBE(dmatx,bmatx);


%%%%%%%%%%%%%%%%%%%%%%%%%%%%%%%%%%%%%%%%%%%%%%%%%%%%%%%%%%%%%%%%%%%%%%%%%%%%
%%%%%%%%%%%%%    Calculate the element stiffness matrices       %%%%%%%%%%%%%
%%%%%%%%%%%%%%%%%%%%%%%%%%%%%%%%%%%%%%%%%%%%%%%%%%%%%%%%%%%%%%%%%%%%%%%%%%%%

    estif = estif + transpose(bmatx)*dbmat;

%%%%%%%%%%%%%%%%%%%%%%%%%%%%%%%%%%%%%%%%%%%%%%%%%%%%%%%%%%%%%%%%%%%%%%%%%%%%
%%%%%%%%%%%%%%%%%%%%%%%%%    End of Gaussian Integration
%%%%%%%%%%%%%%%%%%%%%%%%%%%%%%%%%%%%%%%%%%%%%%%%%%%%%%%%%%%%%%%%%%%%%%%%%%%%

  end

 end

%%%%%%%%%%%%%%%%%%%%%%%%%%%%%%%%%%%%%%%%%%%%%%%%%%%%%%%%%%%%%%%%%%%%%%%%%%%%
%%%%%%%%%%%%    Assemble the element stiffness matrices
%%%%%%%%%%%%%%%%%%%%%%%%%%%%%%%%%%%%%%%%%%%%%%%%%%%%%%%%%%%%%%%%%%%%%%%%%%%%

 [globK] = I_ASMBLK(ielem,nevab,lm,estif,globK);

 end

%%%%%%%%%%%%%%%%%%%%%%%%%%%%%%%%%%%%%%%%%%%%%%%%%%%%%%%%%%%%%%%%%%%%%%%%%%%%
%%%%%%%%%%%%    END OF ASSEMBLY FOR "estif" OF "ielem"
%%%%%%%%%%%%%%%%%%%%%%%%%%%%%%%%%%%%%%%%%%%%%%%%%%%%%%%%%%%%%%%%%%%%%%%%%%%%

iRuns = 1 ;
plyconfig=1;
%%%%%%%%%%%%%%%%%%%%%%%%%%%%%%%%%%%%%%%%%%%%%%%%%%%%%%%%%%%%%%%%%%%%%%%%%%%%
%%%%%%%%%%        Read the nodal loads and assemble into          %%%%%%%%%%
%%%%%%%%%%                  Global Force Vector                   %%%%%%%%%%
%%%%%%%%%%%%%%%%%%%%%%%%%%%%%%%%%%%%%%%%%%%%%%%%%%%%%%%%%%%%%%%%%%%%%%%%%%%%
```

```
[eload] =
I_LOADPS(nelem,numnp,nnode,nevab,ndofn,ngaus,posgp,weigp,coord,lnods,matno,props,iRuns);

  [asmblF] = I_FORCE(nelem,nevab,lm,eload);

%%%%%%%%%%%%%%%%%%%%%%%%%%%%%%%%%%%%%%%%%%%%%%%%%%
%%%%%%%%         Solve for Displacements              %%%%%%%%
%%%%%%%%%%%%%%%%%%%%%%%%%%%%%%%%%%%%%%%%%%%%%%%%%%

[displ,eldis] = I_BCSOLVE(ndofn,coord,asmblF,globK,lm,nelem,nevab,numnp,nnode,iRuns);

%%%%%%%%%%%%%%%%%%%%%%%%%%%%%%%%%%%%%%%%%%%%%%%%%%
%%%%%%%%        Solve for GAUSS POINT STRESSES              %%%%%%%%
%%%%%%%%%%%%%%%%%%%%%%%%%%%%%%%%%%%%%%%%%%%%%%%%%%

  strsp=zeros(nstre,ngaus*ngaus,nelem);
  sgtot=zeros(nstr1,ngaus*ngaus,nelem);

[sgtot,strsp]=I_STREPS(nelem,matno,props,ntype,nmats,nnode,ndofn,coord,ngaus,nstre,nevab,nstr1,eldis,l
nods,iRuns);

%
[sy,sigy_653,sigy_629,sigy_605,sigy_581,sigy_557,sigy_533,sigy_334,sigy_356,sigy_378,sigy_400,sigy_
422,sigy_444,sigy_466,sigy_488,sigy_510 ] = stress_hole(sgtot,coord);
[sy,stress_mat] = stress_hole(sgtot,coord)

disp(' DISPLAY NODAL STRESS BY MATLAB PROGRAMMING')

stress_mat

sigy_653,sigy_629,sigy_605,sigy_581,sigy_557,sigy_533,sigy_334,sigy_356
sigy_378,sigy_400,sigy_422,sigy_444,sigy_466,sigy_488,sigy_510

disp(' DISPLAY CORRESPONDING STRESS BY EXACT EQUATION')

sy

disp('displacement near boundary')

disp_node15 = displ(29:30)
disp_node29 = displ(57:58)
disp_node273 = displ(545:546)
disp_node524 = displ(1047:1048)
disp_node510 = displ(1019:1020)

disp('displacement near hole')

disp_node653 = displ(1305:1306)
disp_node637 = displ(1273:1274)
disp_node661 = displ(1321:1322)
disp_node645 = displ(1289:1290)

RunTime = toc
```

APPENDIX – C

Program for the Stochastic Finite Element Analysis of Notched

Composite Laminates

```
clear all;
close all;
clc;

% tic;
format long;

%%%%%%%%%%%%%%%%%%%%%%%%%%%%%%%%%%%%%%%%%%%%%%%%%%%%%%%%%%%%%%%%%%%%%%%%%%%%%%%%%%%%%%%%%%%%%%%%%%%%%%%%%%%%%%%
%%%
 %%%%%%%%%%%%%%            In the organization of the program
%%%%%%%%%%%%%%%
%%%%%%%%%%%%%%  Local and Global variables are referred to by the
%%%%%%%%%%%%%%   names so that any variable is given a single name
%%%%%%%%%%%%%%%
%%%%%%%%%%%%%%          all throughout the program, in order to avoid
%%%%%%%%%%%%%%              confusion over variable names
%%%%%%%%%%%%%%%
%%%%%%%%%%%%%%%%%%%%%%%%%%%%%%%%%%%%%%%%%%%%%%%%%%%%%%%%%%%%%%%%%%%%%%%%%%%%%%%%%%%%%%%%%%%%%%%%%%%%%%%%%%%%%%%
%%%

dummy=0;        % Dummy variable is used to pass  I_GETDAT and I_GETARR
nelem=0;

%%%%%%%%%%%%%%%%%%%%%%%%%%%%%%%%%%%%%%%%%%%%%%%%%%%%%%%%%%%%%%%%%%%%%%%%%%%%%%%%%%%%%%%%%%%%%%%%%%%%%%%%%%%%
ndofn=0;        %                                                       %
nnode=0;        %     Initialize all the relevant variables which are   %
ngaus=0;        %                                                       %
ntype=0;        %     passed to the data functions so that all the relevant  %
nmats=0;        %                                                       %
numnp=0;        %     data is passed back through the same variables.   %
nstre=0;        %                                                       %
nstr1=0;

%%%%%%%%%%%%%%%%%%%%%%%%%%%%%%%%%%%%%%%%%%%%%%%%%%%%%%%%%%%%%%%%%%%%%%%%%%%%%%%%%%%%%%%%%%%%%%%%%%%%%%%%%%%%%%%
%%%

props = 0;
lnods = 0;
coord = 0;

nlami = 300;

[ao,do] =I_DISAO(nlami);   %% Pass the characteristic length values for both point and average stress
criterion
[xc_unc,yc_unc] = hole_uncert(nlami);      %% Controls the eccentricity of hole center

for ilami = 1 : nlami
```

```
fprintf(' \n TENSILE ANALYSIS of  [0/90]4s uncontrolled hole simulation no:%d \n',ilami);

kgaus = 0;   % Keep track over the Gauss points in each entire structure.

%%%%%%%%%%%%%%%%%%%%%%%%%%%%%%%%%%%%%%%%%%%%%%%%%%%%%%%
%%%%%%%%%%%%        I_GETDAT - Contains relevant scalar variables
%%%%%%%%%%%%%%%%%%%%%%%%%%%%%%%%%%%%%%%%%%%%%%%%%%%%%%%


[nelem,ndofn,nnode,ngaus,ntype,nmats,numnp,nstre,nstr1,ntotg,iRuns,Length,Width,Dia]=I_GETDAT(du
mmy);

%%%%%%%%%%%%%%%%%%%%%%%%%%%%%%%%%%%%%%%%%%%%%%%%%%%%%%%
%%%%%%%%%%%%      I_GETARR – Contains all the Relevant Data in Array from   %%%%%%%%
%%%%%%%%%%%%%%%%%%%%%%%%%%%%%%%%%%%%%%%%%%%%%%%%%%%%%%%

% fg = fopen('propg.m','w');
% fprintf(fg,'\n\n\t\t\t--------------------------------------\n');
% fprintf(fg,' \t        properties at each and every Gauss point');
% fprintf(fg,'\n\t\t\t--------------------------------------\n\n');

[props,tetag,plytk,matno,propg,lnods,coord,ThetaPly] =
I_GETARR(nelem,ngaus,ndofn,nnode,ntotg,ilami,xc_unc,yc_unc,Length,Width,Dia);

%%%%%%%%%%%%%%%%%%%%%%%%%%%%%%%%%%%%%%%%%%%%%%%%%%%%%%%
%%%%%%%%%%%%%%%%%%%%%              Establish the Nodal Connectivity          %%%%%%%%%
%%%%%%%%%%%%%%%%%%%%%%%%%%%%%%%%%%%%%%%%%%%%%%%%%%%%%%%

nevab = ndofn*nnode;
globK = zeros(numnp*ndofn); % Initialize the Global "K" matrix for each element

[lm,id] = I_ELCON(ndofn,nnode,nelem,numnp,lnods);

%%%%%%%%%%%%%%%%%%%%%%%%%%%%%%%%%%%%%%%%%%%%%%%%%%%%%%%
%%%%%%%%%%%%%%%            Start Computing the Stiffness Matrices
%%%%%%%%%%%%%%%%%%%%%%%%%%%%%%%%%%%%%%%%%%%%%%%%%%%%%%%

for ielem = 1 : nelem              % Loop over total number of element

%%%%%%%%%%%%%%%%%%%%%%%%%%%%%%%%%%%%%%%%%%%%%%%%%%%%%%%
%%%%%%%%%%%%        Get the Coordinates of Each Node in the Element
%%%%%%%%%%%%%%%%%%%%%%%%%%%%%%%%%%%%%%%%%%%%%%%%%%%%%%%

 for inode = 1 : nnode
  lnode = round(abs(lnods(ielem,inode)));
  for idime = 1 : ndofn
   elcod(idime,inode) = coord(lnode,idime);
  end
 end

 shape = zeros(8,1);
 deriv = zeros(2,8);
 xjacm = zeros(2,2);
 cartd = zeros(2,8);
 estif = zeros(nevab,nevab);
```

```
%%%%%%%%%%%%%%%%%%%%%%%%%%%%%%%%%%%%%%%%%%%%%%%%%%%%%%%%%%%%%%%%%%%%%%%%%%%%
%%%%%%%%%%%%%%%%%%%%%%%%%%    Start Gaussian Integration    %%%%%%%%%%%%%
%%%%%%%%%%%%%%%%%%%%%%%%%%%%%%%%%%%%%%%%%%%%%%%%%%%%%%%%%%%%%%%%%%%%%%%%%%%%

 kgasp = 0;   % Keep track over the Gauss points in each element.

 [posgp,weigp] = I_GAUSSQ(ngaus);

 for igaus = 1 : ngaus                % Loop over each Gauss point along "Zi" axis
                                      % i.e., horizontally, starting from left.
  for jgaus = 1 : ngaus               % Loop over each Gauss point along "Eta" axis
                                      % i.e., vertically, starting from bottom.
    kgasp = kgasp + 1;
    kgaus = kgaus + 1;

    lprop = matno(kgaus);
    ThetaPly = tetag(kgaus,:);
    thick = sum(plytk(kgaus,:));

%%%%%%%%%%%%%%%%%%%%%%%%%%%%%%%%%%%%%%%%%%%%%%%%%%%%%%%%%%%%%%%%%%%%%%%%%%%%
%%%%%%%%%%    Evaluate the Shape functions, Derivatives, etc.    %%%%%%%%%%%%
%%%%%%%%%%%%%%%%%%%%%%%%%%%%%%%%%%%%%%%%%%%%%%%%%%%%%%%%%%%%%%%%%%%%%%%%%%%%

    exisp = posgp(igaus);
    etasp = posgp(jgaus);

    [dmatx] = I_MODPS(ntype,nstre,nmats,lprop,propg,ThetaPly,kgaus);

    [shape,deriv] = I_SFR2(exisp,etasp);

   [xjacm,djacb,gpcod,cartd]=I_JACOB2(ielem,kgasp,ndofn,nnode,shape,deriv,elcod);

%%%%%%%%%%%%%%%%%%%%%%%%%%%%%%%%%%%%%%%%%%%%%%%%%%%%%%%%%%%%%%%%%%%%%%%%%%%%
%%%%%%%%%%%    Evaluate the 'B' matrix and 'DB' matrices
%%%%%%%%%%%%%%%%%%%%%%%%%%%%%%%%%%%%%%%%%%%%%%%%%%%%%%%%%%%%%%%%%%%%%%%%%%%%

[bmatx] = I_BMATPS(nnode,cartd);

[dbmat] = I_DBE(dmatx,bmatx);


%%%%%%%%%%%%%%%%%%%%%%%%%%%%%%%%%%%%%%%%%%%%%%%%%%%%%%%%%%%%%%%%%%%%%%%%%%%%
%%%%%%%%%%%    Calculate the Element Stiffness Matrices
%%%%%%%%%%%%%%%%%%%%%%%%%%%%%%%%%%%%%%%%%%%%%%%%%%%%%%%%%%%%%%%%%%%%%%%%%%%%

    estif = estif + transpose(bmatx)*dbmat*dvolu;

%%%%%%%%%%%%%%%%%%%%%%%%%%%%%%%%%%%%%%%%%%%%%%%%%%%%%%%%%%%%%%%%%%%%%%%%%%%%
%%%%%%%%%%%%%%%%%%%%%%%%%%    End of Gaussian Integration
%%%%%%%%%%%%%%%%%%%%%%%%%%%%%%%%%%%%%%%%%%%%%%%%%%%%%%%%%%%%%%%%%%%%%%%%%%%%

  end

 end
```

```
%%%%%%%%%%%%%%%%%%%%%%%%%%%%%%%%%%%%%%%%%%%%%%%%%%%%%%%%%%%%%%%%%%%%%%%%%%%%
%%%%%%%%%%%    Assemble the Element Stiffness Matrices
%%%%%%%%%%%%%%%%%%%%%%%%%%%%%%%%%%%%%%%%%%%%%%%%%%%%%%%%%%%%%%%%%%%%%%%%%%%%

 [globK] = I_ASMBLK(ielem,nevab,lm,estif,globK);


 end

%%%%%%%%%%%%%%%%%%%%%%%%%%%%%%%%%%%%%%%%%%%%%%%%%%%%%%%%%%%%%%%%%%%%%%%%%%%%
%%%%%%%%%%%%%%%%      End of Assembly for "estif" of "ielem"
%%%%%%%%%%%%%%%%%%%%%%%%%%%%%%%%%%%%%%%%%%%%%%%%%%%%%%%%%%%%%%%%%%%%%%%%%%%%

%%%%%%%%%%%%%%%%%%%%%%%%%%%%%%%%%%%%%%%%%%%%%%%%%%%%%%%%%%%%%%%%%%%%%%%%%%%%
%%%%%%%%%%%%          Read the nodal loads and assemble into          %%%%%%%%%%
%%%%%%%%%%%%                Global Force Vector                       %%%%%%%%%%
%%%%%%%%%%%%%%%%%%%%%%%%%%%%%%%%%%%%%%%%%%%%%%%%%%%%%%%%%%%%%%%%%%%%%%%%%%%%

 [eload] =
I_LOADPS(nelem,numnp,nnode,nevab,ndofn,ngaus,posgp,weigp,coord,lnods,matno,props,iRuns);

 [asmblF] = I_FORCE(nelem,nevab,lm,eload);

%%%%%%%%%%%%%%%%%%%%%%%%%%%%%%%%%%%%%%%%%%%%%%%%%%%%%%%%%%%%%%%%%%%%%%%%%%%%
%%%%%%%%%%          Solve for Displacements          %%%%%%%%%%%%%%%%%%%%%%
%%%%%%%%%%%%%%%%%%%%%%%%%%%%%%%%%%%%%%%%%%%%%%%%%%%%%%%%%%%%%%%%%%%%%%%%%%%%

[displ,eldis] =I_BCSOLVE(ndofn,coord,asmblF,globK,lm,nelem,nevab,numnp,nnode,iRuns);


%%%%%%%%%%%%%%%%%%%%%%%%%%%%%%%%%%%%%%%%%%%%%%%%%%%%%%%%%%%%%%%%%%%%%%%%%%%%
%%%%%%%%%          Solve for Gauss Point Stresses     %%%%%%%%%%%%%%%%%%%%%
%%%%%%%%%%%%%%%%%%%%%%%%%%%%%%%%%%%%%%%%%%%%%%%%%%%%%%%%%%%%%%%%%%%%%%%%%%%%

 strsp=zeros(nstre,ngaus*ngaus,nelem);
 sgtot=zeros(nstr1,ngaus*ngaus,nelem);


[sgtot,strsp]=I_STREPS(nelem,matno,props,propg,tetag,ntype,nmats,nnode,ndofn,coord,ngaus,nstre,nevab,
nstr1,eldis,lnods,iRuns);

%%% Compare the Results of Reference, Exact and MATLAB© Solution    %%%%%%%%%%%%%

[sigy_ref,sigy_exact,stress_mat] = ref_whitney(props,ThetaPly,coord,sgtot,Width,Dia,xc_unc,ilami)

%%%% Calculate the stresses by both Point stress and Average stress criterion  %%%%%%%%%%%%

[sigavg,stress_mat,point_maxstress]=I_AVGSTR(sgtot,coord,ilami,ao,do,Width,Dia,xc_unc);

end

 %% Display the displacements at loading boundary
%%%%%%%%%%%%%%%%%%%%%%%%%%%

Vdispl_29(ilami,1)=displ(58);
Vdispl_273(ilami,1)=displ(546);
```

```
Vdispl_524(ilami,1)=displ(1048);


sigY_653(ilami,1) = stress_mat(1,1);
sigY_629(ilami,1) = stress_mat(1,2);
sigY_605(ilami,1) = stress_mat(1,3);
sigY_581(ilami,1) = stress_mat(1,4);
sigY_557(ilami,1) = stress_mat(1,5);
sigY_533(ilami,1) = stress_mat(1,6);
sigY_334(ilami,1) = stress_mat(1,7);
sigY_356(ilami,1) = stress_mat(1,8);
sigY_378(ilami,1) = stress_mat(1,9);
sigY_400(ilami,1) = stress_mat(1,10);
sigY_422(ilami,1) = stress_mat(1,11);
sigY_444(ilami,1) = stress_mat(1,12);
sigY_466(ilami,1) = stress_mat(1,13);
sigY_488(ilami,1) = stress_mat(1,14);
sigY_510(ilami,1) = stress_mat(1,15);

equv_stress(ilami,1)= sigavg ;
max_stress(ilami,1)=point_maxstress;

end

stddev_sigy_653=std(sigY_653);

mequv_stress = mean(equv_stress);
standdev_equvstress =std(equv_stress);
coeff_var_equvstres = (standdev_equvstress/mequv_stress)*100;

mmax_stress= mean(max_stress);
standdev_maxstress =std(max_stress );
coeff_var_maxstress = (standdev_maxstress/mmax_stress)*100;

=================================================================================
========== Output for equivalent stress by average stress criterion ==========
=================================================================================

fk = fopen('out_uncert_equ_stress.m','w');
fprintf(fk,'\n\n\t\t\t----------\n');
fprintf(fk,' \t      Equivalent stress value after total simulation no.%d',nlami);
fprintf(fk,'\n\t\t\t----------\n\n');

for  ilami = 1 : nlami
 fprintf(fk,'\n----------\n');
 fprintf(fk,'\nSimulation : %d\t  %13.10f  \n',ilami,equv_stress(ilami,1));
end

fprintf(fk,' \t  Mean Equivalent stress: %13.10f  \n\n',mequv_stress);
fprintf(fk,' \t  Standard Dev.of Equivalent stress: %13.10f  \n\n',standdev_equvstress);
fprintf(fk,' \t  Coefficient of Var. of Equivalent stress: %13.10f  \n\n',coeff_var_equvstres );

=================================================================================
========== Output for maximum stress by point stress criterion=== ==========
=================================================================================
```

```
for  ilami = 1 : nlami
 fprintf(fk,'\n----------\n');
 fprintf(fk,'\nSimulation : %d\t   %13.10f  \n',ilami,max_stress(ilami,1));
end

fprintf(fk,' \t   Mean maximum stress: %13.10f  \n\n',mmax_stress);
fprintf(fk,' \t   Standard Dev.of maximum stress: %13.10f  \n\n',standdev_maxstress);
fprintf(fk,' \t   Coefficient of Var. of maximum stress: %13.10f  \n\n',coeff_var_maxstress );


disp(' DISPLAY MEAN STRESS NEAR HOLE')

msigY_653 = mean(sigY_653);
msigY_629 = mean(sigY_629);
msigY_605 = mean(sigY_605) ;
msigY_581 = mean(sigY_581) ;
msigY_557 = mean(sigY_557) ;
msigY_533 = mean(sigY_533) ;
msigY_334 = mean(sigY_334) ;
msigY_356 = mean(sigY_356) ;
msigY_378 = mean(sigY_378) ;
msigY_400 = mean(sigY_400) ;
msigY_422 = mean(sigY_422) ;
msigY_444 = mean(sigY_444) ;
msigY_466 = mean(sigY_466);
msigY_488 = mean(sigY_488) ;
msigY_510 = mean(sigY_510) ;

disp('DISPLAY MEAN DISPLACEMENT NEAR BOUNDARY')

mVdispl_29  = mean(Vdispl_29) ;
mVdispl_273 = mean(Vdispl_273);
mVdispl_524 = mean(Vdispl_524) ;

standard_dev_sigY_653 = std(sigY_653);
Coeff_Var_sigY_653 =  (standard_dev_sigY_653/msigY_653)*100;

 sigy_ref
 sigy_exact

fprintf(fk,' \t   mean Stress at hole edge: %13.10f  \n\n',msigY_653);
fprintf(fk,' \t   std. dev of Stress at hole edge: %13.10f  \n\n',stddev_sigy_653);
fprintf(fk,' \t V Displacement at boundary node 29: %13.10f  \n\n',mVdispl_29);
fprintf(fk,' \t V Displacement at boundary node 273: %13.10f  \n\n',mVdispl_273);
fprintf(fk,' \t V Displacement at boundary node 524: %13.10f  \n\n',mVdispl_524);

save all;
fclose('all');
```

APPENDIX – D

Program for the Calculation of Characteristic Length Values using Point Stress Criterion and Average stress Criterion

```
function [chlen]= I_AOCAL(dummy)

format short;

nstre=3;

ThetaPly=[ 0 90 0 90 0 90 0 90 90 0 90 0 90 0 90 0]*pi/180;

choose_crieterion =input('if average stress crit. put 1, for point stress put 2 >>');
D=input('Diameter of the hole in meter >> ');
matl_prop=input('If Shashank matl prop put 1 or put 2 >>');
hole_size=input('put 1 or 2 or 3 correspond to hole dia 5.1 , 6.35 or 7.54  >>');

if choose_crieterion==1
   disp('Characteristic lengths by Average stress criterion')
else choose_crieterion==2
   disp('Characteristic lengths by Point stress criterion')
end

if matl_prop==2
  props = [ 135.036e9  8.2e9  0.264   0.016   4.172e9   1.25e-4  16];
else matl_prop==1
 props = [ 113.9e9 7.985e9 .29 0.020 3.13e9 1.25e-4 16];
end

qm126 = zeros(nstre,nstre);
qmxys = zeros(nstre,nstre);
matxA = zeros(nstre,nstre);

yung1 = props(1);
yung2 = props(2);
nue12 = props(3);
nue21 = props(4);
shr12 = props(5);

plytk = props(6);
nplys = props(7);

%%%%%%%%%%%%%%%%%%%%%%%%%%%%%%%%%%%%%%%%%%%%%%%%%%%%%%%%%%%%%%%%%%%%%%%%%%%%
%%%%%%%%%%%%%%%%%%   On-Axis Stiffness Matrix   %%%%%%%%%%%%%%%%%%
%%%%%%%%%%%%%%%%%%%%%%%%%%%%%%%%%%%%%%%%%%%%%%%%%%%%%%%%%%%%%%%%%%%%%%%%%%%%

qm126(1,1) = yung1/(1.0 - nue12*nue21);
qm126(2,2) = yung2/(1.0 - nue12*nue21);
qm126(1,2) = nue12*yung2/(1.0 - nue12*nue21);
qm126(2,1) = qm126(1,2);
```

```
qm126(1,3) = 0.0;
qm126(2,3) = 0.0;
qm126(3,1) = 0.0;
qm126(3,2) = 0.0;
qm126(3,3) = shr12;

for iplys = 1 : nplys

 theta = ThetaPly(iplys);

 m = cos(theta);
 n = sin(theta);

 qmxys(1,1) = m^4*qm126(1,1) + n^4*qm126(2,2) + 2*m^2*n^2*qm126(1,2) + 4*m^2*n^2*qm126(3,3);
 qmxys(2,2) = n^4*qm126(1,1) + m^4*qm126(2,2) + 2*m^2*n^2*qm126(1,2) + 4*m^2*n^2*qm126(3,3);
 qmxys(1,2) = m^2*n^2*(qm126(1,1)+qm126(2,2)) + (m^4 + n^4)*qm126(1,2) -
4*m^2*n^2*qm126(3,3);
 qmxys(2,1) = qmxys(1,2);
 qmxys(1,3) = m^3*n*qm126(1,1) - m*n^3*qm126(2,2) + (m*n^3 - m^3*n)*(qm126(1,2) +
2*qm126(3,3));
 qmxys(3,1) = qmxys(1,3);
 qmxys(2,3) = m*n^3*qm126(1,1) - m^3*n*qm126(2,2) + (m^3*n - m*n^3)*(qm126(1,2) +
2*qm126(3,3));
 qmxys(3,2) = qmxys(2,3);
 qmxys(3,3) = m^2*n^2*(qm126(1,1) + qm126(2,2)) - 2*m^2*n^2*qm126(1,2) + (m^2 -
n^2)^2*qm126(3,3);

 botom = -(nplys/2)*plytk;

 hite1 = botom + iplys*plytk;
 hite2 = botom + (iplys-1)*plytk;

 matxA = matxA + qmxys*( hite1 - hite2 );
end

dmatx = matxA/(nplys*plytk);

chlen= zeros(25,1);

if hole_size==2          % [ 0/90]4s d1 experimental result of Ibrahim
sigN= 1e9*[ 0.6367
   0.6033
   0.5519
   0.5961
   0.6251
   0.6019
   0.5867
   0.5824
   0.6308
   0.5834
   0.6217
   0.5677
   0.6097
   0.5968
   0.6034
   0.6210
```

```
   0.6067
   0.5979
   0.6239
   0.6171
   0.5720
   0.5972
   0.6202
   0.6086
   0.5954];

if matl_prop==2

sigO=1e6*[1054.091488                    % Experimental  data
1030.753547
1032.54181
949.6748522
989.8087039
1024.146645
986.4741842
1044.915626
988.7720121
1035.611714
1042.604502
1186.50682
1177.6654
1161.763354
1138.652417
1071.574314
1105.961224
1146.585381
1155.08265
1177.410225
868.697975
1073.69245
1130.841518
1180.079268
1072.356867
];

else

for i=1:25
   ratio=(sigN(i)/sigO(i));

t=0.002; % laminate thickness

A= dmatx*t; % Axial stiffness matrix

% a=inv(A);

Ktinf= 1+ sqrt((2/A(2,2))*(sqrt(A(1,1)*A(2,2)-A(1,2))+(A(1,1)*A(2,2)-A(1,2)^2)/(2*A(3,3))));

% equn of SC Tan 3.70
R=D/2;
% R=0.00376; %radius of the hole
right=0;
```

```
if choose_crieterion==1

for ao=0.001:0.00001:0.1
  if(right~=ratio)
    xzi=R/(R+ao);
    Nu=(2*(1-xzi));
    den=(2-xzi^2-xzi^4+(Ktinf-3)*(xzi^6-xzi^8));
    right=Nu/den;
     if (right>ratio)
       chlen(i)=ao;
       break, end
  end
end

elseif choose_crieterion==2

for do=0.0001:0.000001:0.1
  if(right~=ratio)
    xzi=R/(R+do);
    Nu=2;
    den=(2+xzi^2+3*xzi^4-(Ktinf-3)*(5*xzi^6-7*xzi^8));
    right=Nu/den;
     if (right>ratio)
       chlen(i)=do;
       break, end
  end
end

end


end

if  choose_crieterion==1

chlen=chlen*1000; % display all the value of characterstic length
mean_chlen =mean(chlen) % mean of characterstic length
stand_chlen =std(chlen)

coeff_variation=(stand_chlen/mean_chlen)*100

max_ao = max(chlen)
min_ao = min(chlen)

else  choose_crieterion==2

chlen=chlen*1000                % display all the value of characterstic length
mean_chlen =mean(chlen)         % mean of characterstic length
stand_chlen =std(chlen)

coeff_variation=(stand_chlen/mean_chlen)*100

max_do = max(chlen)
min_do = min(chlen)

end
```